Final Report – March 2018

Thermal Shock Technology

E16PC00010

BSEE

March 15 2018

Document Revision History

Revision No.	Revision Date	Revision Description	Prepared By	Approved By
A	Jan 12 2018	Issued for BSEE comment	NTP	AEG
B	Mar 15 2018	BSEE Comments Addressed	NTP	AEG

TABLE OF CONTENTS

Abbreviations and Nomenclature

API	American Petroleum Institute
BOP	Blow Out Preventer
BSEE	Bureau of Safety and Environmental Enforcement
CFD	Computational Fluid Dynamics
COP	ConocoPhillips
FEA	Finite Element Analysis
GOM	Gulf of Mexico
HSE	Health, Safety and Environment
HPHT	High Temperature High Pressure
OCS	Outer Continental Shelf
UH	University of Houston
WWC	Wild Well Control, Inc.
LT	Lower Tertiary
UTA	University of Texas at Austin
SCP	Sustained Casing Pressure
MD	Measured Depth
TVD	True Vertical Depth
k	Thermal conductivity

1 EXECUTIVE SUMMARY

Historically, the concern of thermal stresses induced in a well by completion and production operations was not considered early in the developing petroleum industry. Wells were completed and assumed to remain functional and intact for the producing lifetime. As well integrity problems appeared, they were fixed, but a holistic evaluation of thermal stresses induced on a well by completion, production, and intervention operations was not routinely considered. Considering the comparatively low thermal and mechanical gradients imposed on early wells, this is not surprising. In the second half of last century, well depths increased along with temperatures and pressures. Along with this development, awareness of safety hazards and desire to establish best practices, guidelines and regulations governing well construction and operation was emerging.

The advent of geothermal wells, HPHT wells and thermal stimulation of viscous hydrocarbons greatly increased awareness of thermal induced hazards. Instances of casing buckling or wellheads growing out of the ground emphasized the potential of thermal effects. Additionally, conventional wells were drilled deeper, hydraulic fracturing treatments were larger in volume, and workover operations became more frequent. All these factors increased the effect of temperature changes in the well.

It is proposed that the occurrence of a thermal shock may be defined as a magnitude of temperature change over the time at which it changes. Therefore thermal shock may or may not occur depending on various conditions in the wellbore.

The intent of this project is to investigate whether or not thermal shock has been adequately considered in the design and operation of OCS wells and to establish whether or not whether there are any gaps in knowledge. This final report covers the completion of the Thermal Shock Technology E16PC00010. The summary of findings is shown below.

1.1 Overall Project Summary:

The summary of findings of the overall project goals and objectives are summarized with the initial objective to investigate whether or not thermal shock has been adequately considered in the design and operation of OCS wells and to establish whether or not whether there are any gaps in knowledge:

1. ***Identify source and magnitudes of thermal gradients produced during OCS well drilling, completion and production.***
   - Stimulating a well results in significantly higher thermal gradients in the well than drilling, completion and production. Stimulation also causes more damage to the cement than a normal production/shut-in cycle and that damage can extend a significant distance up the well bore.

2 Develop an acceptable definition of thermal shock and identify operating conditions that could result in a thermal shock.

- Wells with a bottom hole temperature of 350°F or above combined with a minimum ambient temperature as low as 40°F.
- Thermal shock could be initiated by shutting in a producing well and allowing it to cool to ambient or by stimulating a well. The thermal shocks are more severe during stimulation and damage is mainly caused by the cyclical nature of the load.
- Thermal shock depends primarily on the temperature range of that shock but also the rate at which temperature changes. The rate of cooling of the well depend on the operations considered, e.g. natural cooling post shut-in or cooling during well stimulation for example.

3 Evaluate thermal shock damage potential to well bore components and barriers.

- Thermal shock can potentially cause damage to various well bore components. The consideration of thermal effects is much better understood with regards to tubulars and is typically accounted for in well design software such as WellCAT and StressCheck. These are programs that are used for the design of the casing and tubing used within a well. The damage potential to settable barriers such as cement carries a greater uncertainty due to the inherent material characteristics of cement. The severity of this damage to cement is highly dependent on factors such as cement composition used, quality of the cement itself and placement of cement. It should be noted that damage does not necessarily result in an actual loss of barrier/zonal isolation

4 Assess applicability of previously-reported computer simulation or failure analyses to address thermal shock risks.

- The reports recognizes that well design software WellCAT is widely used within the industry in the design of the components of a wellbore. It is noted that WellCAT is well suited for the determining the thermal loads on the various components as this is one of its main functions. WellCAT and its module StressCheck are very applicable to designing the tubulars for thermal shock. However, these programs assume competent cement sheaths are in place. It would be prudent to examine the sensitivity of the tubular design to cement barrier breakdown over the course of the well life and revisit the cement design if the results of that sensitivity analysis warrant it.

5 Identify ways to mitigate thermal shock effects and ways to avoid the creation of a thermal shock environment.

- While thermal shock environments may not be completely unavoidable due to the inherent nature of oil and gas wells, proper design of tubulars and the tubular connections in accordance to current industry recommended practices will help mitigate against thermal shock. The cement composition, uniformity of cement mixing and quality of placement of cement is crucial to mitigate the thermal shock effects. The potential for thermal shock damage to cement should be examined across the entire well bore.

6 ***Evaluate thermal shock resistance of various well barriers utilized in the industry, both mechanical and settable fluid.***

- Tubulars, when thermal loading is accounted for in the design have very good thermal shock resistance when considering typically used steel grades, etc. In addition there are established guidelines for de-rating steel for various temperature exposures. It was found that the cements used in OCS wells have a range of resistances; some cements performed poorly against thermal shock while some performed very well. Thermal shock resistance is needed throughout the cement barrier system and isn't just an issue at bottom of the well.

7 ***"Identify gaps in current well design methods contributing to loss of well integrity caused by thermal shock."***

- The findings of this project show that the industry has made good strides in ensuring that technology used in the past for shallower Outer Continental Shelf (OCS) wells is suitable for these deeper and hotter wells that will experience thermal shock. However a better understanding of the conditions faced in the deeper and hotter wells and the need to increase the performance of the cement barriers throughout the well is a knowledge gap that exists.

2 INTRODUCTION AND PROJECT OBJECTIVES

The background to this project was a request by BSEE for research into the effects of thermal shock on oil wells, specifically in the outer continental shelf (OCS). In its broad agency announcement, [1], BSEE posed a potential problem that required further research as follows:

"If a High Temperature well (greater than 350° F) is shut in, the well may go into thermal shock when the temperature of the well drops to equilibrium."

In an OCS deep water well, equilibrium could be as low as 35° F (i.e. sea water temperature at the sea bed). The temperature of the well fluids could be as high as 350° F. Therefore large temperature gradients and temperature changes can exist during the operation of a well. The magnitude of temperature changes during well operations as well as the rate of change of temperature could be considered a thermal shock.

The aim of this project was to explore whether shut in and other operations could lead to a thermal shock event in an oil and gas well, research the circumstances under which a such events could occur and most importantly quantify whether thermal shock could damage the well barrier systems in place. Well barriers are the means by which the pressurised fluids in the reservoir are controlled to prevent the unintended release of reservoir fluids into the environment.

Figure 1 illustrates a Deepwater HPHT well showing various temperature gradients experienced throughout the life of a well.

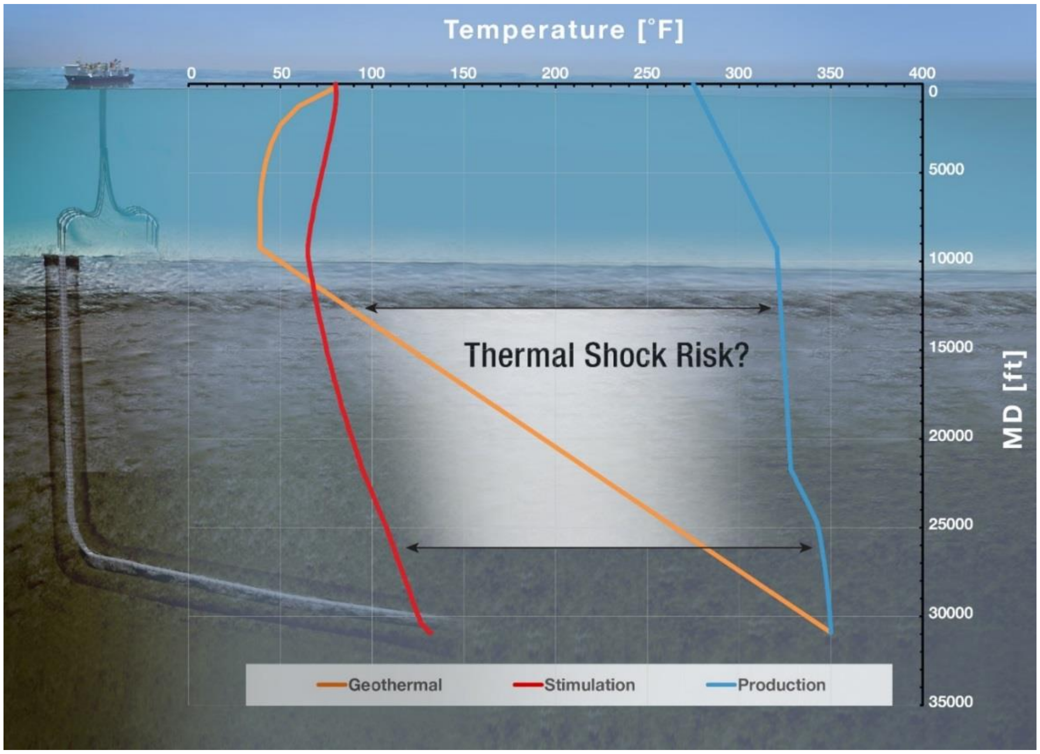

Figure 1 **Deepwater well gradients**

The geothermal gradient (orange) traces the temperature under static conditions from the surface at 80°F, to the subsea mudline surface at 39°F, to the bottom of the well at 350°F or greater. The production gradient (blue) traces the temperature during production from the bottom of the well at 350°F to the mudline at 321°F, to the surface at 72°F. The stimulation gradient (red) simulates a stimulation operation showing a temperature change from surface at 80°F, mudline at 65°F, bottom of the well at 127°F, followed by perforation at 350°F. These three gradients, while illustrative only, are demonstrations of the various temperature profiles potentially experienced in all wells. This illustration also shows the potential temperature changes that can occur along the entire well bore during different well operations. The rate of temperature change was also thought to be an important in consideration in a thermal shock.

A single definition of thermal shock has not yet been widely adopted across the oil and gas industry. A thermal shock definition must therefore be better defined. Working with the project team and BSEE that definition and quantification was developed within this project.

3 FORMATION OF INDUSTRY ADVISORY GROUP

Several major operators with wells in the Gulf of Mexico were contacted to be members of the industry advisory group (IAG). As expected, there was mixed response for IAG membership, as a significant amount of time and effort is required on a voluntary basis.

The focus for this task was attracting interest from major operators. While it may be beneficial to also gain input from drilling contractors and equipment vendors, it was considered a better strategy to wait until the project had developed specific questions. This approach to seek advice was used rather than adopting a blanket invite approach.

Some operators had indicated a willingness to participate in the project but expressed concern over some of the terminology used in the project description with ‘thermal shock’ in particular causing some concern, particularly in the context of shut-in. Some operators do not consider a shut-in as an event that will provide a significant thermal shock.

The following operators were willing to participate in the project:

- ConocoPhillips
- Chevron
- Apache

The following shows companies and their respective personnel that represented the IAG for the project.

Project Industry Advisory Group

Name	Company	Job Title
Gary Limb	ConocoPhillips	Principal Engineer, Well Integrity
Robert Martin	Chevron	Cementing Specialist
Steven Riedinger	Chevron	Cementing Specialist
Steve Willson	Apache	Senior staff Technical Advisor – geomechanics and pore pressure
Joe Savoy	Wild Well Control	Well Operations Manager, Marine
Alistair Gill	Wild Well Control	VP Advanced Engineering
Larry Watters	CSI Technology	Chief Engineer
Nathan Pinkston	Wild Well Control	Senior Engineer
Richard A. Schultz	University of Texas at Austin	Senior Research Scientist

3.1 Industry Advisory Group - Feedback

Feedback on the literature review of current guidelines and proposed thermal shock load histograms respectively was received from Chevron and ConocoPhillips (COP) and was considered in the project:

ConocoPhillips:

- The definition of thermal shock was queried by ConocoPhillips; maximum and minimum temperatures at depth are common well design parameters, however rate of change of temperature is not. COP suggested clarifying the definition of thermal shock being used for the project and to provide some plausible examples of how "thermal shock" can be detrimental to the well.

Chevron:

- Chevron suggested that some of the failure modes such as radial cracking from tensile failure, shear failure, de-bonding, etc. are defined. Also, suggested emphasizing that failure of the cement does not necessarily result in loss of isolation.
- Chevron queried the bottom hole temperature for Lower Tertiary operations in Deepwater suggesting 350°F was on the high side for static temperature, with 250°F being more typical with some starting to approach 300°F. Also reaching 350°F at 25,000 ft as the initial well schematic depicts would be a very high temperature gradient to achieve for Deepwater.
  - WWC increased the true vertical depth (TVD) of the wells to reflect Chevron's input.
- Chevron also suggested that surface pipes be cemented to mudline, as per CFR 250.421
  - Since this well is based very closely on an OCS well completed in the GOM it was decided to have only the cement in the 36x28 annulus cemented to mudline.
- Chevron questioned how the FEA model is managing the mud left behind pipe above the top of cement.
  - This was addressed within Section 6 Well Barrier Design and Response.
- Chevron also suggested conditioning the hole for days seemed long and would have expected this period to be measured in hours but accepted that things vary from operator to operator.
  - The times listed were initial estimates and the sensitivity to this was addressed in the FEA.
- The initial temperature profiles provided to the IAG were just the starting position. The speed at which temperature changes occur was explored in the FEA, however it was found that analysis convergence issues limited the rates of change that could be achieved in certain cases.
- Chevron also questioned the well schematics showing each string cemented back into the previous string and pointed out that this is not very common. To assist in alleviating annular pressure build up, those annuli are typically left open on purpose to act as a relief point.
  - Feedback was be taken into account in future well configurations

- Chevron also questioned the choice of 5 ½” and also suggested that the use of vacuum insulated tubing be considered in the project as it is often utilized to reduce annulus temperatures to reduce annular pressure build-up.
  - This can be taken into consideration for future well configurations, the original 5 ½” tubing was used since it is based on an actual design.

4 LITERATURE REVIEW

The task definition used for this report is complex and is attached as Appendix B, this differed slightly from the task definition originally supplied at time of tender. The key items adjusted were the definition of thermal shock being used in the review, the initial well configuration and the materials used to drive the literature search.

The intent of this task was to ensure that the objectives of this project had not been met by other published research and to determine whether previously published work would be of use to the current project.

4.1 Literature Review Of Thermal Shock Of Well Barriers

Document searches were primarily conducted online in using various key word combinations generated from the task definition.

This flagged tens of thousands of possible technical paper titles from sources including:

- Society of Petroleum Engineers
- Offshore Technology Conference
- American Petroleum Institute
- American Rock Mechanics Association
- International Petroleum Tech Conference
- International Society for Offshore and Polar Engineering
- International Society for Rock Mechanics
- Petroleum Society of Canada

In order to sort through such a large number of titles the searches were restricted, when possible, to peer reviewed papers only. This restriction enabled a list of a few hundred papers to be generated that meriting further review.

It was clear from the literature that thermal shock in the context of wells in general has been examined by others. But the literature review also suggests that thermal shock, as defined in Appendix B and as it effects the entire well barrier system, has not been thoroughly investigated for OCS wells and the further research within this project is justified.

The literature review identified a number of key areas of research and sources of relevant information that will be given further discussion, namely:

- Researched published literature on thermal stimulation to enhance rock fracturing. [3 et al].

- Research into the effects of injecting cold fluid into cased or uncased holes, [4 et al]. Similar research work that was identified during the previous BSEE project, [7], "Well Stimulation Effects on Annular Seal of Production Casing in OCS Oil and Gas Operations" also appeared during this review.
- There are many technical papers relating to thermal shock in the context of geothermal and steam assisted gravity drainage (SAGD) wells that have been published by multiple authors, [4 and 6 et al].
- Thermal effects on well tubular design is well recognized in literature, [12, 13 et al]
- Guidelines already exist for design and construction of well heads and wells in general for HPHT condition, [18, 19 and 20]

4.1.1 Thermal Shock Due To Cold Fluid Injection

Since the increased usage of unconventional oil extraction methods, such as fracking, multiple authors have investigated the effects of injecting cold fluid into the well bore, [3, 4, 7and 11]. This is clearly relevant to this project as well stimulation will be part of the load history for the OCS wells. However, the literature review suggests that most if not all of the work of this type is focused on the open hole or last cased hole section of the well, where the temperature difference are typically the greatest (perhaps understandably).

Objectives 1 through 5 of this project were to examine thermal shock more widely both in terms of location within the well and the circumstances where a thermal shock can occur and do damage to the barrier systems within the well, particularly the cement. There appears to be little attention paid to the upper sections of the well during stimulation, presumably because the assumption has always been that lower temperature deltas result in less damage. Therefore it is reasonable to state that the project objectives have not been met elsewhere.

4.1.2 Thermal Wells and SAGD - Lessons to be Learned

The temperatures involved in Thermal wells may exceed those likely to be encountered in OCS wells, even those with HPHT, nevertheless it was felt prudent to review this arena to confirm whether or not relevant information or lessons learned could be applied to the current project.

The review found a number of papers that looked at the well in its entirety including the interaction of all the constituent parts, [5 is typical]. This was generally contrary to what had been found in literature relating to OCS wells where individual parts have been considered by many but the well as a system less so. It should be pointed out that many of these wells, particularly of the SAGD type are typically much shallower and their construction differs from typical OCS wells in a number of ways, e.g. fewer casings. Nevertheless, lessons were learned from this work to apply to the current project, particularly in terms of the possible merits of adopting a more holistic approach to numerically modelling the well.

4.1.3 Thermal Shock on Well Components and Barriers

Design of well tubulars is well documented throughout literature and the importance of thermal effects is also clearly recognised and design guidelines exist for well tubulars and other well components all acknowledging the importance of temperature and temperature cycling in the loads to be considered in the design, [18,19 and 20]. There does not appear to be much if any literature concerning the specific effects of thermal shock on a well bore as a whole. As per Section 4.1.1, the focus seems to have been on the bottom hole section. Based on the limited returns during the literature search from the key phase “thermal shock” there does not appear to be a consensus within the oil and gas industry over what that term means and therefore objective 2 remains to be satisfied within this project.

4.1.4 Thermal Shock due to Shut-in

Note that also within the objectives for this project is the need to examine the temperature changes caused by shutting in a well and what damage they may do to the barrier systems. Literature review has uncovered very little work specific to shutting in a well and any negative consequences that may have. API recommended practice identifies that in an HPHT context shut-in temperature effects may be relevant, [19], and identifies a survival load condition post shut-in when cooling of the tubulars at the top of the well may increase tension while shut-in pressures are still acting. This is the closest description to what BSEE outlined in its BAA found in regulatory related documents. This is also supported by work done by a joint industry project (JIP) for the Minerals Management Service in 2001, [16].

Otherwise, literature review has not uncovered any particular concerns over shut-in. In fact most of the papers reviewed did not identify shut-in as a design driver, at least for well tubulars, [13 is typical]. This supports one operators view that shut-in does not result in a thermal shock.

Other literature examines the temperature effects of shut-in on well bore and annular fluids but doesn’t describe a thermal shock.

It is clear from the design guidelines that are available that the cold shut-in condition may be important to certain barriers, tubing in particular, and merits further investigation.

4.2 Literature Review Of Computer Models Investigating Thermal Shock

The purpose of this subtask is to review the capabilities of the simulation tools proposed, identify any gaps and make recommendations on how to fill those gaps.

Research was done to explore the capabilities of commercially available software that is specifically used for the design and planning of oil and gas wells.

After reviewing various commercially available software packages it was identified that very few offer a combined capability that can accommodate the entire wellbore system throughout all phases of its life cycle. It was determined that of the software's reviewed WellCAT, [22], is best suited to handle the tasks involved in modelling the wellbore architecture relevant to this project. A potential gap identified was the modelling of the cement with regards to a stress analysis of the cement interaction with the casings. The only material properties used as inputs for cement are density, specific heat and conductivity. It assumes that axial loads in cemented casing sections result in no axial displacement. This assumption is reasonable for casing analysis, but the cement in the annulus needs to be analysed as part of the system to determine if there is any damage to the cement or potential for de-bonding/micro-annuli development in the cement.

Therefore a combination of WellCAT and ABAQUS, [23], were used to model the wellbores. This will allow for the use of the capabilities of WellCAT such as the load sequencing, thermal profile development for inputs in ABAQUS. The use of ABAQUS will allow for more detail modelling and analysis of the cement and failure of the cement. The modelling techniques used in ABAQUS in the FEA was an extension of the FEA performed in "Well Stimulation Effects on Annular Seal of Production Casing in OCS Oil and Gas Operations" (BSEE#728) and was validated by physical testing.

The literature review of this software included the following:

4.2.1 Drill Bench – Schlumberger

Drill Bench, [25], is software that is used for understanding the hydraulics during all phases of the drilling operations. Its core function is built around the well-control workflow, covering pressure control, well control and blowout control. The functions of this software would not be considered directly applicable to the type of modelling that is required for this project since it is not a tool typically used for the casing design of a well.

4.2.2 EDrilling - EDrilling AS

EDrilling, [25], has various modules of software available that are used for planning to deliver a "Life Cycle Drilling Simulation with advanced dynamic drilling models and diagnosis technology. It is similar to Drill Bench as it is primarily focused on the hydraulics during drilling and also production. The functions of this software would not be considered directly applicable to the type of modelling that is required for this project since it is not a tool typically used for the casing design of a well.

4.2.3 TubeFlowPIC – BTechSoft

TubeFlowPIC, [26], is software that is designed for wellbore intervention, drilling and completions. It has the capability to model complex well configurations with its database of standard pipe sizes for configuring well tubulars, capillary strings, coiled tubing and drill strings. It has the capability to calculate the transient temperature history of a well, but it currently does not have this information available as an output. The company is currently modifying the software to add this output, but it will not be available in time for use in this project. At this time the availability is not known.

4.2.4 WellCAT – Landmark Solutions

WellCAT, [22], is software that is intended to design and model the entire wellbore. It has the capability to handle most, if not all loading situations that a well might experience throughout its life cycle. This includes drilling loads, cementing loads, production loads and external loads applied to the well head such as loadings on the blowout preventer (BOP). It has the capability to analyse tubing/casing loads and movement, buckling behavior, design integrity and can simulate fluid flow and heat transfer to allow for full transient analysis. It also has the capability to model various tubing hangers, packers, connections.

WellCAT is widely used throughout the industry to design wells both onshore and offshore and is used in HPHT well design. WellCAT software is suited for the tasks of this project due to its vast capabilities and is used by many operators.

4.2.5 ABAQUS –Dassault Systemes

The general purpose FEA software ABAQUS, [23], will be used in combination with WellCAT to fill in any gaps. ABAQUS is well suited to the type of analysis required as it can accommodate advanced models for all the materials likely to be encountered from the steel casing to the cement and the formation. It has an extensive failure modelling capability which can include de-bonding, fracture and crack growth as well as cyclic plasticity.

4.2.6 Proprietary software developed by others

The literature review did uncover work done by others that is similar in principal of designing for thermal shock which is similar to the work required for this project. Total developed a coupled thermal and structural model of a SAGD well to improve the design of such wells, [5]. This software is the property of the operator and so will not be available to this project, but the principals guiding its development may be of use.

There are also other FE software tools that have been used by others investigating well structural behaviour, [27], but these don't offer anything above and beyond what ABAQUS can provide.

4.3 Literature Review Of Failure and Risk Assessments Of Thermal Shock

The search for literature concerning failure of well barriers uncovered limited published information concerning the failure of well barrier elements as a result of thermal shock. There is much literature concerning well barrier and well integrity failure in general. As recently as 2016, Wu et al, [118], performed a study that provides failure rates for well barriers, but does not attribute failure to a specific mechanism, though failure mechanisms are categorised. King et al, [14], also conducted a review of well and well barriers though concluded that the failure rate of oil and gas wells that result in a release of hydrocarbons to the environment as extremely low and while barrier failures occur with greater frequency, provided a multi-barrier philosophy had been adopted in the well design this rarely led to a loss of well integrity. This work also categorises the failures by barrier type, age of the well, its geographic location and its type. Tubular connections were found to be the dominant barrier failure type but modern connection designs have drastically reduced their prevalence. High Pressure/High Temperature wells were found to have a higher failure rate than their lower pressure and temperature counterparts.

There have been various studies surrounding the prevalence and management of sustained casing pressure (SCP). A 2001 JIP, [16] looked at best practice for the prevention and management of SCP and recognised the importance of temperature cycling and designing all pressure barriers for the correct temperature extremes. While there was no mention of thermal shock per se, the need to consider the cold shut-in condition, (when production fluids have cooled during an extended shut in), in the design of tubing and casing strings was recognised and provides the closest description yet found of the BSEE BAA posed definition of thermal shock, [1].

More recently, work has been performed to predict SCP build-up and gas influx rates as functions of time given a cement column of known permeability exists in the annulus, [17]. However, the assumption here is that even an intact undamaged cement column will allow gas migration through it. The gas influx rate being inversely proportional to the length of the cement column. This doesn't account for damaged cement or the presence of a micro-annulus between cement and casing nor the causes of the same.

US regulatory guidelines recognize the challenges of SCP and that all parts of the well should be designed with extreme temperature considerations per API, [21]; although thermal shock is never mentioned explicitly.

It would reasonable to conclude that thermal shock has not specifically been investigated in the context of SCP and that the current research work was not repeating previous work.

5 DETERMINE THERMAL SHOCK AND WELL LOAD HISTOGRAMS

The section outlines the approach used to develop the thermal loads and wellbore load histogram that were used to investigate the effects of thermal shock in OCS well bore integrity. Thermal shock refers to thermal changes generated during well construction or operation that contribute to stresses in various well barriers. The well and its barriers must withstand these stresses and remain a closed flow path for produced well fluids.

The process used for this task was to use the information gathered as part of the literature review and to develop the various following subtasks:

- Obtain wellbore schematics of a well that would be typical for a HPHT well in the OCS;
- It was intended that wells would be categorized to account for water depth, target depth and pressure and temperature ranges; shelf, deep-water and HPHT would seem a sensible split of likely well profiles and construction and analyzed. However, due to the complex nature of modelling the entire well a single well design with varying cement mixes was used.

These various subtask lead to the development of the well load histograms and well configurations that will be used in the more detailed modelling of wells subsequent tasks if required.

It is proposed that the occurrence of thermal shock may be defined as a magnitude of temperature delta over the time at which it changes. Therefore thermal shock may or may not occur depending on various conditions in the wellbore. The results of this task will be used to investigate the potential of thermal shock in Task 4. Depending on the results of Task 4, the definition of thermal shock may be modified as needed.

5.1 Objectives

The objective of this task was to develop and present the proposed well schematics and well loading histograms developed from information compiled earlier in the project. The results will be used for the modelling of various well configurations in subsequent tasks.

5.2 Obtain Wellbore Schematics for OCS Wells

Various searches for publicly known wellbore schematics of a HPHT OCS in the GOM were performed. This included online searches using the BSEE well data query as well as discussions with operators. Wellbore schematics are considered proprietary information and are not public knowledge, especially if the well is still under construction or still in the production phase. Information regarding various HPHT wells throughout the world is available, particularly in the North Sea. Using available information from various sources a “generic” well was developed. The casing/tubing, hangers, connections etc. will be comprised of commonly used sizes and material grades. This generic schematic will be considered a base case and may be modified as required based on the feedback from the industrial advisory group and BSEE and or if analysis findings warrant.

The focus for this project is OCS wells. In particular it was felt that the Lower Tertiary (LT) GOM would be a good starting point given the target depths in that play, (25000°F t to 35000°F t TVD range) would be deep enough to generate the bottom-hole temperature of 350°F to be compatible with the definition of thermal shock shown in Appendix B.

Figure 2 shows a well design similar to GOM wells. Since actual well schematics are proprietary and generally not available to the public, WWC presented the proposed configuration to the advisory group for feedback.

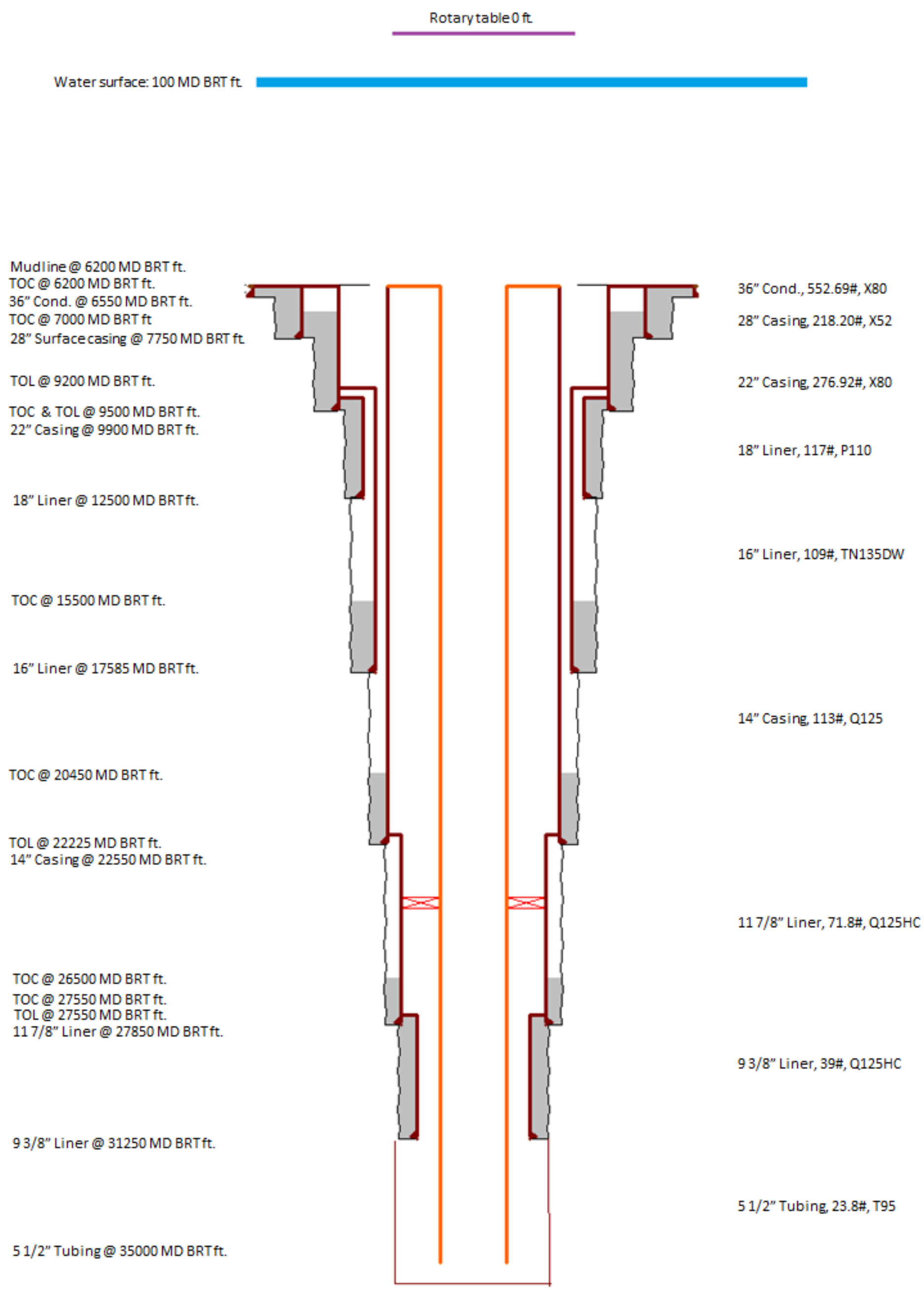

Figure 2 **Representative Wellbore Schematic**

5.3 Categorize OCS Wells

At least 3 categories of wells were originally envisaged to account for water depth, target depth and pressure and temperature ranges to provide a sensible split of likely well profiles and construction; for example shelf, deep-water and HPHT. However, the project team considered it more appropriate to start with the generic wellbore as defined previously and obtain feedback from the advisory group to categorize as necessary and to allow for sensitivity studies to analyze the effects various well depths, casing programs, etc., have on the response to thermal shock. After initial results it was determined that it is more beneficial to the project objectives to focus on varying the cement mixes and stimulation rates.

The use of a generic wellbore still provides the ability to achieve the project objective but allows a more efficient analysis approach in the FEA.

5.4 Develop Temperature Profiles and Load History for Wells

Primary outputs from this subtask are appropriate load histograms and a clear definition of thermal shock. This sub-task made use of the range of tools available. Since developing a single computer model of the well and all barriers is not feasible due to the length scales involved in the well; and the potential need to resolve the temperature and pressure fields and subsequently the stress field in 3D. Therefore a combination of models and tools was used. For this study the commercially available well design software. Any gaps found in the software with regards to thermal shock of a well is addressed by the use of the general purpose FEA software ABAQUS.

The drilling and completions phase of a well is a small part of the life a well when compared to the production phase. Also in the production phase the fluid flows through the well at different temperatures, pressures and viscosity than that is used for drilling/completions. However, to fully understand the effects thermal shocking may have on the well, this phase must be considered. The load history has been simplified to assume that there were minimal issues during this phase. Table 1 shows a representation of the load sequencing histogram for the drilling and completion phase of the well. This histogram was considered as the base load history for the wells and was modified as required based on feedback from the industrial advisory group and BSEE regarding the proposed well schematic. However, based on modelling limitations the drilling and completion phase did not include the actual temperature changes from circulation during cementing.

Table 1Well load histogram for drilling and completion phase of well life cycle

Operation	Time Duration (Scale)	Comments
1. Drill Surface Casing Hole	Days	
2. Log Surface Casing Hole	Hours	
3. Condition Surface Casing Hole	Hours	
4. Run Surface Casing	Hours	
5. Cement Surface Casing	Hours	
6. Drill Intermediate Casing Hole	Days	Thermal shock of surface casing ^
7. Log Intermediate Casing Hole	Hours	
8. Condition Intermediate Casing Hole	Hours	
9. Run Intermediate Casing	Hours	
10. Cement Intermediate Casing	Hours	
11. Drill Production Casing Hole	Days	Thermal shock of intermediate casing
12. Log Production Casing Hole	Hours	
13. Condition Production Casing Hole	Hours	
14. Run Production Casing	Hours	
15. Cement Production Casing	Hours	
16. Drill Production Liner Hole	Days	Thermal shock of production casing
17. Log Production Liner Hole	Hours	
18. Condition Production Liner Hole	Hours	
19. Run Production Liner	Hours	
20. Cement Production Liner	Hours	
21. Clean-up Production Liner for Tie-back	Hours	
22. Run and Set Production Tie-back	Days	

^ depends on shoe depth

The majority of the well life is in the production phase which may be anywhere from 10-20 years for a deep-water well. For this investigation at life cycle of 20 years has been assumed for the development of the loading histogram. The main purpose of this histogram is capturing a set and sequence of likely loads a well will be subjected to during its lifespan, such as shut-ins, well stimulations, etc. The load history was based on experience for wells in the GOM region. It includes mandatory shut-ins when testing safety equipment, storms and planned stimulations/reservoir management. The base load histogram for the production phase is shown in Table 2. This load history was considered a base case to study the entire production life of the well. Other comparative cases were performed as well.

Table 2 Well load histogram for 20 year production phase of well life cycle

Operation	Events per year	Duration (Scale)	Comments
Shut in to test actuated master valve	12	Hours-Days	Potential for thermal shock during any shut-in
Shut in to test subsurface safety valve	2	Hours-Days	
Shut in due to weather induced events	3	Days	
Shut in due to production/equipment problems	4	Hours-Days	
Shut in for reservoir management	1 / 1.5 years	Days	
Stimulation	1 / 4 years	Days	Thermal shock
Potential number of shut ins over a 20 year life cycle			438

Additional casing loads from BOP's, over-pull, etc. is accounted for well configurations. It is anticipated that these loads will have a small contribution to overall loading when compared to the thermal loads.

5.5 WellCAT Analysis

The commercial software tool WellCAT was used to develop the global thermal profiles for the well. The loading histogram previously mentioned was used as input for both the drilling and production phases. Temperature profiles for the well were generated for the various construction and production operations. A temperature vs time history profile is generated for the entire depth of the wellbore for the various strings. The temperature profiles and preload conditions will be applied to a global and local FEA model in The FEA. A various range of temperature conditions will be assessed. Initial temperature profiles are based on ambient air temperature of 80 deg. Fahrenheit, mudline temperature of 40 deg. Fahrenheit and bottom hole static temperature of 350 deg. Fahrenheit.

Figure 3 shows the representative temperature versus depth profile of the wellbore at various points in time during the drilling and completion phase for the production casing string. Profiles for the annulus, conductor, surface casing, etc. are generated and used for input as well. The resulting profiles for the wellbore temperatures are used as inputs into the FEA models in the FEA.

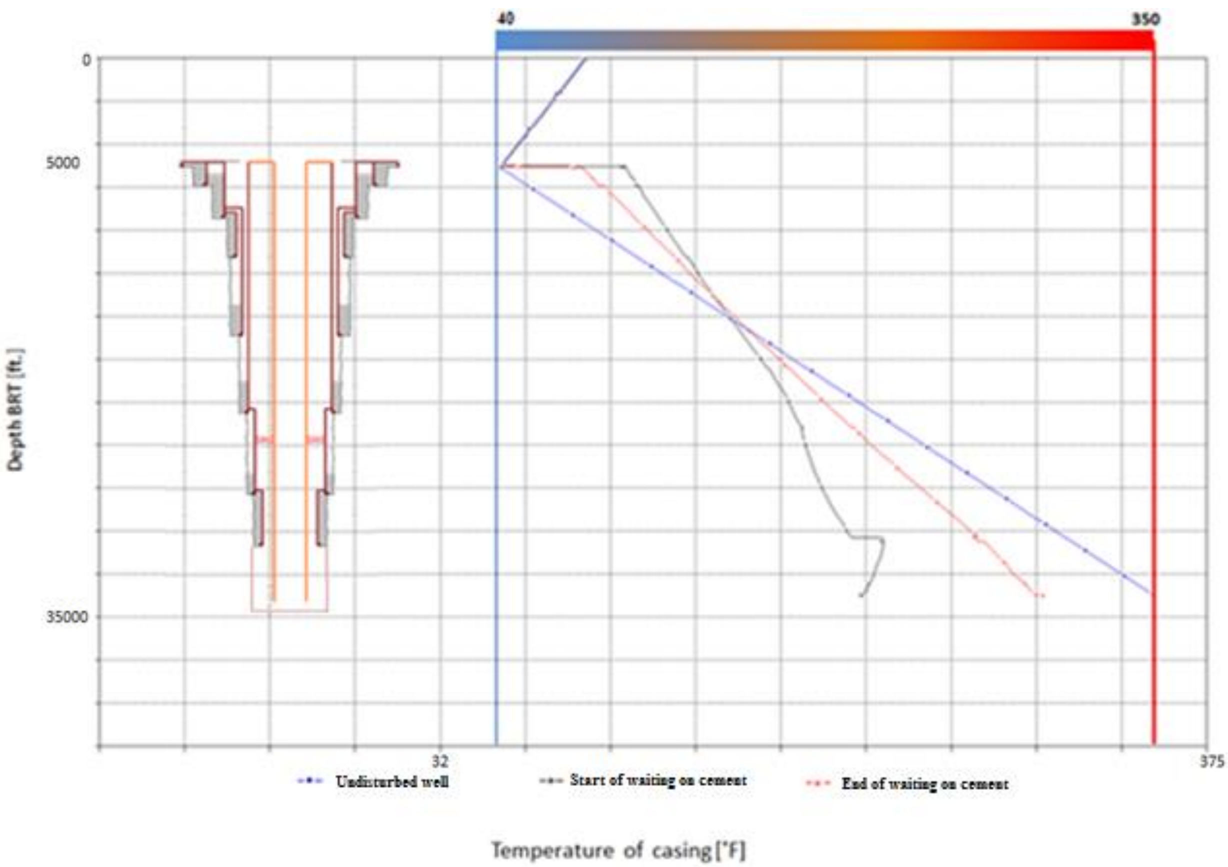

Figure 3 **Temperature profile for well during final cementing phase of drilling**

Figure 4 shows the representative temperature versus depth profile of the wellbore at various points in time duration the production phase for the production casing string. Profiles for the annulus, conductor, surface casing, etc. were generated as well. The resulting profiles for the wellbore temperatures were used as inputs into the FEA models in the FEA.

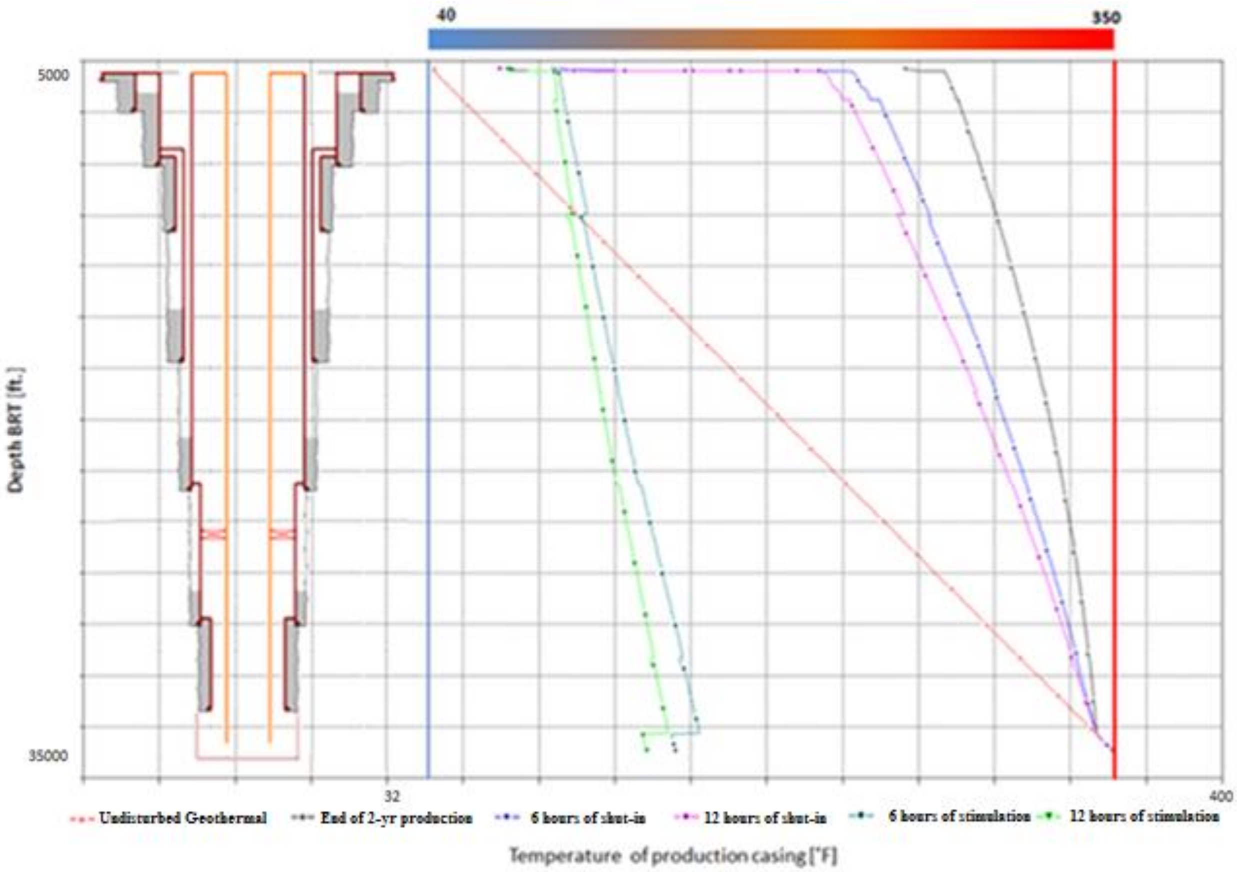

Figure 4 **Temperature profile for well for various operations during production phase**

Figure 5 shows the representative temperature versus depth profile of the formation near the wellbore at various points in time during the production phase. The resulting profiles for the wellbore temperatures were used as inputs into the FEA models in The FEA to set initial geostatic conditions and use as validation of the resulting temperature distribution in the formation in the FEA model.

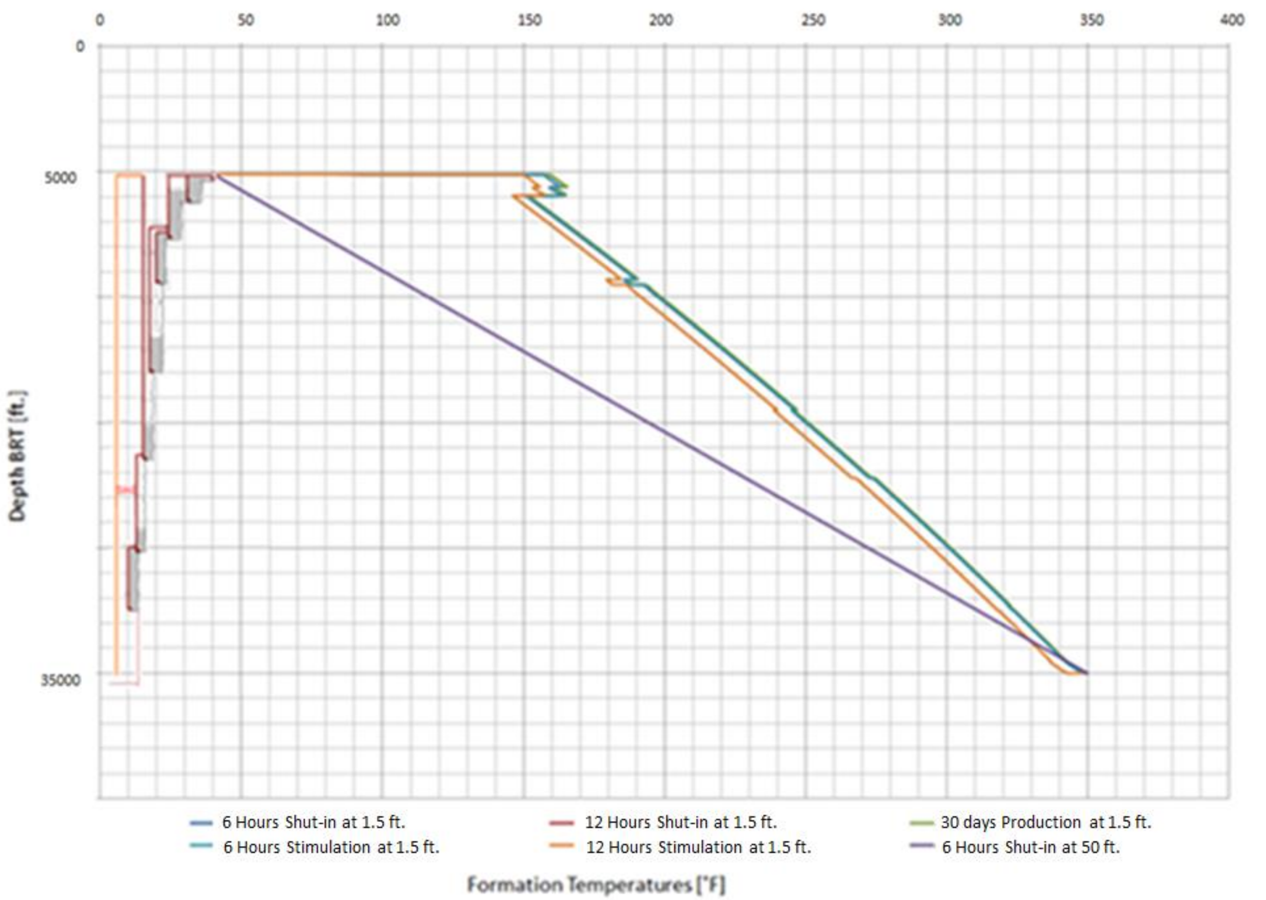

Figure 5 **Temperature profile in formation near wellbore**

5.6 ABAQUS FEA

ABAQUS FEA was used to develop further the thermal profile and load histogram of the well and its constituents. The intent of this subtask was to develop efficient methods for building a global FEA model that the loading history and conditions is applied.

A global axisymmetric finite element model of the entire wellbore was selected as this best modelled the global wellbore system while maintaining computational efficiency. This model could simultaneously account for thermal and mechanical loads imposed on the well.

The formation surrounding the wellbore was explicitly accounted for in the axisymmetric model. The formation is modelled as a homogenous solid which is vary in layers vertically along the wellbore to allow for varying the elasticity of the formation. .

5.7 Task Findings

Potentially there are various thermal loadings and well configurations that could cause a thermal shock scenario for OCS wells that could result in a loss of one or more well barriers. However, based on the temperature profiles; stimulating operations particularly when injecting with a fluid that is substantially cooler than the temperature of the producing wellbore, seem to pose the highest risk to damaging components of the well. It was observed that stimulation operations generate a larger temperature gradient from the production temperatures when compared to the gradients caused by the production phase followed by shut-in conditions at the same time points.

5.7.1 Thermal Shock Definition

At the outset of the project the definition of thermal shock was developed from the statements in the BSEE BAA, [1] as:

- Wells with a bottom hole temperature of 350°F or above combined with a minimum ambient temperature as low as 40°F.
- Thermal shock could be initiated by shutting in a producing well and allowing it to cool to ambient or by stimulating a well.
- Thermal shock not only depends on the temperature range but also the rate at which temperature changes. The rate of cooling of the well would depend on the operations considered, e.g. natural cooling post shut-in or cooling during well stimulation for example.

It is proposed that thermal shock may be defined as a magnitude of temperature change over the time at which it changes. Therefore thermal shock may or may not occur depending on various conditions in the wellbore. The results of this task were used to investigate the damage potential of various thermal shocks in the FEA.

6 WELL AND BARRIER RESPONSE

6.1 Summary

The FEA modelling performed revealed some significant findings, namely:

- That a shut-in of a producing Deepwater HPHT well does represent a thermal shock that can damage cement, particularly in the upper part of the well, however a large accumulation of production/shut-in cycles is required to significantly damage the barrier.
- The HPHT well investigated was able to maintain zonal isolation for a complete production life of 20 years, assuming a good cement job had been completed in the first instance.
- Stimulating a well does significantly more damage to the cement than a normal production/shut-in cycle and that damage can extend a significant distance up the well bore. It therefore represents a greater risk to the well barrier.
- Because the FE model encompasses the entire wellbore, damage locations can be readily identified in one well model. To WWC's knowledge this is the first time this has been achieved for a deep water well.
- The modelling indicates that production/shut-in damage is restricted to the upper cement annuli whereas stimulation damages the deeper cement barriers because the temperature changes are greatest in each case at the top and bottom of the well respectively.
- The cement designs and quality of placement of cement in the wellbore during completions is critical to the performance of the well. Although one cement mix design is not always adequate for all situations and environments it was found that in general more brittle cements are less durable and failure will occur at fewer cycles. This is true for all wells but is more pronounced in the HPHT variety. A high compressive or tensile strength does not always indicate the ability to withstand a greater number of load cycles; rather a balance of high compressive strength or tensile strengths coupled with a lower elastic modulus seemed to perform the best.

6.2 FEA Global Response Modelling And Tie In Known FEA Model Data

A finite element model of the full measured depth (MD) of the well bore has been constructed, see Figure 6. This takes into account all tubular strings from conductor to production tubing along with both liquid and cement filled annuli through the full depth of the well.

The Explicit FEA solver was used in the scale modelling performed in the previous BSEE work "Well Stimulation Effects on Annular Seal of Production Casing in OCS Oil and Gas Operations" (BSEE#728) as it is better suited to handle the extreme non-linearity behavior of cement. However when modelling the entire wellbore geometry there are considerations regarding the selection of the FEA solver used due to the computational requirements of the large model involved. To reduce the computational expense required of modelling an entire well an axi-symmetric model was used and was therefore only able to model vertical well configurations. In addition, the Explicit solver was not compatible with axi-symmetric models and thus the Standard Implicit FEA solver within ABAQUS was used. Material models used in Task 4 and 5 were selected to allow for interoperability between the Standard and Explicit solvers. Due to the complexity and convergence issues that were encountered during the project a single geometry wellbore was investigated instead of multiple configurations to achieve the objectives of the project.

Various cement designs based on mixes in use today in various OCS cementing operations for surface, intermediate, and production depths were utilized in the analysis to study the effects of cement these designs on the response of the wellbore when exposed to thermal events.

Large departure well effects were studied using local FEA model to compare a deviated versus non-deviated section of a well and are discussed in Section 6.3.

The model also included an appropriate representation of the formation, with stiffness varying as appropriate with depth.

The material strength properties defined for laboratory scale testing were used; to help with convergence issues and model stability the individual components were assembled using "hard contact" or tie constraints. De-bonding and micro-annulus cracking are therefore investigated using the individual damage intensities in tension or compression respectively as well as the cracking strains.

The run in and cementing sequence for each tubular is accounted for by performing a series of analysis steps that form the open hole and progressively activates elements representing the tubulars according to the well construction sequence. The cementing process is reflected during the well construction steps in a similar fashion.

Cement is added to the annulus to ensure the string buoyant weight is correct and then either tie constraints or hard contact between the cement and tubulars is activated after the cement placement has occurred.

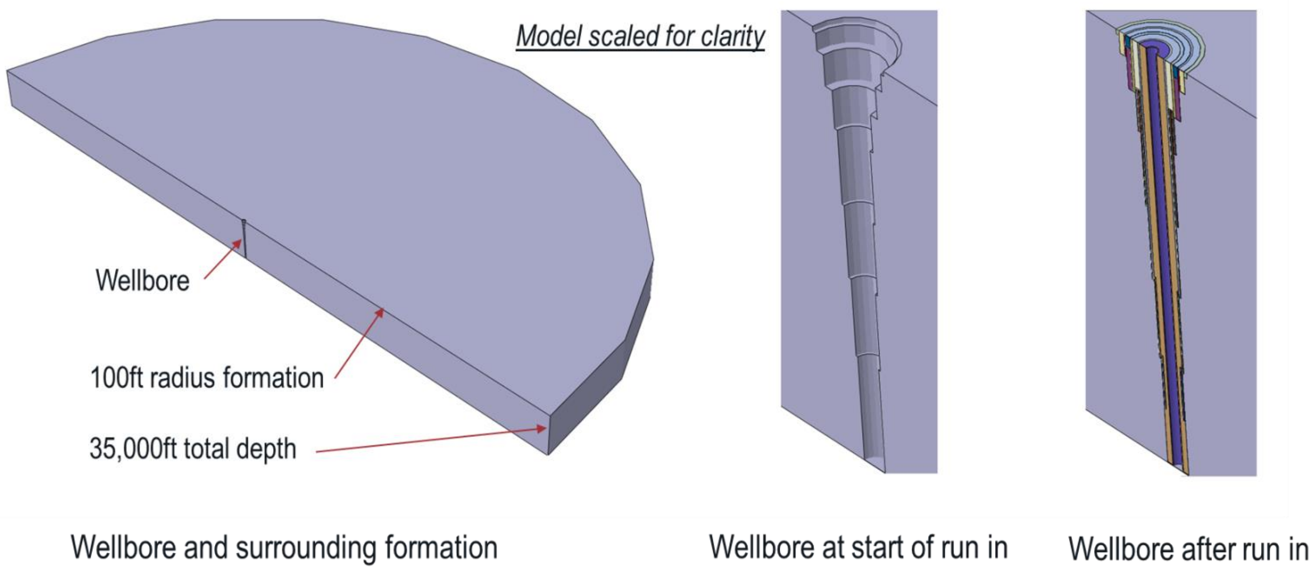

Figure 6 **Global FE model**

The analysis included a 20 step process to simulate the well construction phase as follows:

- Step 1 – Geostatic equilibrium of formation
- Step 2 – Remove open hole material
- Step 3 - Run-in conductor
- Step 4 – Cement conductor
- Step 5 – Run-in casing 1
- Step 6 – Cement casing 1
- Step 7 – Run-in casing 2
- Step 8 – Cement casing 2
- Step 9 – Run-in casing 3 / liner
- Step 10 – Cement casing 3
- Step 11 – Run-in casing 4 / liner
- Step 12 – Cement casing 4
- Step 13 – Run-in casing 5

- Step 14 – Cement casing 5
- Step 15 – Run-in casing 6 / liner
- Step 16 – Cement casing 6/liner
- Step 17 – Run-in casing 7
- Step 18 – Cement casing 7
- Step 19 – Run-in production tubing
- Step 20 – Lock production tubing at packer.

Intermediate steps were also included during the cementing process not shown in the above list.

The well was modelled as an uncoupled heat transfer problem. The temperature field is calculated without consideration of the stress/deformation of constituent parts of the well, which is reasonable in the context of an oil well as the deformation of the steel tubulars does not alter the heat transfer characteristics of the well.

The FE model also accounted for thermal convection as well as conduction for any fluid filled cavities such as annuli. The effects of fluid convection could not be captured explicitly by the FE solid model. However, the effective conductivity of the fluid regions was been modified to account for this. See later discussion under validation, Section 6.2.2.

Once the well run- in sequence was complete the well was brought onto production and the well warmed up to its steady state production temperature. Thermal shock load cases were then carried out.

6.2.1 Thermal Shock Load Cases:

The entire well structure was initialised with the geostatic temperature profile, in this case assuming a mudline temperature of 40˚F and bottom-hole temperature of 350˚F, see Figure 7.

- Production – bottom hole temperature = 350˚F, well flow rate set as 20,000 bpd. Solved until steady state delivery temperature was reached, see Figure 8.
- Shut-in – well flow was halted and the well allowed to cool to ambient, Figure 9 and Figure 10 show profile at 5 days and 60 days respectively
- Stimulation – post shut-in well flow direction was reversed and surface ambient fluid injected – rates 20,000 bpd for 48 hours and 60,000 bpd for 24 hours – cooldown of the hot end of the well, Figure 13 show contours after 48 hours injection at 20,000 bpd, 60,000 bpd is similar.

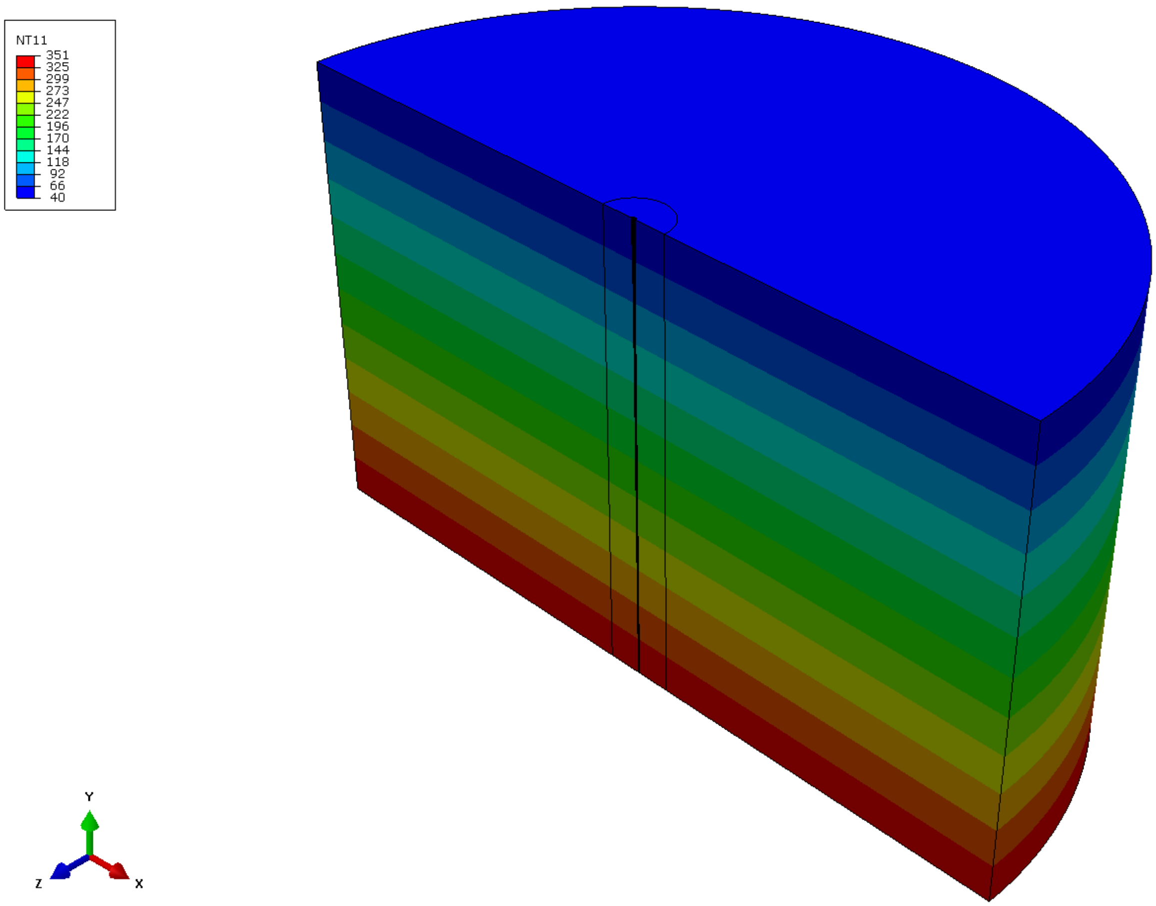

Figure 7 **Global FE model – Initial temperature profile**

Note this view has the x and z coordinates magnified x100 for clarity.

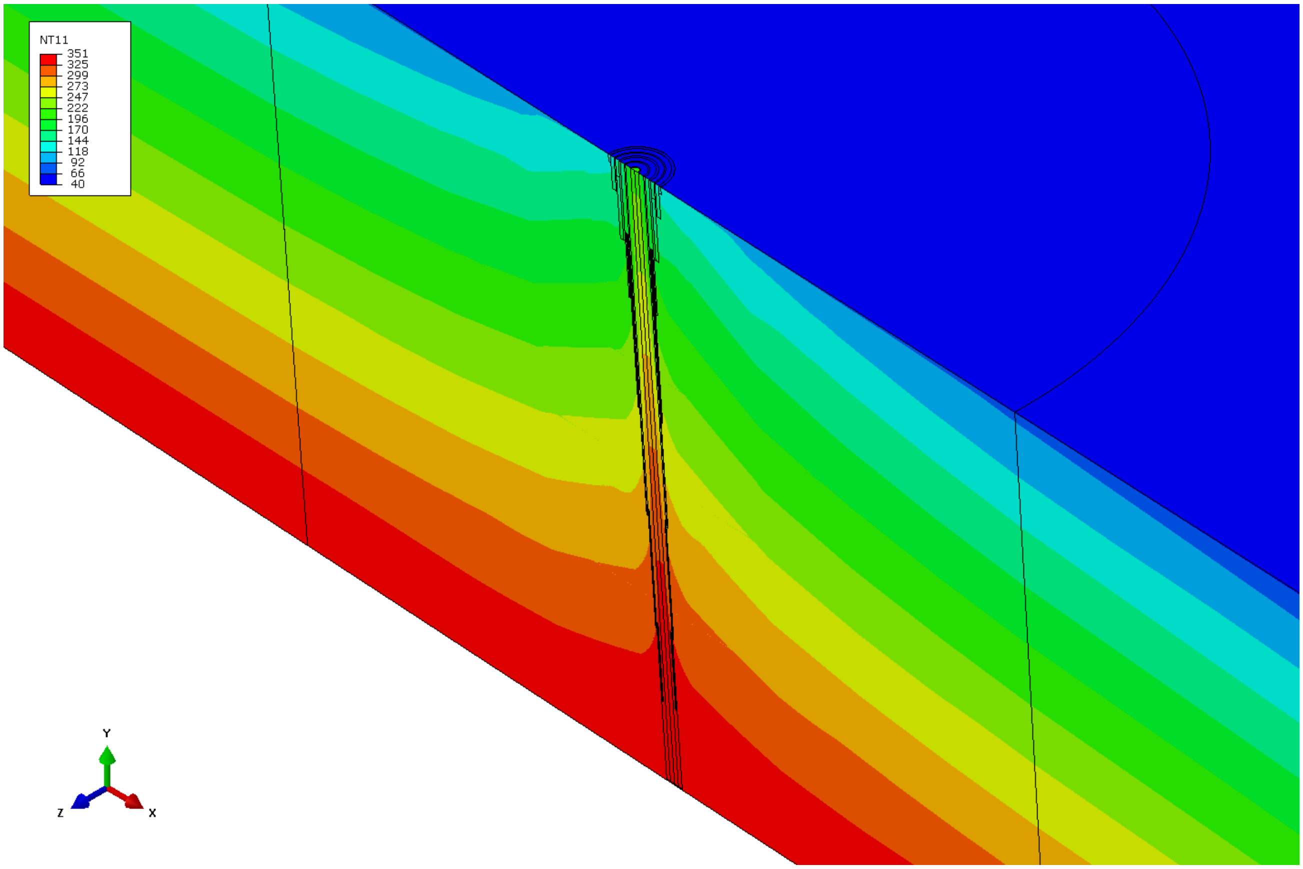

Figure 8 **Global FE model – Production temperature profile 20kbpd**

Note this view has the x and z coordinates magnified x1000 for clarity.

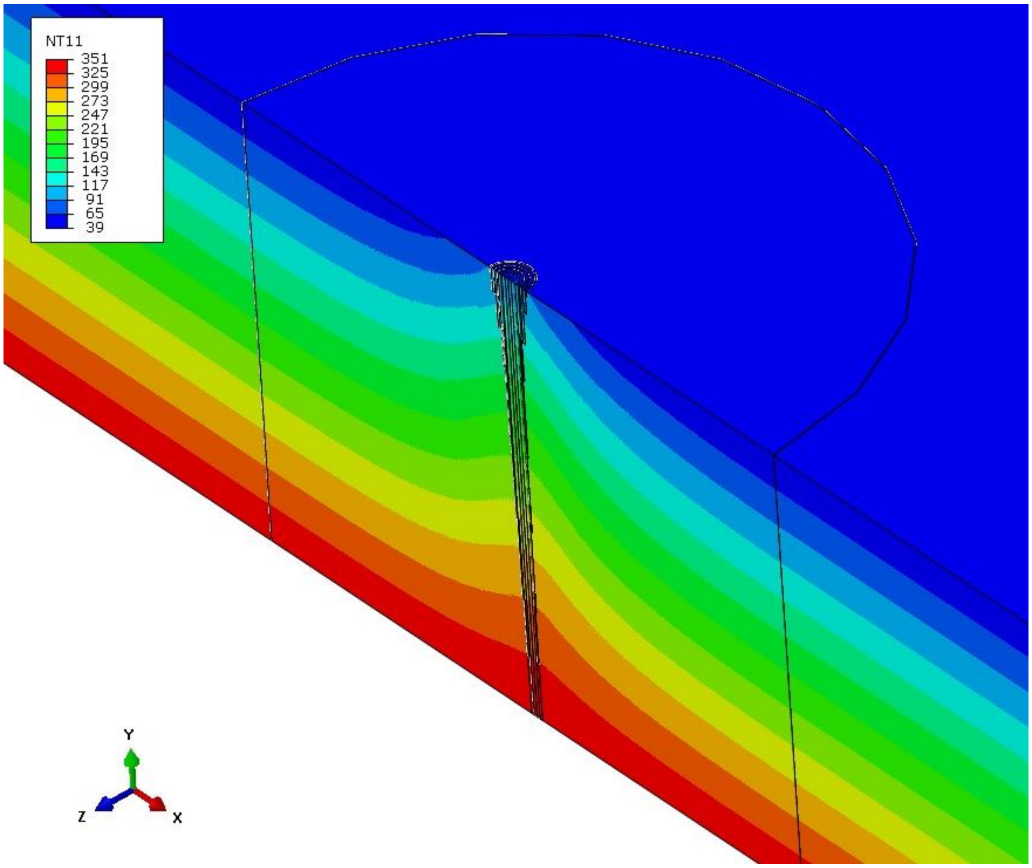

Figure 9 **Global FE model – Shut in temperature profile at approximately 5 days**

Note this view has the x and z coordinates magnified x1000 for clarity.

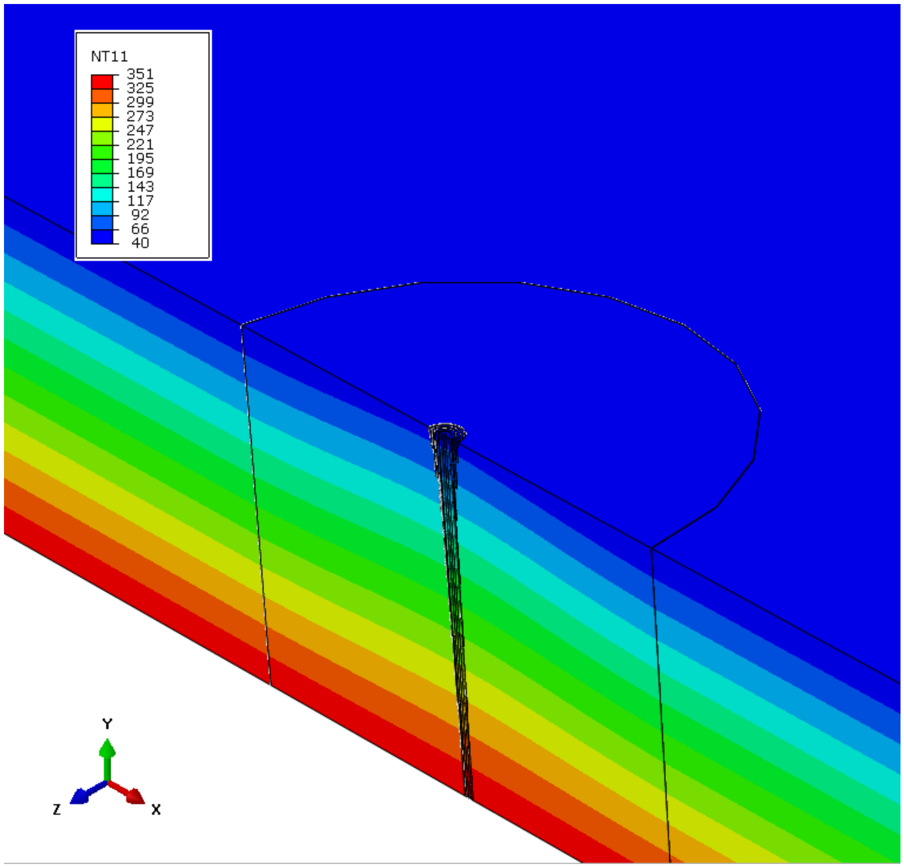

Figure 10 **Global FE model – Shut in temperature profile at approximately 60 days**

Note this view has the x and z coordinates magnified x1000 for clarity.

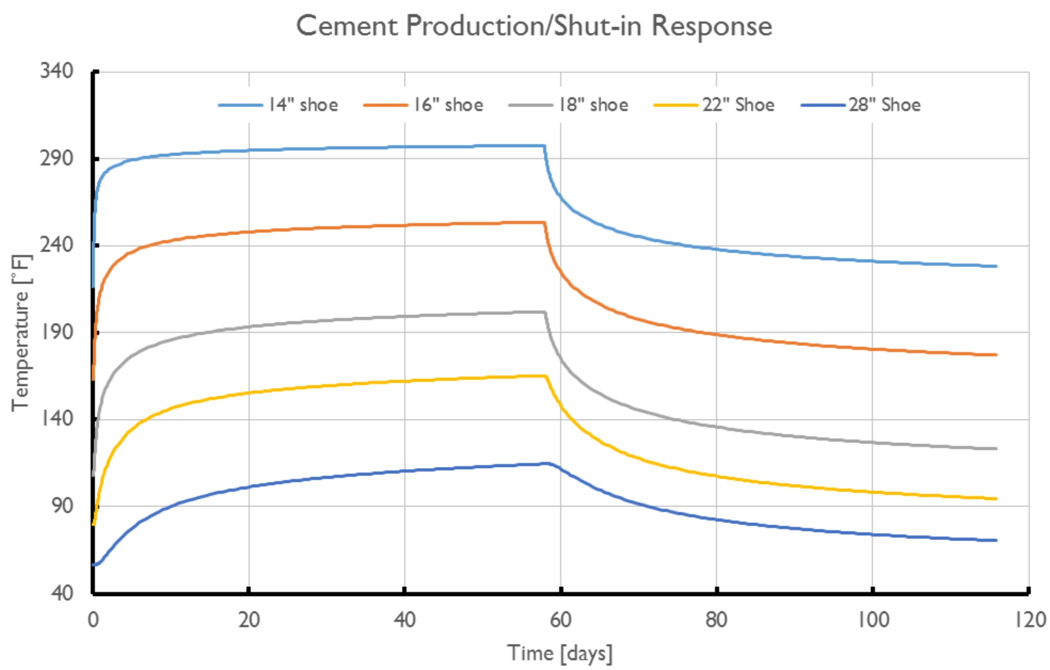

Figure 11 **Global FE model – Well production/shut-in temperature response for 10kbpd**

Figure 11 shows typical temperature histories at different casing shoe depths throughout the well during a production/shut-in cycle. Despite the low ambient temperature at the top of the well the higher temperatures at the base of the well, the maximum temperature range occurs some distance down the well, in this case at the 18” casing shoe.

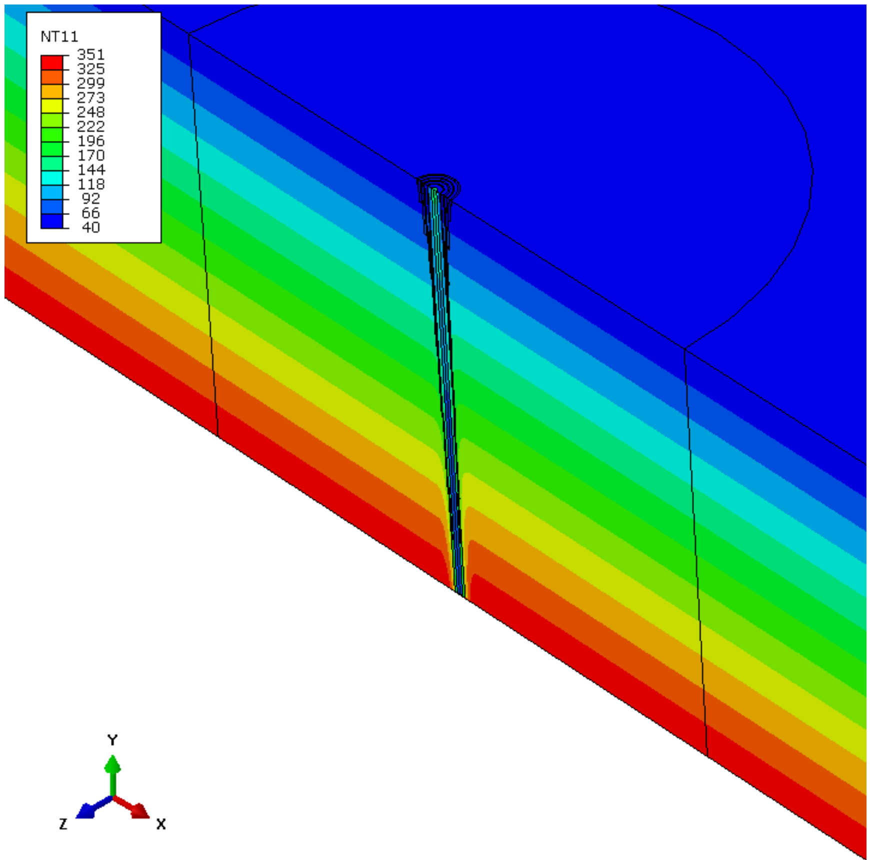

Figure 12 **Global FE model – Well stimulation temperature profile**

Note this view has the x and z coordinates magnified x100 for clarity

6.2.2 FEA v CFD modelling – convective heat transfer verification

The mechanical stresses introduced as a result of temperature effects are dependent upon both the temporal and spatial temperature gradients in addition to temperature magnitudes. Therefore it was considered critical to the objectives of this project that temperature effects were accounted for as accurately as possible.

Finite element models typically can only model conductive heat transfer. Convection within a fluid cannot be simulated directly using solid based finite element models. A fluid's ability to transfer heat may be dominated by convection (fluid movement) if heated from below or from the side. To overcome this, the effective thermal conductivity, k_{eff}, can be adjusted so that the solid transmits thermal energy at the same rate its fluid counterpart. However, the k_{eff} value changes with temperature gradient and hence time, so a single effective conductivity value could not be used here.

To determine appropriate k_{eff} values for both the production tubing and any liquid filled annuli a series of simulations were performed using computational fluid dynamics (CFD) to determine the correct thermal response. A finite element analysis was them compared against the CFD to confirm the correct k_{eff} had been determined.

An example is shown in Figure 13. Here a test model, comprising a 30m section of production tubing was filled with flowing water. Flow and temperature was solved to achieve a delivery temperature using both an FE model and a CFD model. The k value within the FE model was varied. The flow is then stopped and the model is allowed to cool.

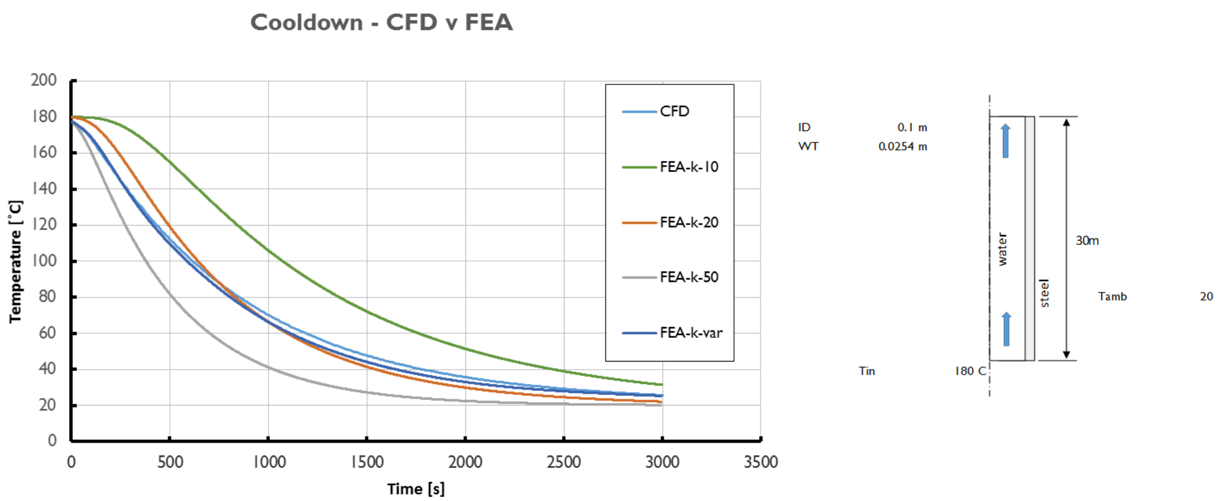

Figure 13 **Local FE model – cooldown response**

It is clear from the cooldown response that the k value chosen made a significant difference. It was also apparent that a single value of k in the FE model fails to match the cooldown response of the CFD model.

However, when the same test was repeated with a variable k value, a good match was achieved. See Figure 14.

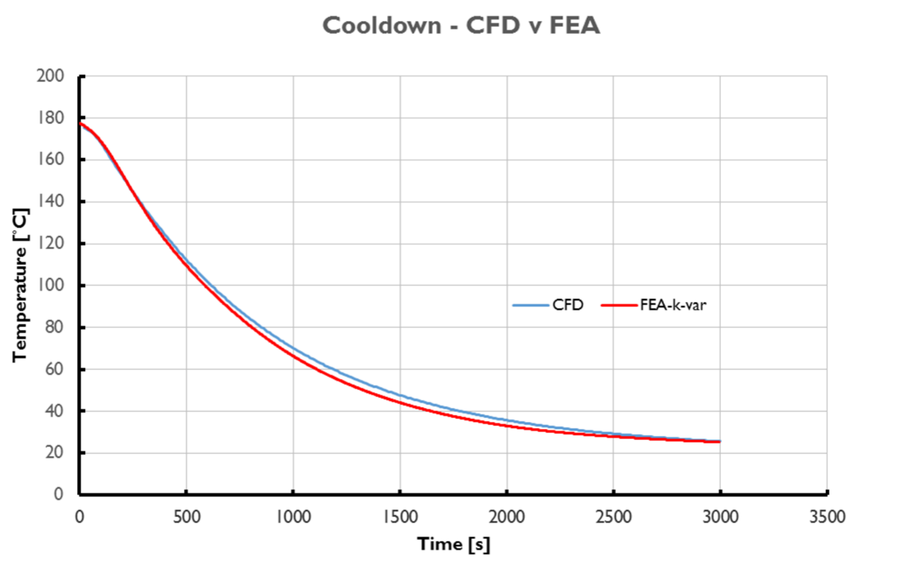

Figure 14 **Local FE model – cooldown response matching**

A series of larger CFD models of different sections of the wellbore were developed to determine k_{eff} for different elevations and wellbore cross-sections. An example is shown in Figure 15. The fluid with the main bore and the annuli is being cooled following a shut-in. The velocity vectors within the main bore and the two adjacent annuli are shown. As can be seen the vectors within the annuli travel upwards near a warmer wall at smaller radius and downwards near the cooler wall at bigger radius due to density variations (i.e. natural convection).

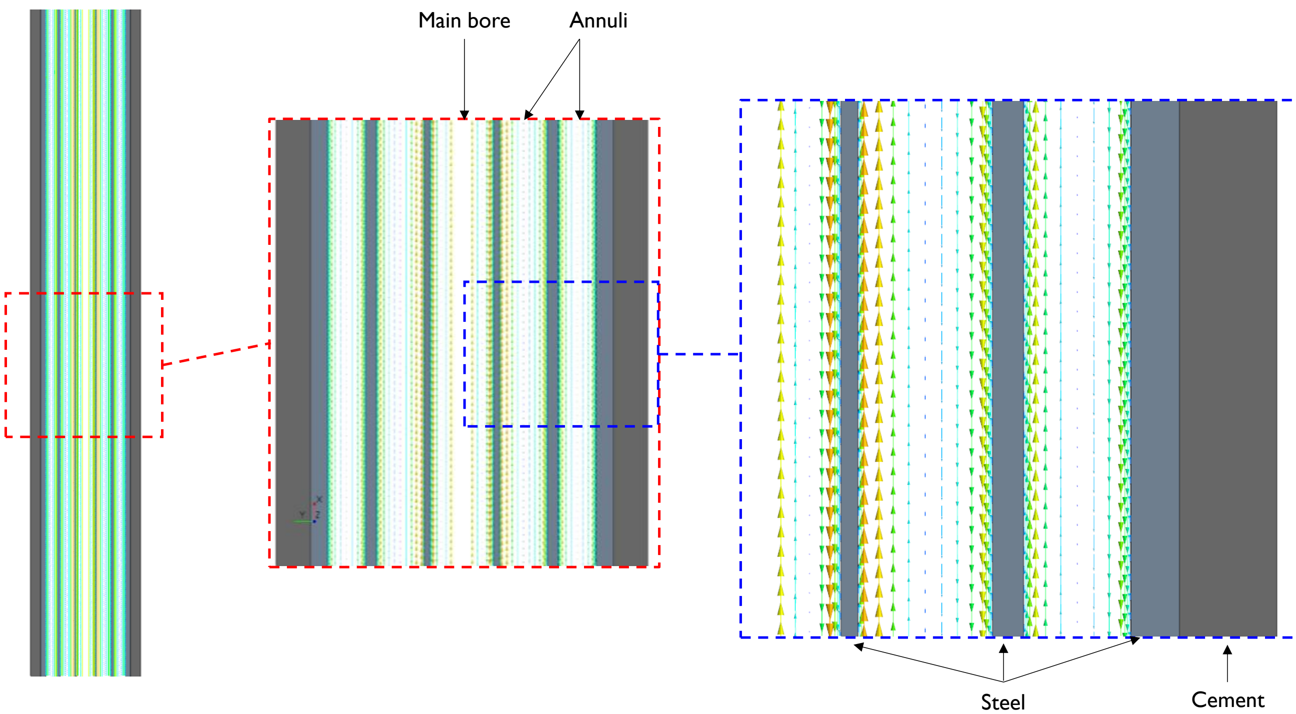

Figure 15 **Local CFD model – thermal response matching – velocity vectors in multiple annuli**

The thermal response model was checked against WellCAT with good agreement.

6.2.3 Global Model Mesh Sensitivity Check

To ensure that the finite element mesh used in the global well models was suitably refined, local highly refined mesh models were used to compare to the thermal response of the coarser global model. See Figure 16. In this case the local model represented a 2D horizontal slice at 1000°F t below mudline.

The 2D local and global models were in very good agreement.

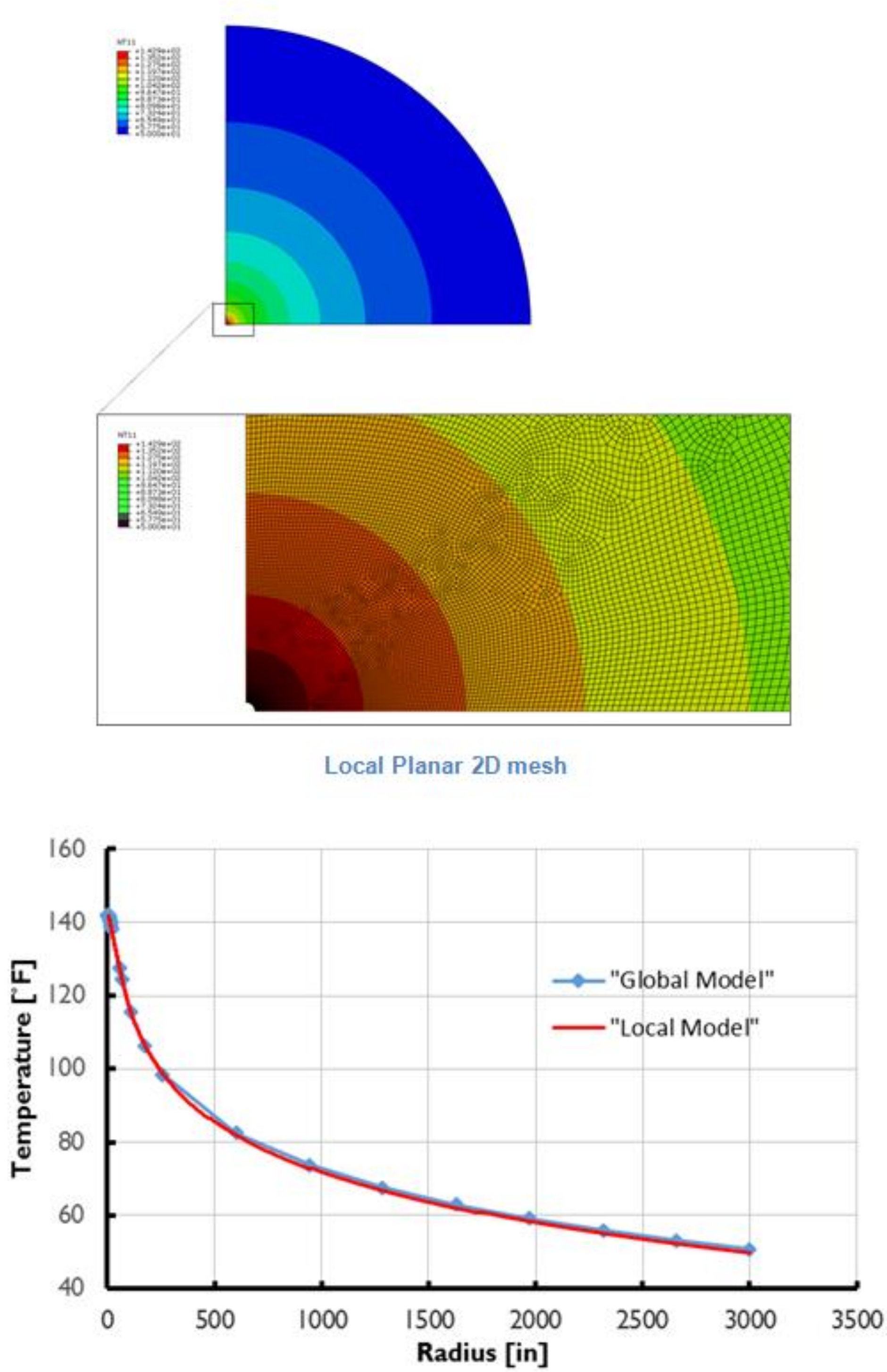

Figure 16 **Mesh refinement checks – Global v Local FEA model**

6.2.4 Thermal Shock Response and tie in known FEA model data

The ABAQUS FE model that solves the thermal and structural response used a similar finite element mesh, simply swapping heat transfer elements for their structural equivalent. The temperature field from the thermal analysis was mapped onto the structural model and the structural response solved. A nominal annular pressure ranging from 25-250 psi due to the thermal expansion of the annular fluids was applied. It was assumed that the annular pressure was monitored and managed per API requirements.

The global model also includes damage models for the cement to identify when and where cement damage occurs. These damage models are validated against experiments – see Task 5.

The cement damage can cause solution stability issues in the global response model that can been difficult to predict. As a result some of the cement materials defined in Task 5 was found to have convergence difficulties in the global model. However, some of the cement properties previously known and validated were used to analyse the well's response with various cement mixes.

Table 3 Cements use in global well

ID		Young's Modulus [psi]	Poisson's Ratio	Strength	
				Comp. [psi]	Tensile [psi]
HDV09675-5-2c	"2c"	2.20E6	0.26	6310	706
Previously defined in prior BSEE project E14PC00037	"A"	4.80E5	0.31	324	58
Previously defined in prior BSEE project E14PC00037	"B"	1.93E6	0.23	3207	387

To evaluate the response and performance of the well over its lifespan the loading histogram as defined in Table 2. The cement used in this load case was the 2c design as shown in Table 3.

In addition to the twenty year life cycle case, a case to perform a comparative analysis to check the well's response to different stimulation rates and cement mixes was completed. In this scenario the well was cycled 4 times with each complete cycle consisting of production, shut-in and stimulation. Due to long analysis times no intermediate production/shut-in cycles were included, however these cases provide valuable information. Table 4 shows the load cases analysed.

Table 4 Well load cases investigated

Case	Cement	Injection Rate	Comments
Full 20yr life cycle	"2c"	20,000 bpd	
Cycle-4x-20-6310	"2c"	20,000 bpd	No intermediate prod/shut-in
Cycle-4x-60-6310	"2c"	60,000 bpd	No intermediate prod/shut-in
Cycle-4x-20-3207	"B"	20,000 bpd	No intermediate prod/shut-in
Cycle-4x-60-3207	"B"	60,000 bpd	No intermediate prod/shut-in
Cycle-4x-20-324	"A"	20,000 bpd	No intermediate prod/shut-in

6.2.4.1 Thermal shock response results

The results of the twenty year life cycle case indicate some damage in the lower portions of the cement in the well. However, the damage does not propagate the entire height of the cement column. It is also observed that the magnitude of damage from stimulating the well is much greater than a typical production and shut-in cycle and occurs at the lower end of the well.

The damage in the cement from after the first year of production/shut-in cycles is shown in Figure 17; and after four years of production/shut-in cycles (prior to the first stimulation occurrence) is shown in Figure 18.

The damage to the element (SDEG) shown is not an indicator that loss of isolation has occurred, a more complete explanation of SDEG is given in Figure 27.

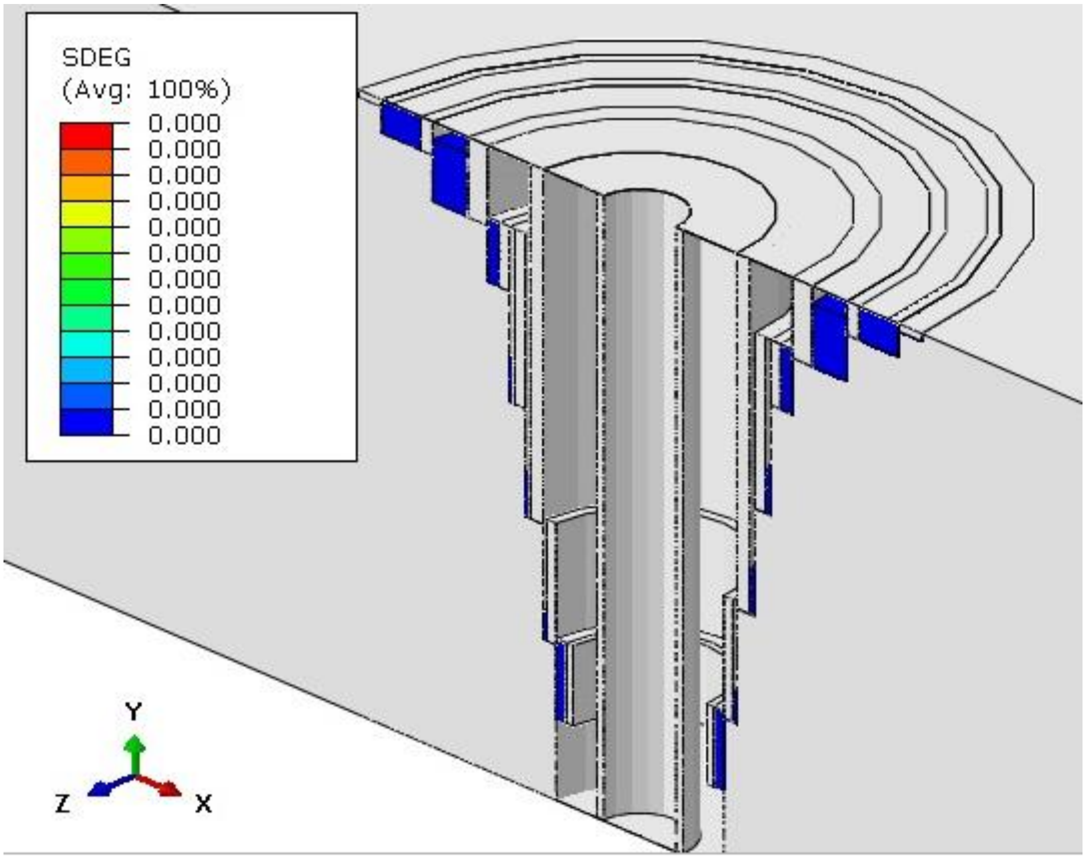

Figure 17 **Cement damage after first year of cycles**

Note this view has the x and z coordinates magnified for clarity.

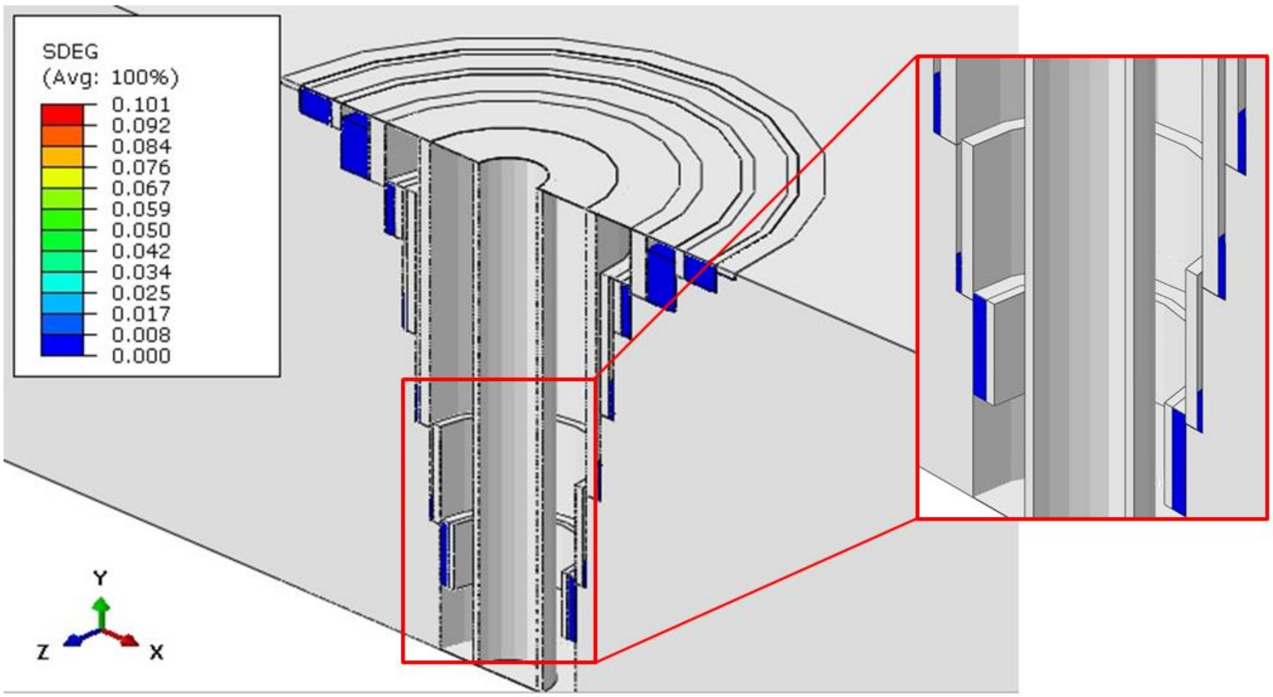

Figure 18 **Cement damage after first four years of cycles**

Note this view has the x and z coordinates magnified for clarity.

The damage in the cement immediately after the first stimulation and warm-up occurrence is shown in Figure 19.

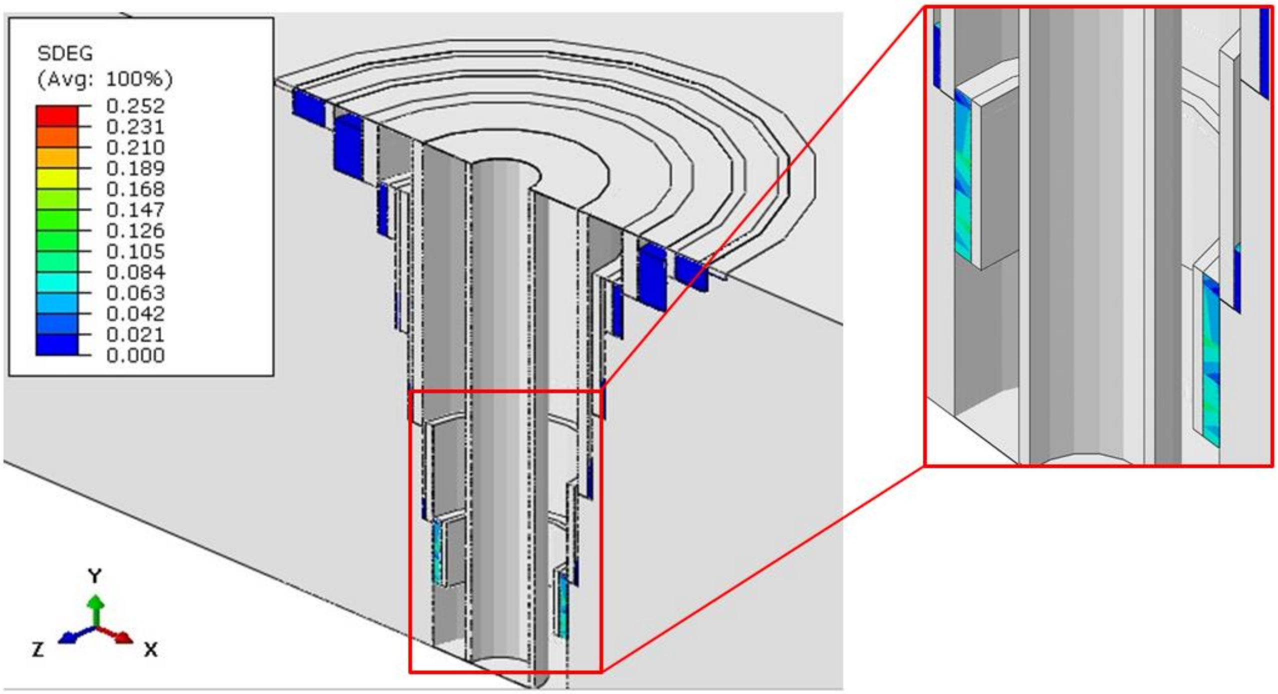

Figure 19 **Cement damage after first stimulation occurrence**

Note this view has the x and z coordinates magnified for clarity.

The damage in the cement after four more years (8 total) of production/shut-in cycles (prior to the second stimulation occurrence) is shown in Figure 20.

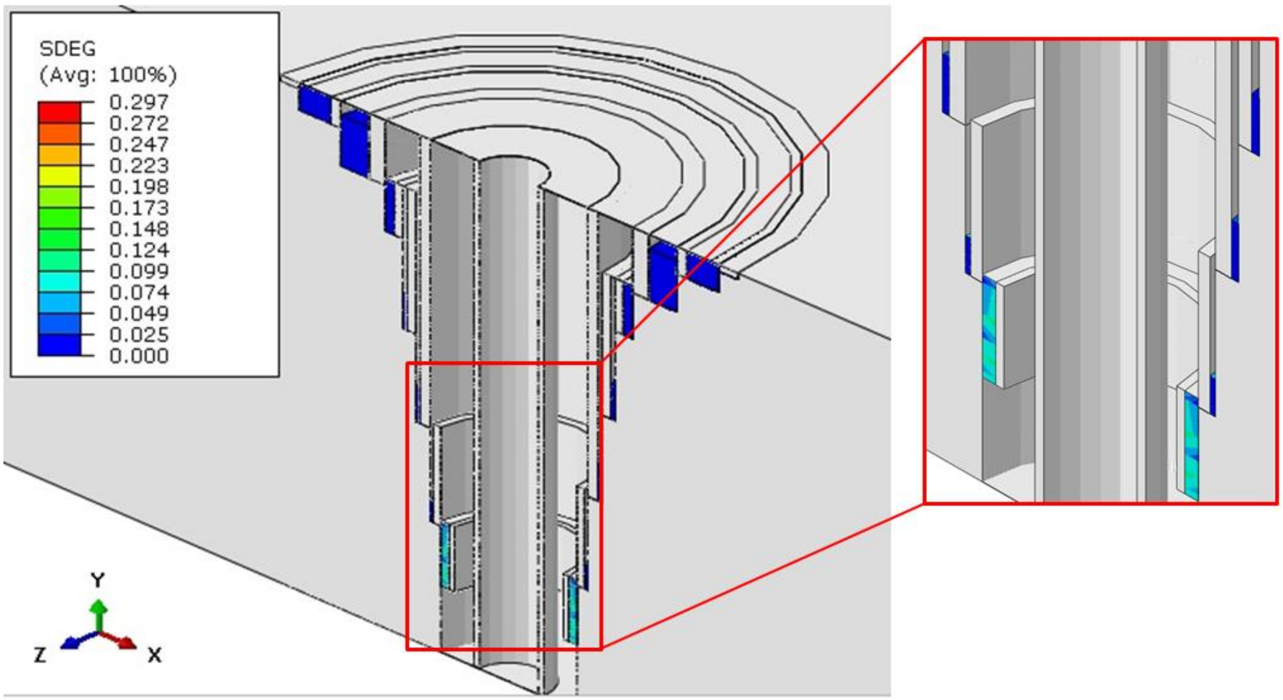

Figure 20 **Cement damage after eight years of cycles**

Note this view has the x and z coordinates magnified for clarity.

The damage in the cement immediately after the second stimulation and warm-up occurrence is shown in Figure 21.

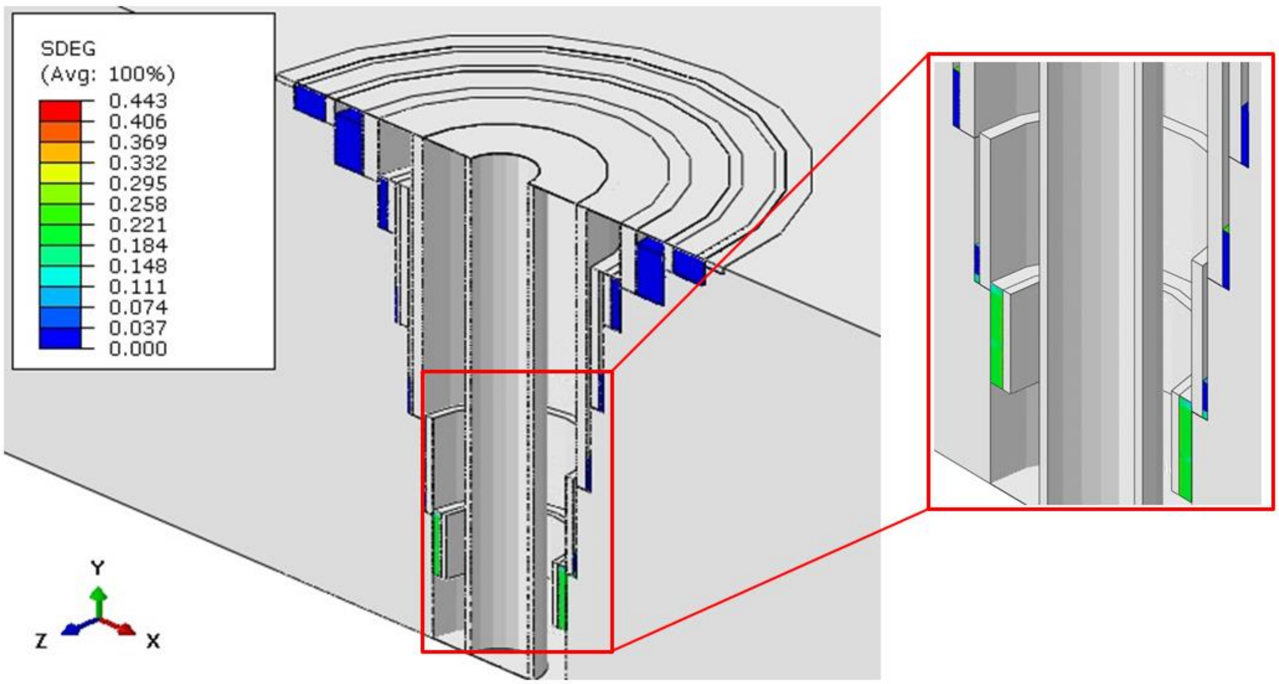

Figure 21 **Cement damage after second stimulation occurrence**

Note this view has the x and z coordinates magnified for clarity.

The damage in the cement after four more years (12 total) of production/shut-in cycles (prior to the third stimulation occurrence) is shown in Figure 22.

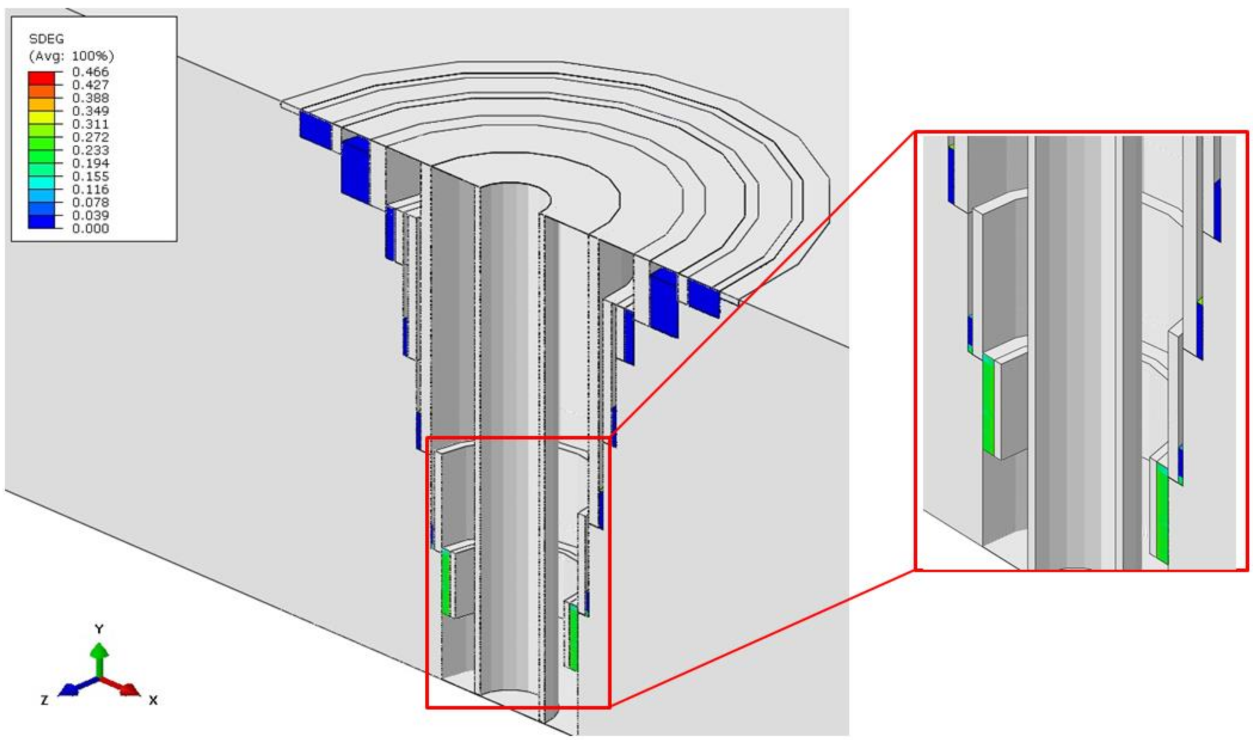

Figure 22 **Cement damage after 12 years of cycles**

Note this view has the x and z coordinates magnified for clarity.

The damage in the cement immediately after the third stimulation and warm-up occurrence is shown in Figure 23

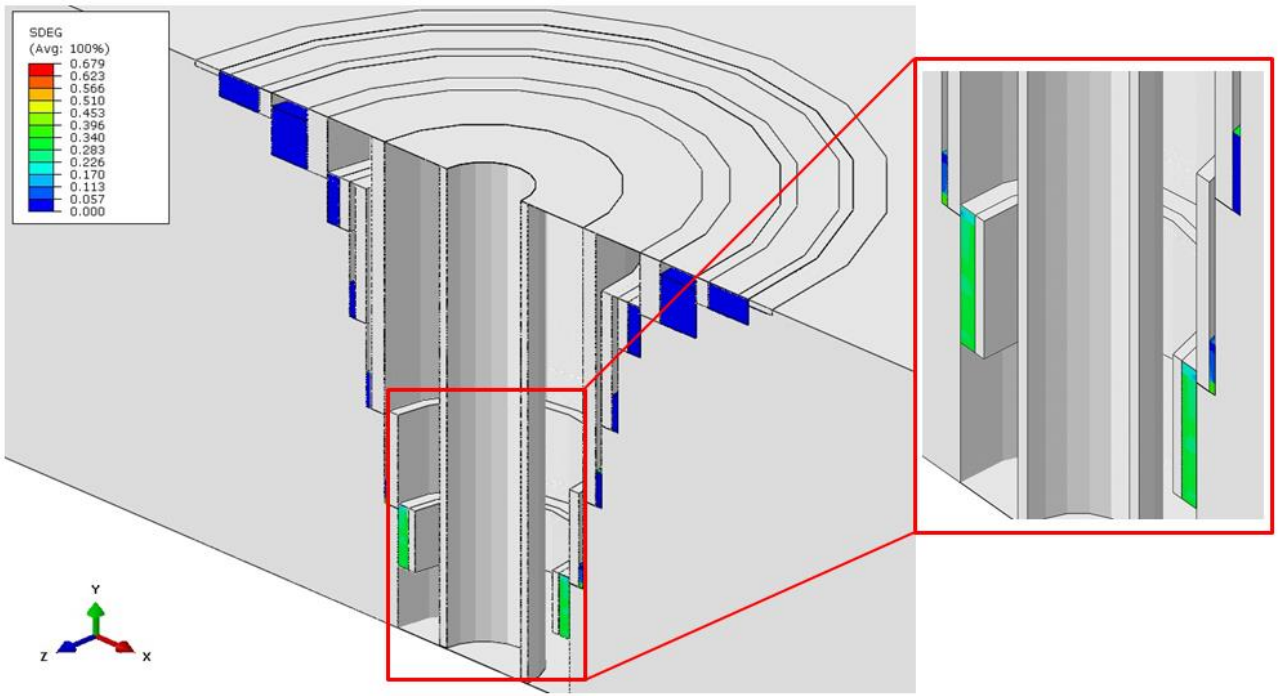

Figure 23 **Cement damage after third stimulation occurrence**

Note this view has the x and z coordinates magnified for clarity.

The damage in the cement after four more years (16 total) of production/shut-in cycles (prior to the forth stimulation occurrence) is shown in Figure 24.

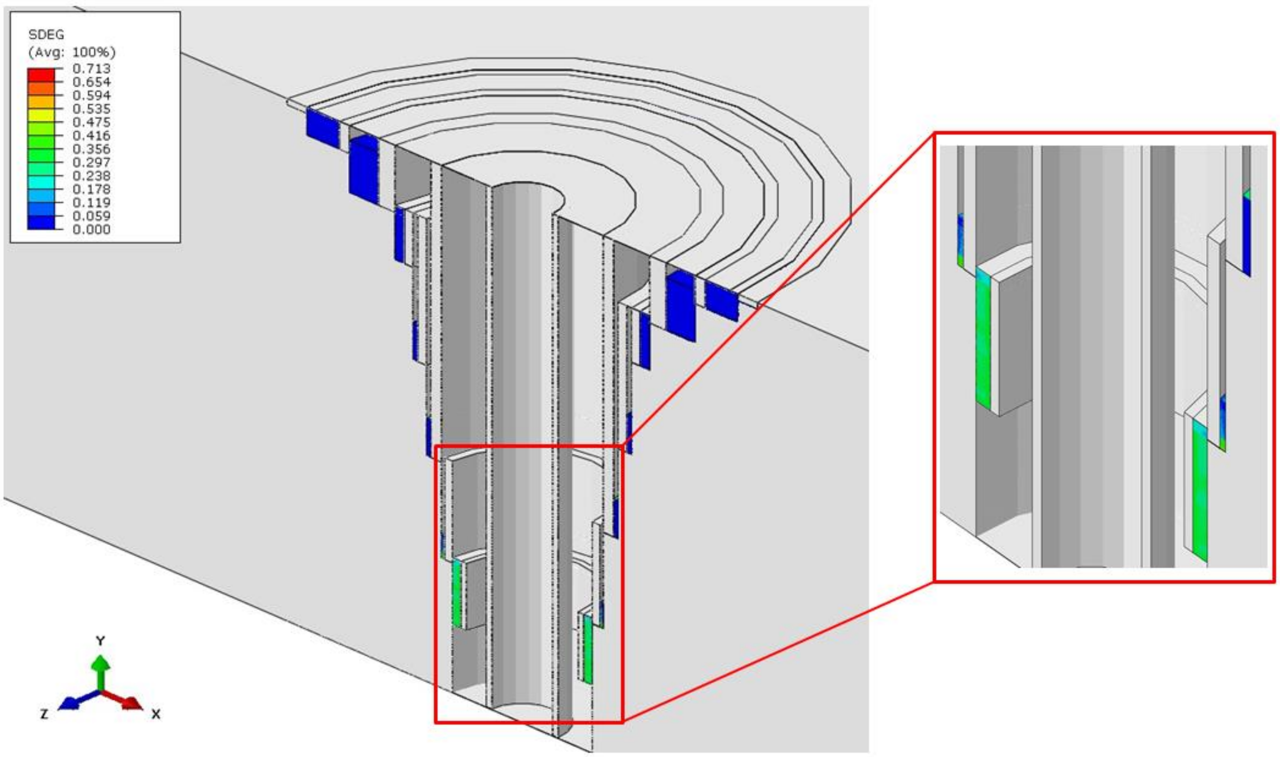

Figure 24 **Cement damage after 16 years of cycles**

Note this view has the x and z coordinates magnified for clarity.

The damage in the cement immediately after the fourth stimulation and warm-up occurrence is shown in Figure 25.

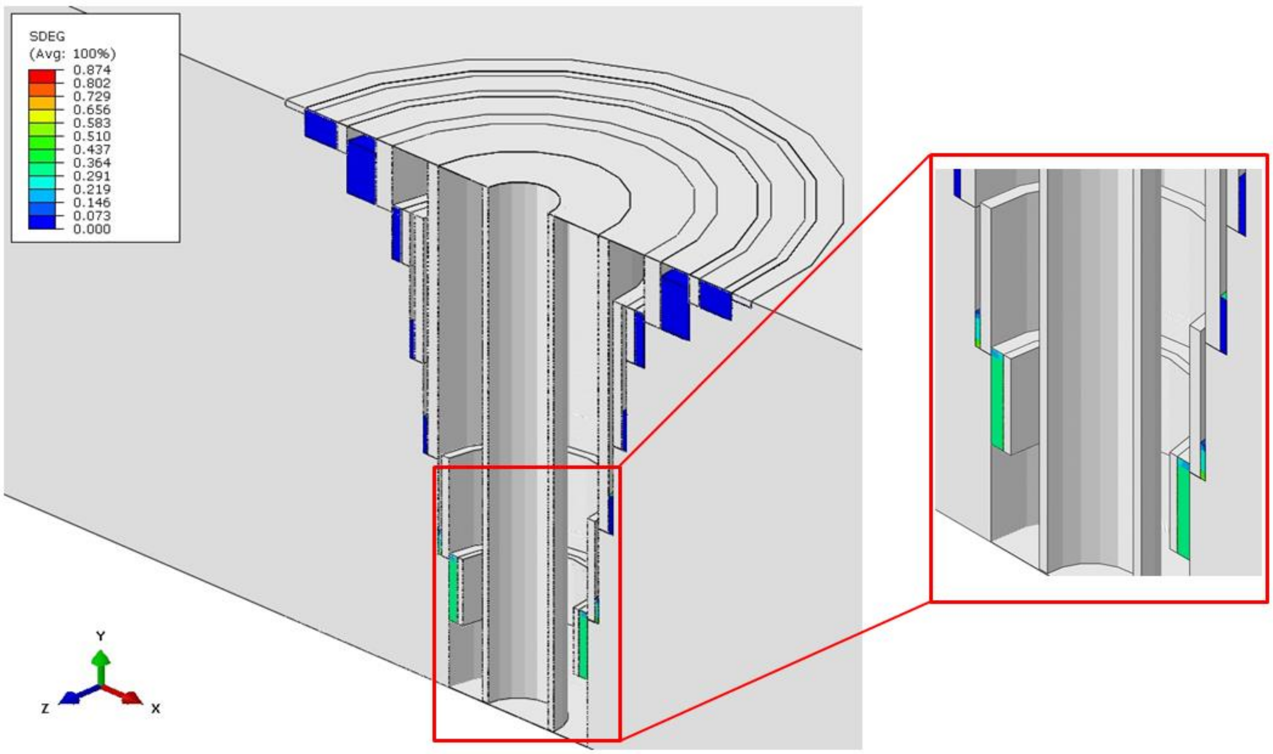

Figure 25 **Cement damage after fourth stimulation occurrence**

Note this view has the x and z coordinates magnified for clarity.

The damage in the cement after four more years (20 total) of production/shut-in cycles (end of assumed production life) is shown in Figure 26

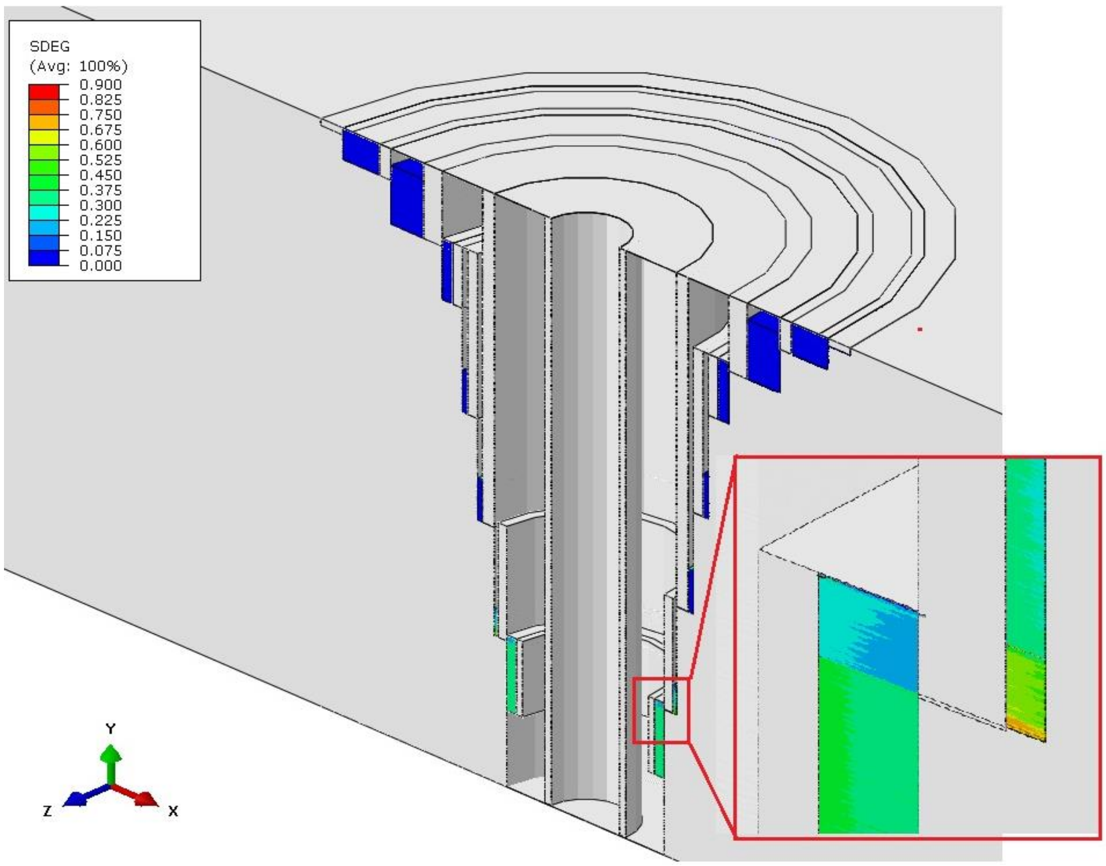

Figure 26 **Cement damage after 20 years of cycles**

Note this view has the x and z coordinates magnified for clarity.

This represents the highest localized damage (SDEG) in the cement. The SDEG values from the FEA have been normalized with respect to 100%, meaning that elements that have reached 100% damage in the model are areas that indicate likelihood for the development of localized cracks/micro-annulus etc. and not a loss of isolation. The validation performed in Task 5 show that it is the magnitude of damage couple with the extent and location of damage is a better indicator of a seal barrier failure. The maximum damage in the cement over the life of the well is shown graphically in Figure 26.

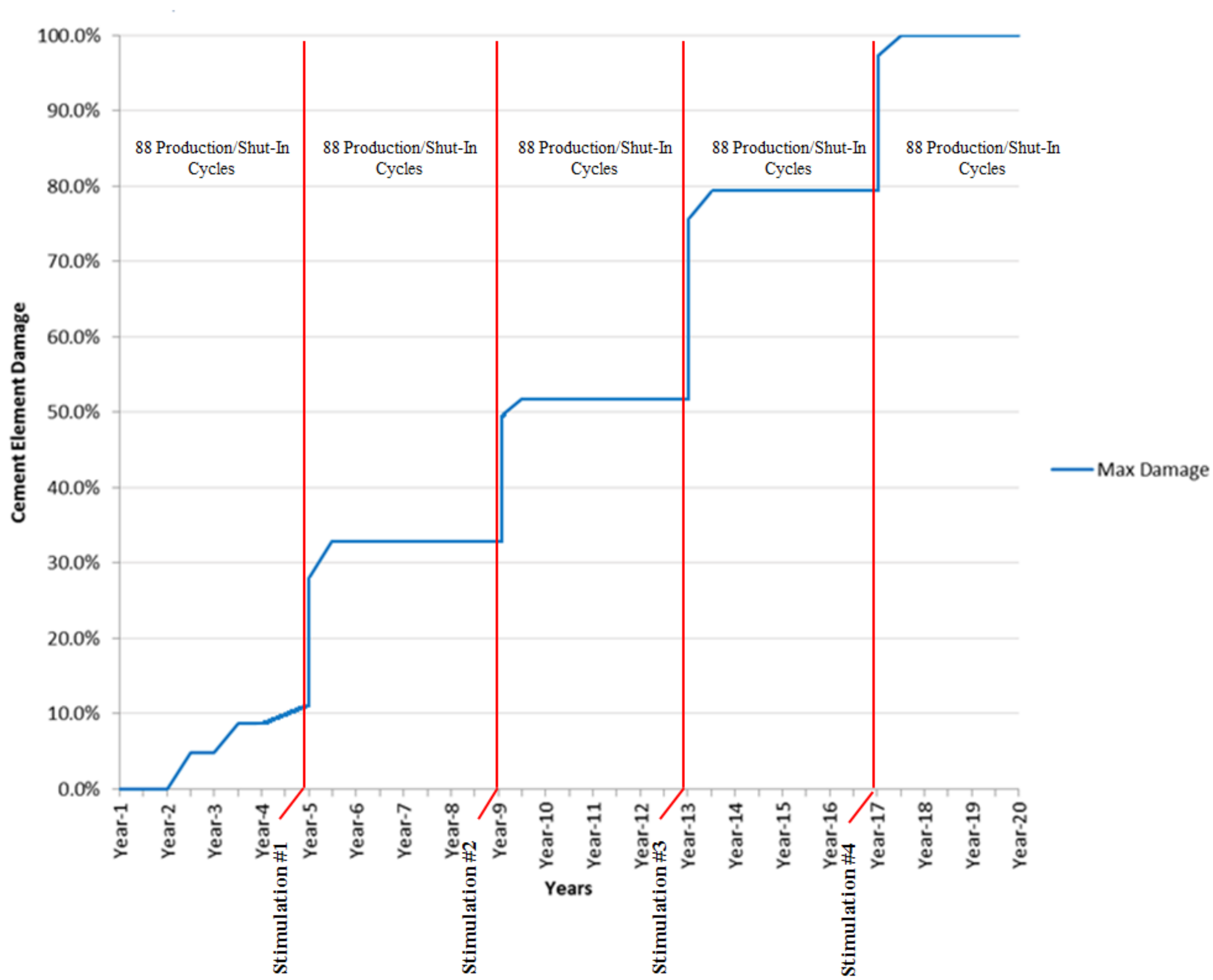

Figure 27 **Maximum local cement damage progression**

The results of the Cycle-4x-20-6310 case are shown in Figure 28 to Figure 31

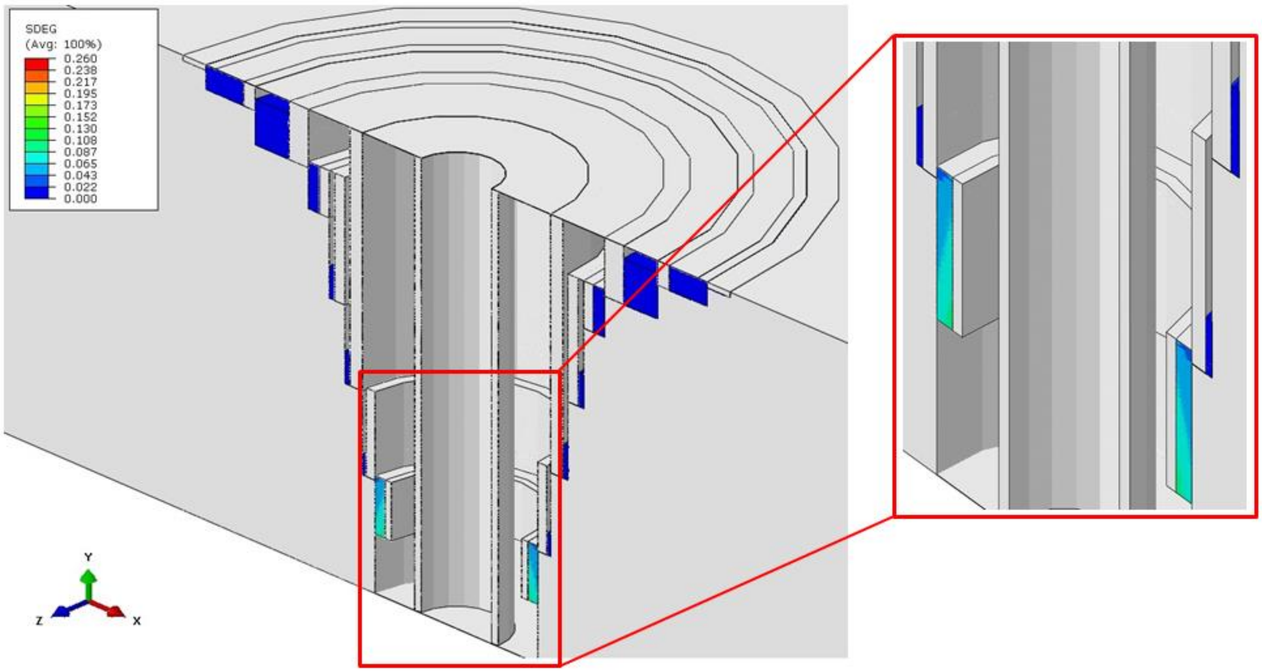

Figure 28 Cycle-4x-20-6310 Case cement damage after first stimulation

Note this view has the x and z coordinates magnified for clarity.

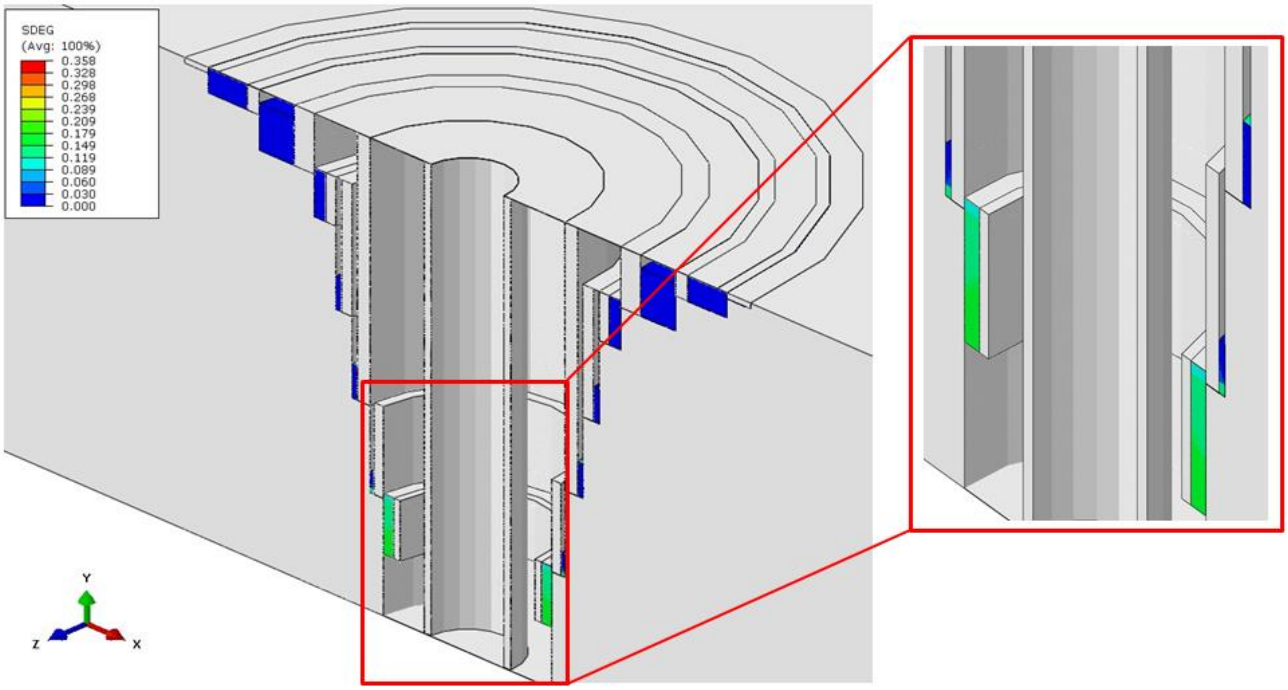

Figure 29 **Cycle-4x-20-6310 Case cement damage after second stimulation**

Note this view has the x and z coordinates magnified for clarity.

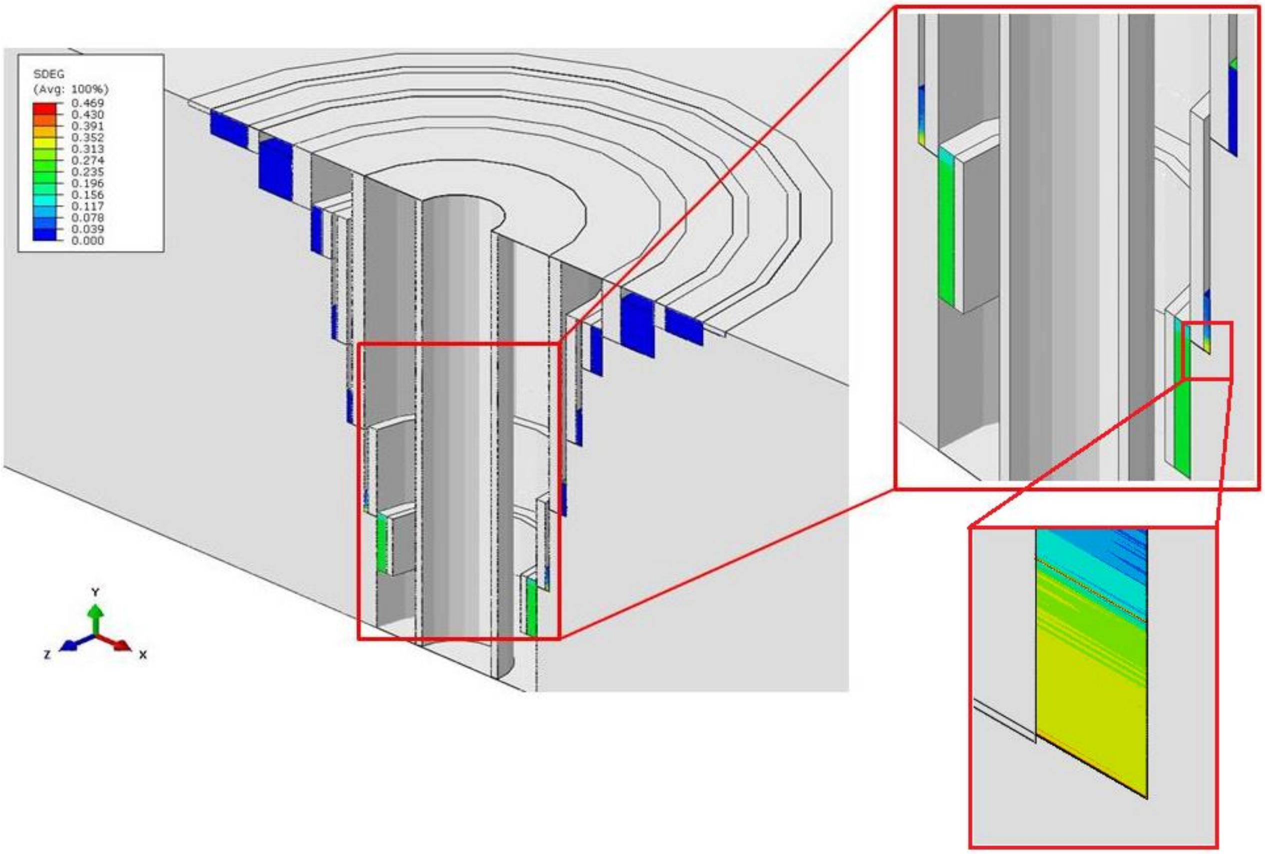

Figure 30 **Cycle-4x-20-6310 Case cement damage after third stimulation**

Note this view has the x and z coordinates magnified for clarity.

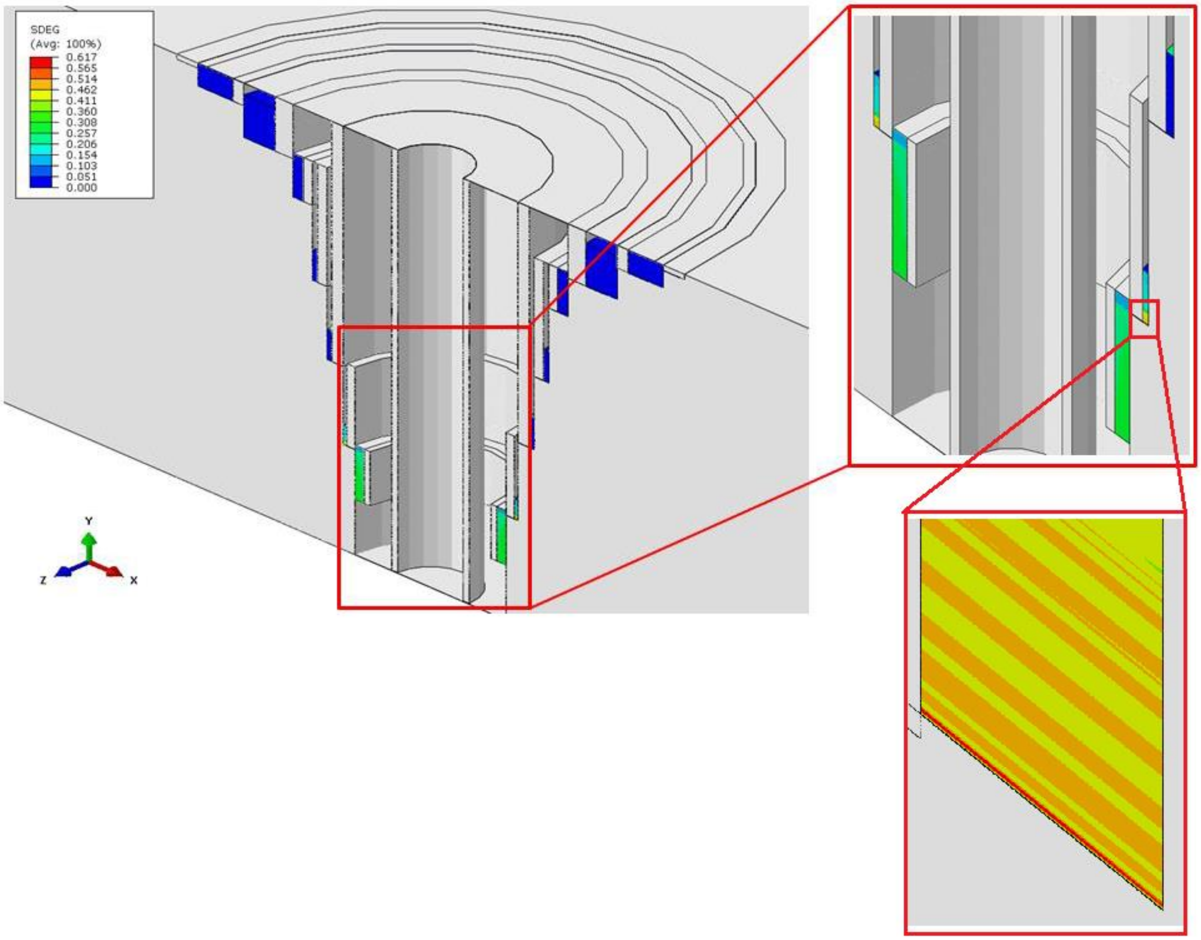

Figure 31 **Cycle-4x-20-6310 Case cement damage after fourth stimulation**

Note this view has the x and z coordinates magnified for clarity.

The results of the Cycle-4x-60-6310 case are shown in Figure 32 to Figure 35.

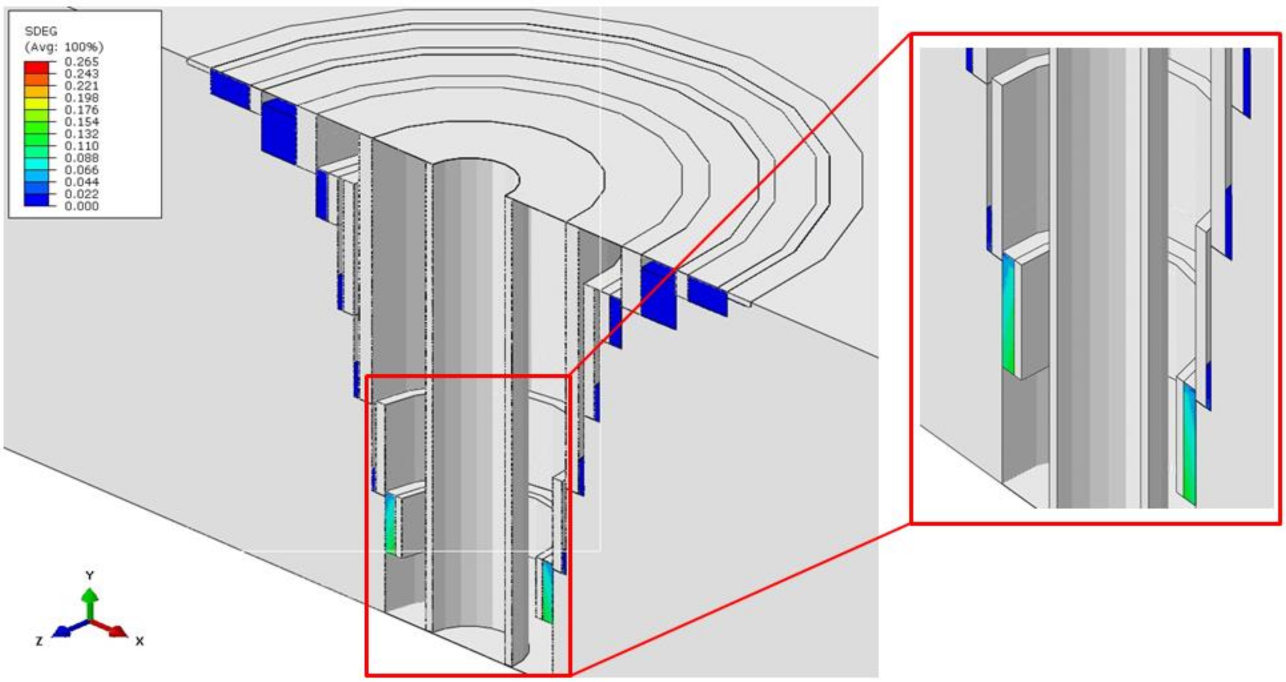

Figure 32 **Cycle-4x-60-6310 Case cement damage after first stimulation**

Note this view has the x and z coordinates magnified for clarity.

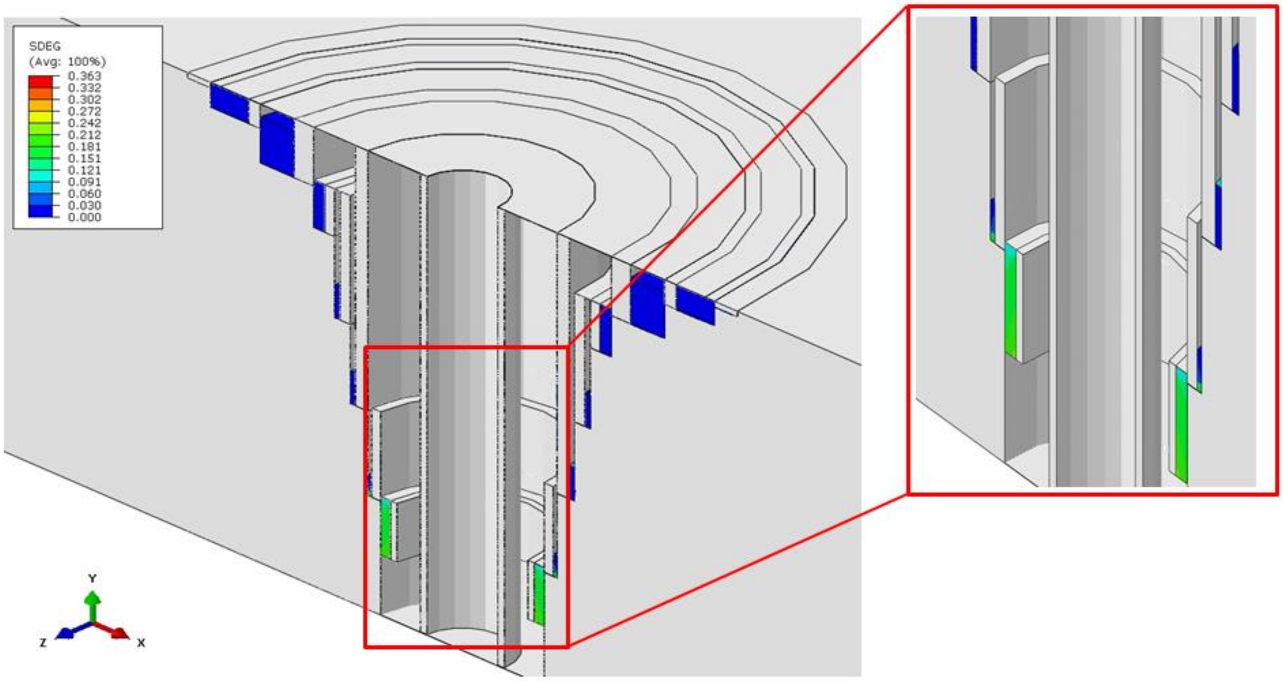

Figure 33 **Cycle-4x-60-6310 Case cement damage after second stimulation**

Note this view has the x and z coordinates magnified for clarity.

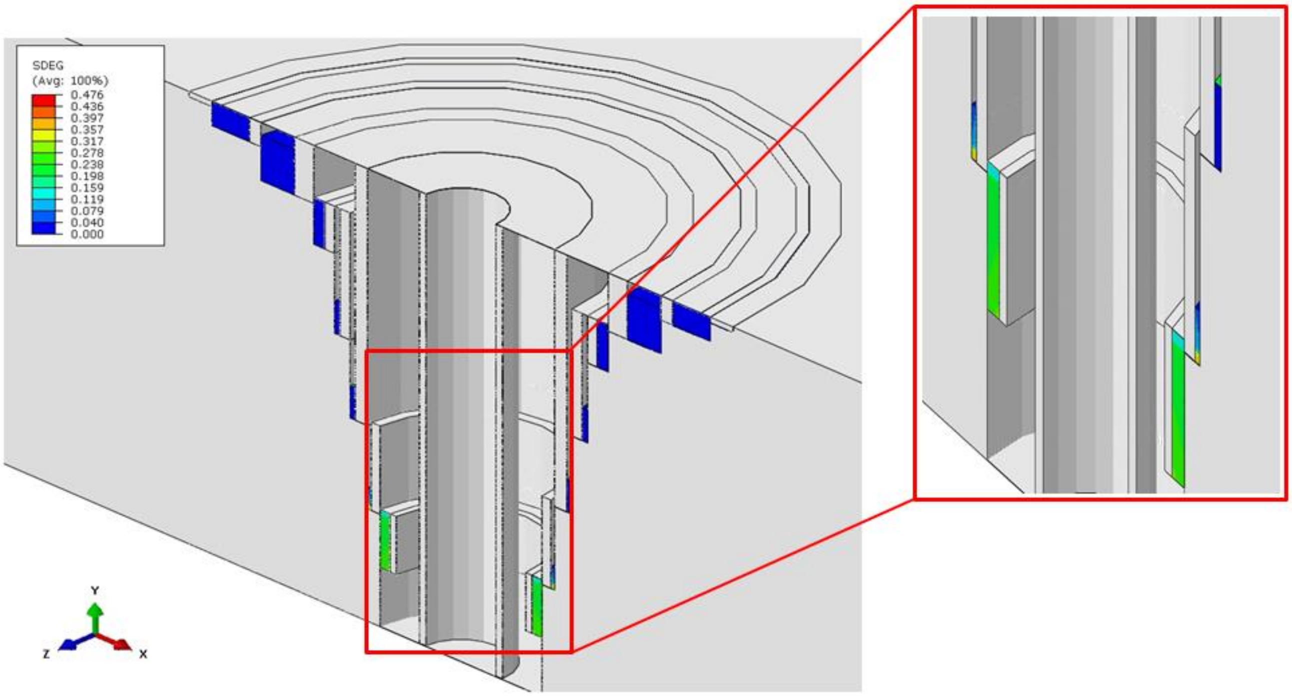

Figure 34 **Cycle-4x-60-6310 Case cement damage after third stimulation**

Note this view has the x and z coordinates magnified for clarity.

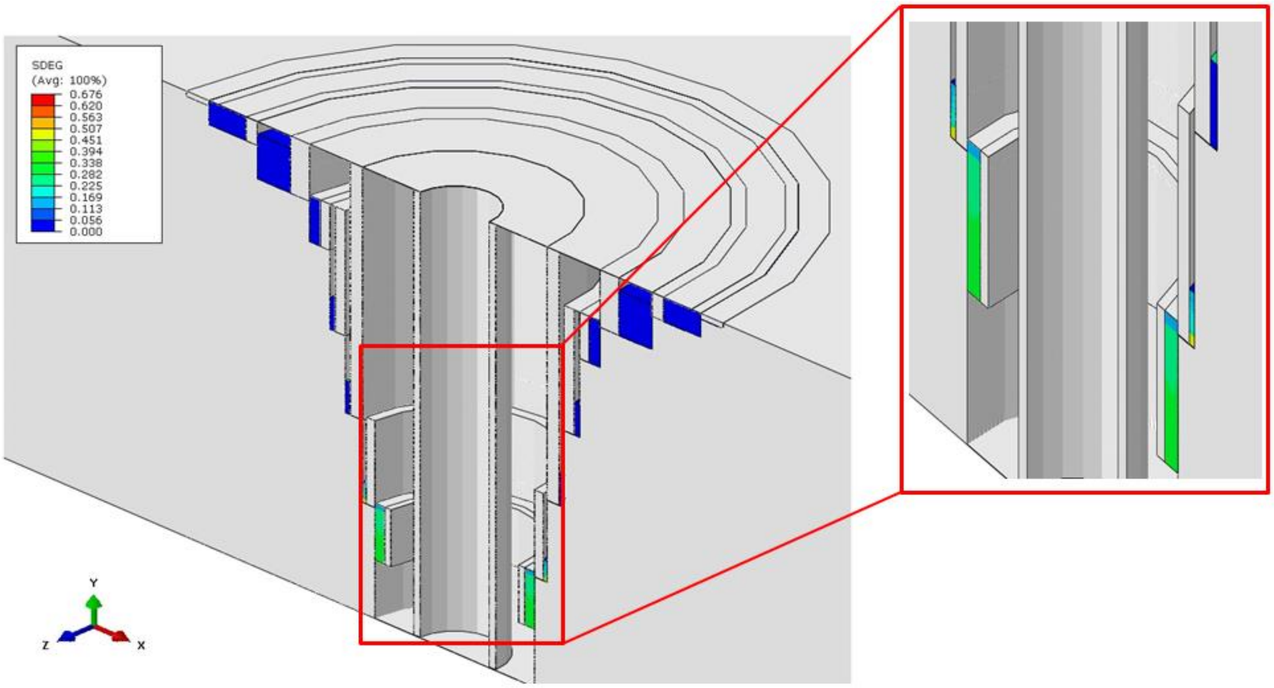

Figure 35 **Cycle-4x-60-6310 Case cement damage after fourth stimulation**

Note this view has the x and z coordinates magnified for clarity.

The results of the Cycle-4x-20-3207 case are shown in Figure 36 to Figure 39.

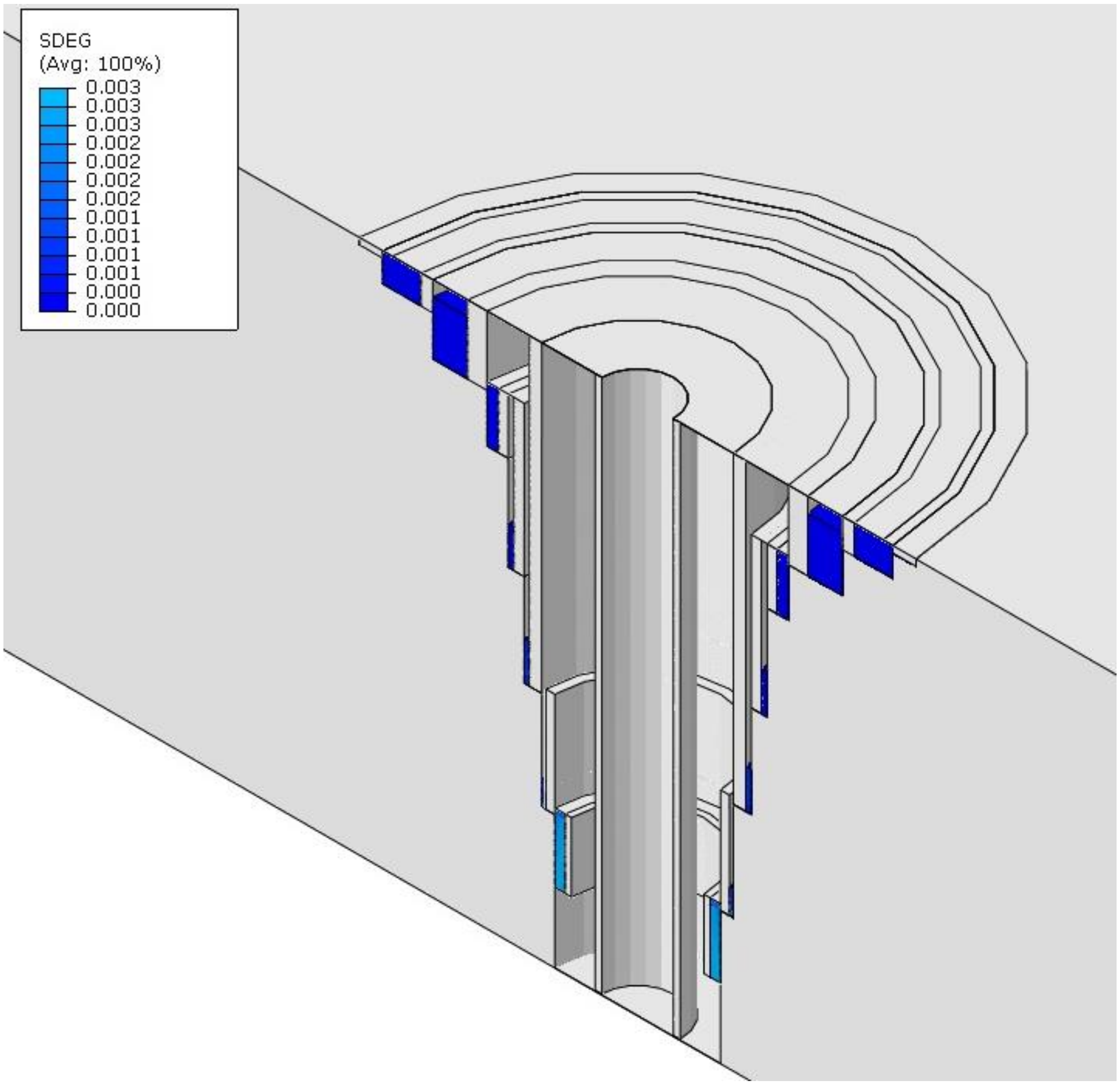

Figure 36 **Cycle-4x-20-3207 Case cement damage after first stimulation**

Note this view has the x and z coordinates magnified for clarity.

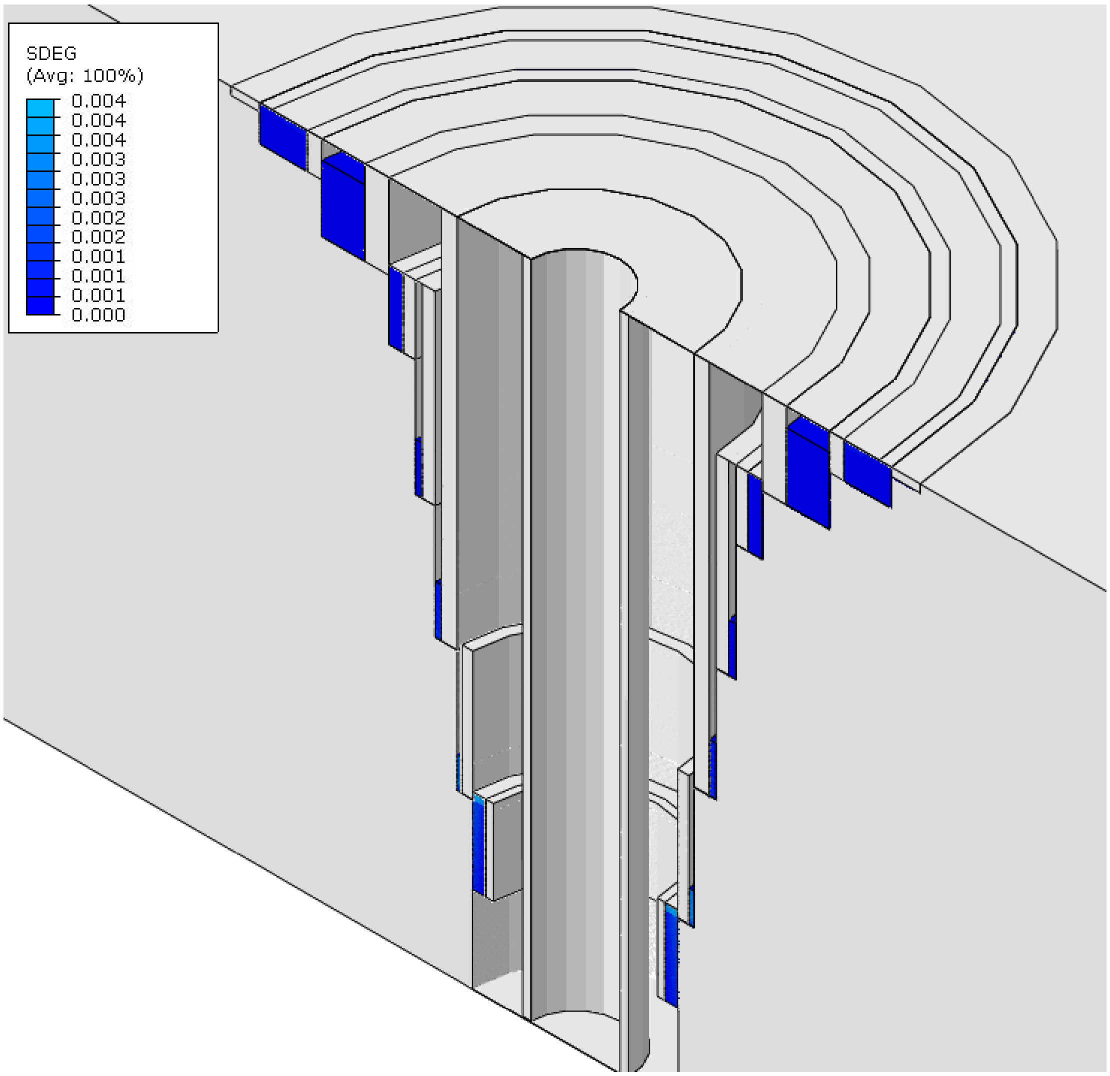

Figure 37 **Cycle-4x-20-3207 Case cement damage after second stimulation**

Note this view has the x and z coordinates magnified for clarity.

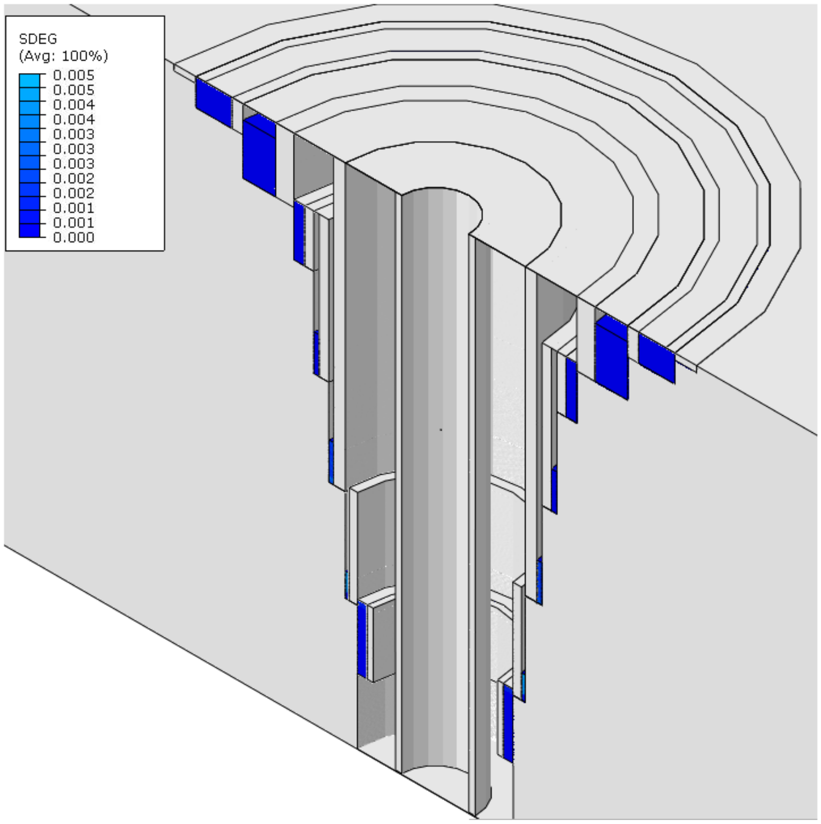

Figure 38 **Cycle-4x-20-3207 Case cement damage after third stimulation**

Note this view has the x and z coordinates magnified for clarity.

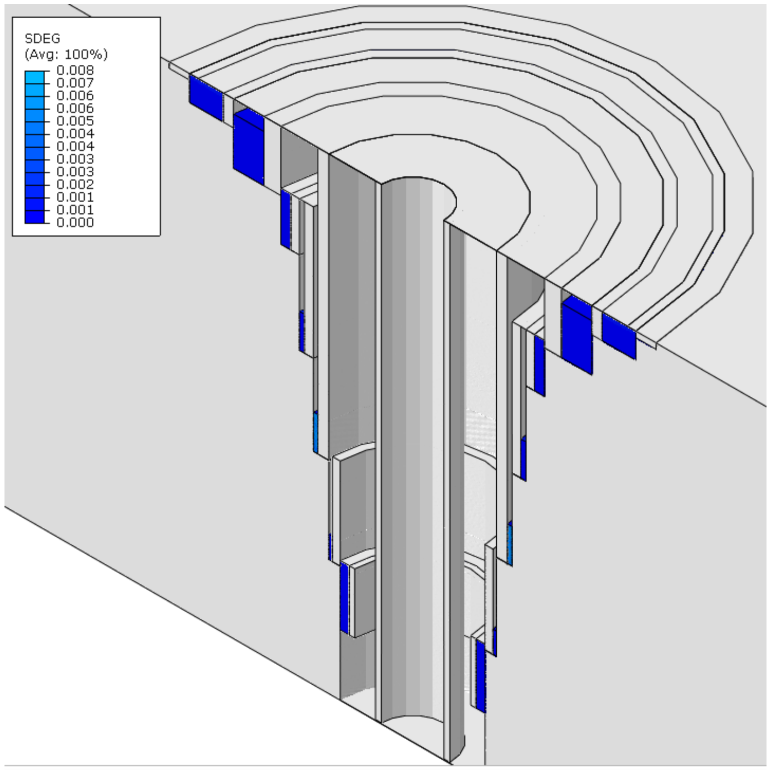

Figure 39 **Cycle-4x-20-3207 Case cement damage after fourth stimulation**

Note this view has the x and z coordinates magnified for clarity.

The results of the Cycle-4x-60-3207 case are shown in Figure 40 to Figure 43.

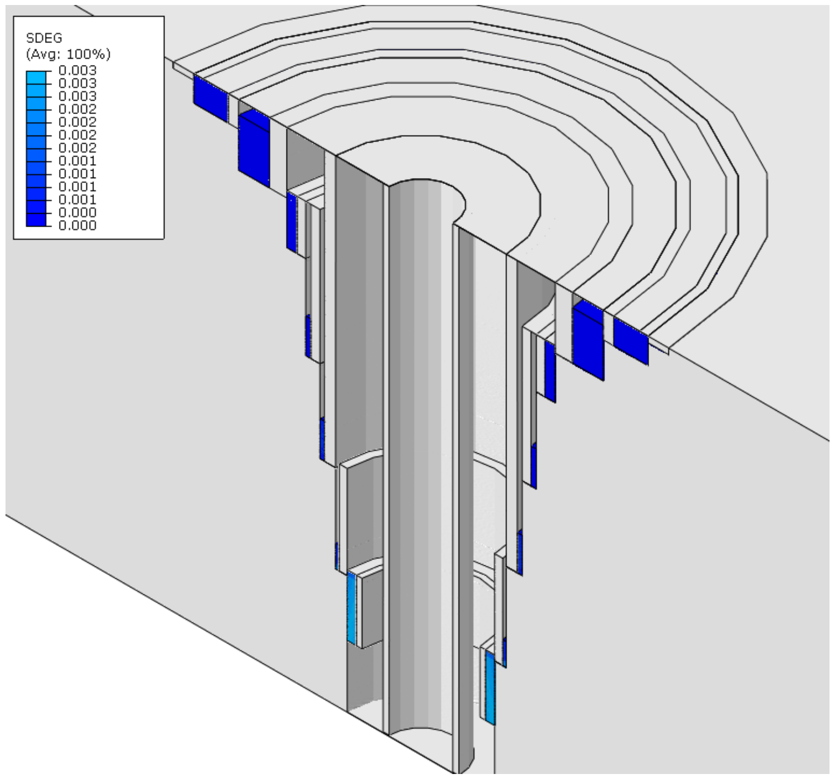

Figure 40 **Cycle-4x-60-3207 Case cement damage after first stimulation**

Note this view has the x and z coordinates magnified for clarity.

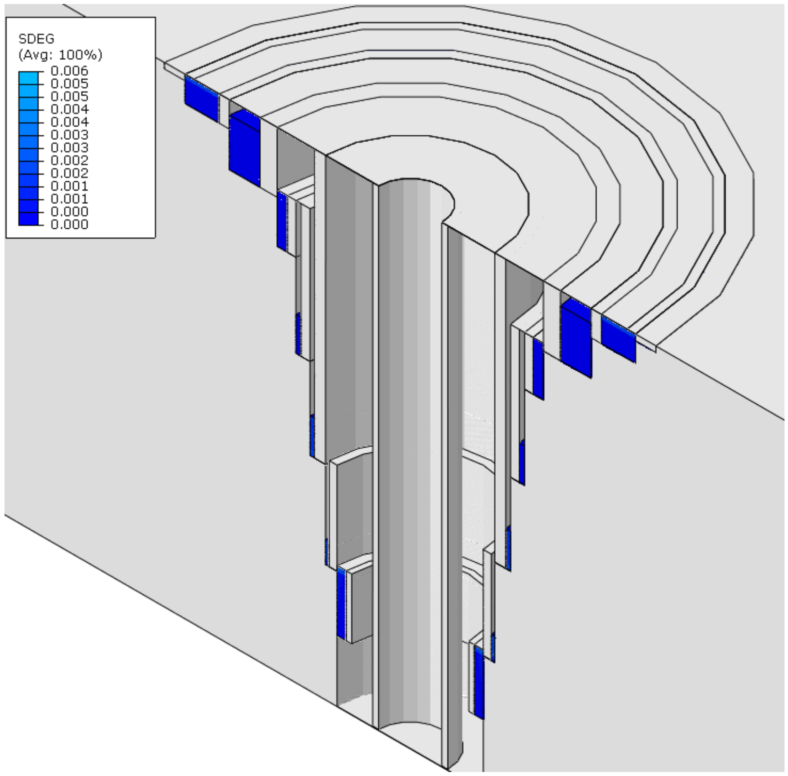

Figure 41 **Cycle-4x-60-3207 Case cement damage after second stimulation**

Note this view has the x and z coordinates magnified for clarity.

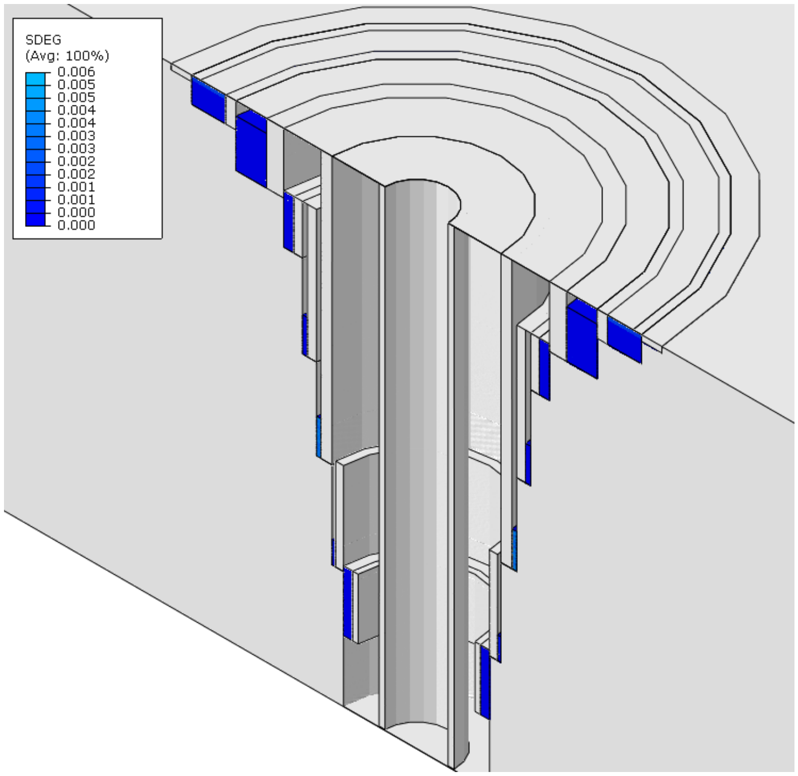

Figure 42 **Cycle-4x-60-3207 Case cement damage after third stimulation**

Note this view has the x and z coordinates magnified for clarity.

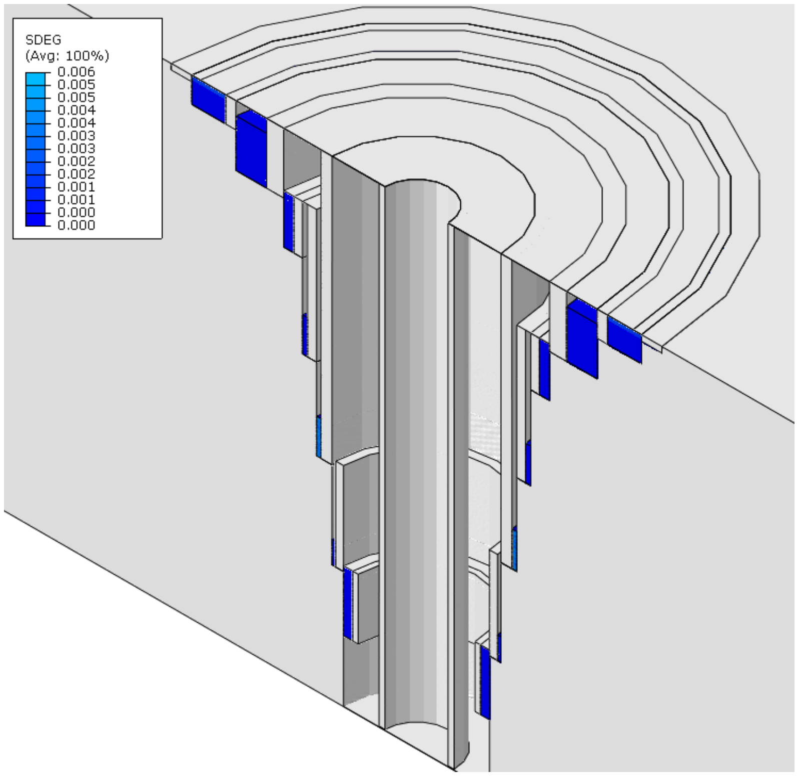

Figure 43 Cycle-4x-60-3207 Case cement damage after fourth stimulation

Note this view has the x and z coordinates magnified for clarity.

The results of the Cycle-4x-20-324case are shown in Figure 44 to Figure 47 .

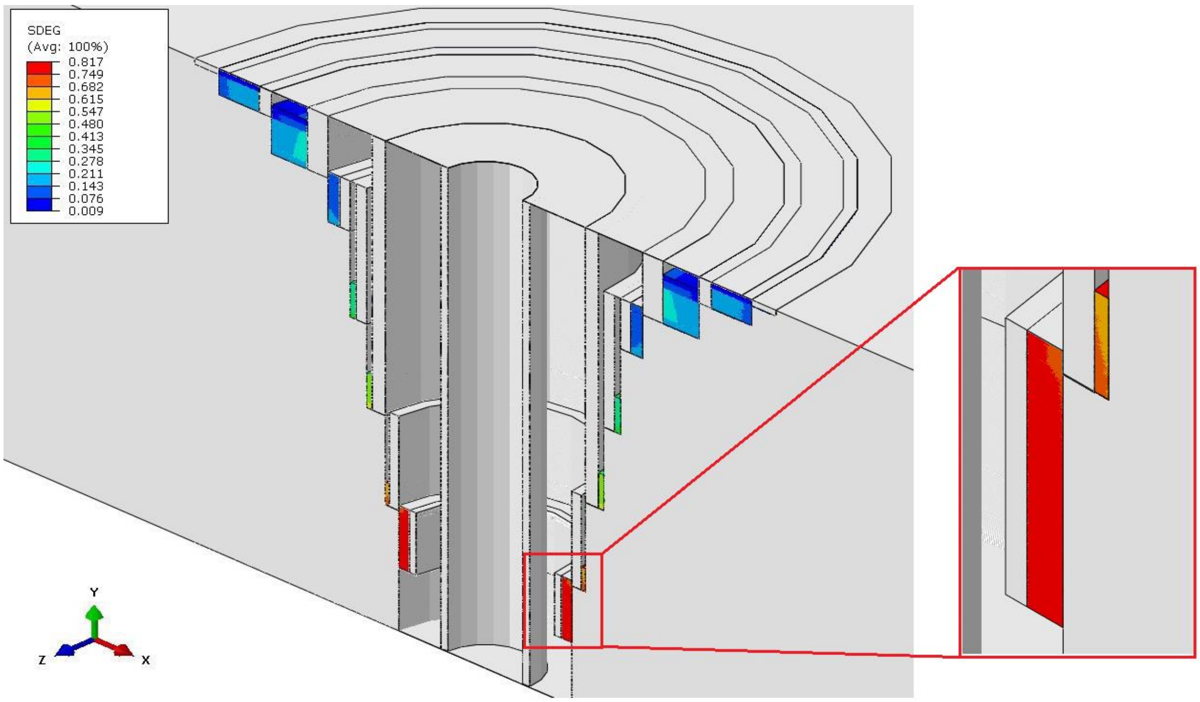

Figure 44 **Cycle-4x-20-324 Case cement damage after first stimulation**

Note this view has the x and z coordinates magnified for clarity.

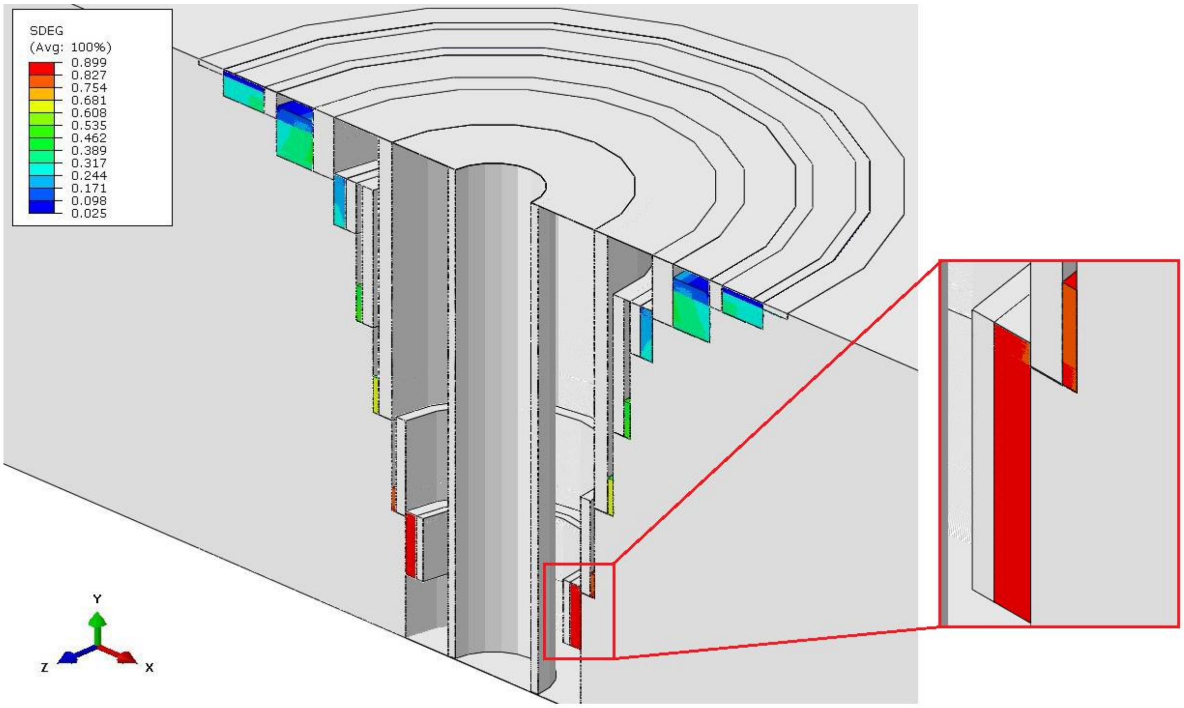

Figure 45 **Cycle-4x-20-324 Case cement damage after second stimulation**

Note this view has the x and z coordinates magnified for clarity.

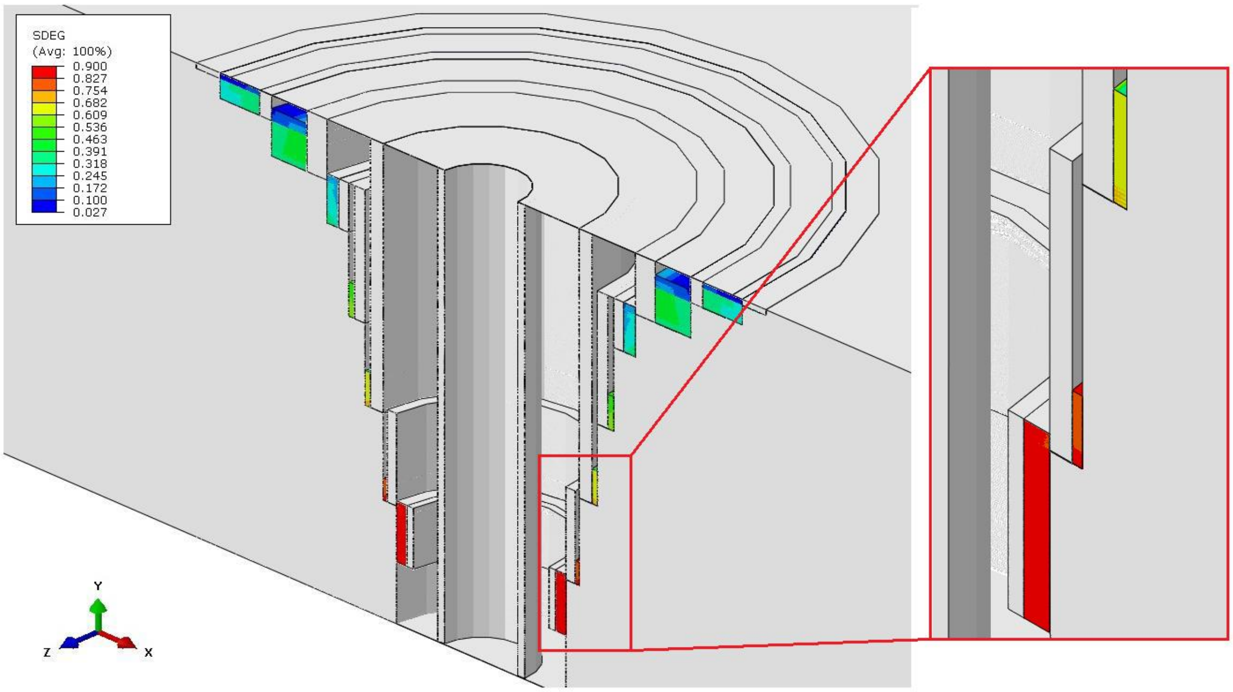

Figure 46 **Cycle-4x-20-324 Case cement damage after third stimulation**

Note this view has the x and z coordinates magnified for clarity.

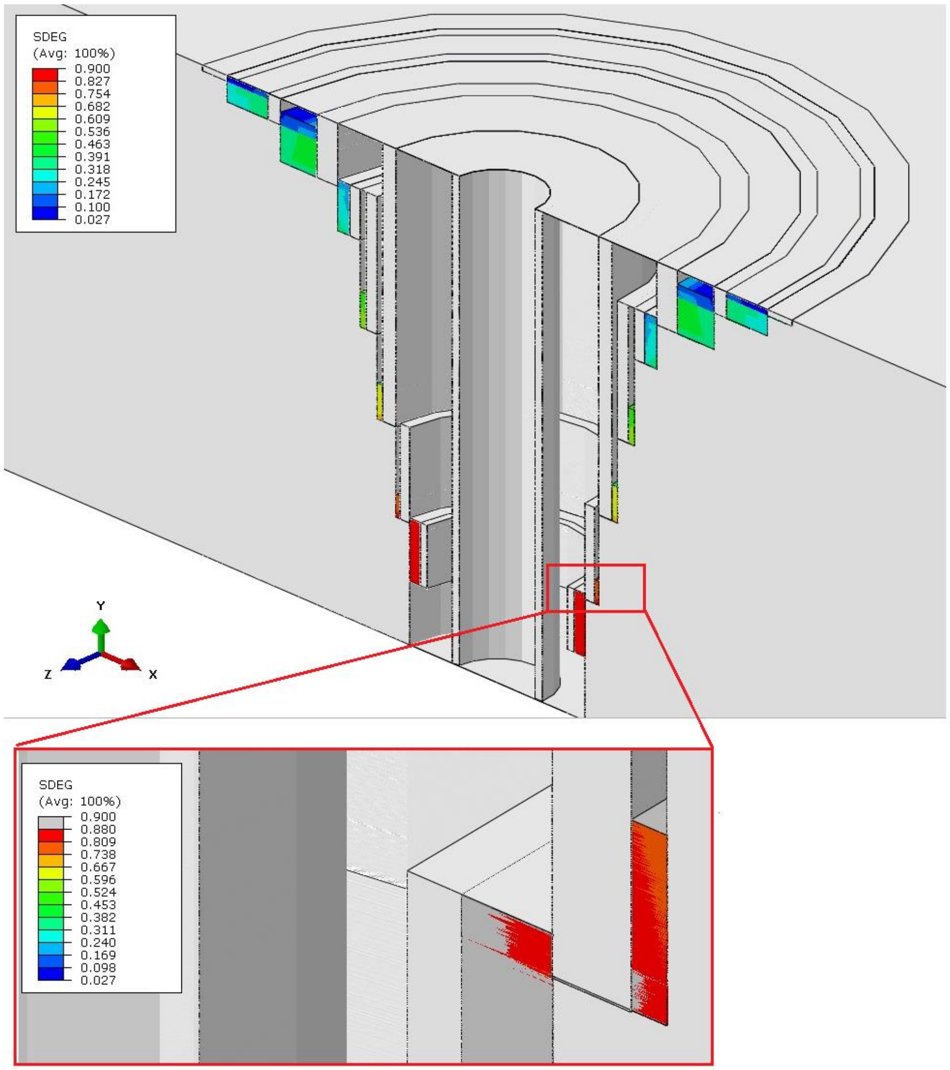

Figure 47 **Cycle-4x-20-324 Case cement damage after fourth stimulation**

Note this view has the x and z coordinates magnified for clarity.

The SDEG values from the FEA have been normalized with respect to 100%, meaning that elements that have reached 100% damage in the model are areas that indicate likelihood for the development of localized cracks/micro-annulus etc. and not a loss of isolation. The validation performed in Task 5 show that it is the magnitude of damage couple with the extent and location of damage is a better indicator of a seal barrier failure. The maximum localized damage in the cement for each case configuration is shown graphically in Figure 48.

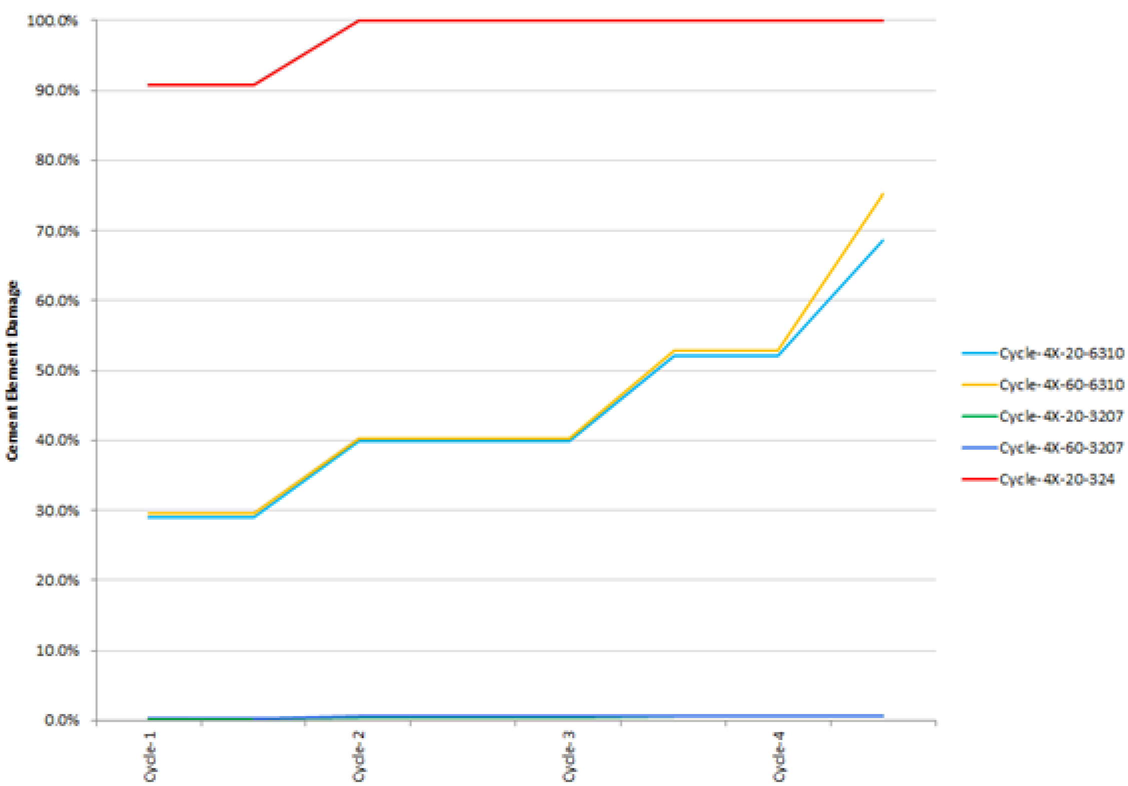

Figure 48 **Maximum localized cement damage comparison**

6.3 Local FEA Modelling and Tie in known Data

Since a deviated well cannot be modelled axi-symmetrically a segment representing a down-hole section of a well was generated for a vertical well and a well that contains a departure angle approximately 0.5 deg/ft. The techniques used to create the structural models and the heat transfer models are similar to the scale modelling and are detailed in the Task 5 section. The computational expense of the local models was reduced by modelling a 375ft diameter x 1,000°F t depth section of soil assumed to be about 30,000°F t below the ocean floor. The formation temperature was assumed to be 350°F and an injection temperature for the stimulation fluid case was assumed to be 80°F.

The well was assumed to have a casing size of 7-5/8” outer diameter with a wall thickness of 3/8”. The diameter of the hole was assumed to be 9-5/8” diameter with the casing placed concentrically.

The models were constructed using the same element types and element count for each. The formation was assumed to be fixed in the vertical direction at the top and bottom of the down-hole segment and fixed in the horizontal direction around the perimeter of the formation limits. To facilitate the comparison of the deviated versus non-deviated wells only thermal effects from the injection case into a very hot environment were considered. To limit analysis run times only one cycle was considered. This allows for a comparison of the two wells.

6.3.1 Local FEA Modelling-Results

The heat transfer analysis results for both the non-deviated well and the deviated well are shown in Figure 49 to Figure 50 respectively.

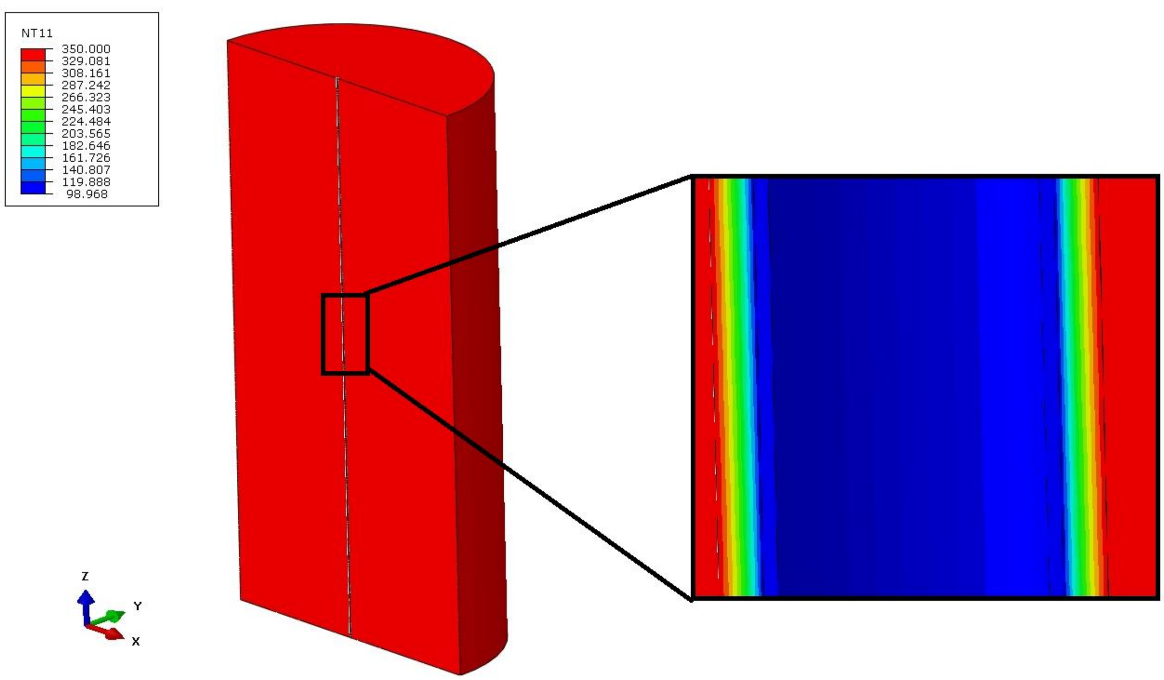

Figure 49 Heat transfer analysis results for vertical well

Note this view has the x and z coordinates magnified for clarity.

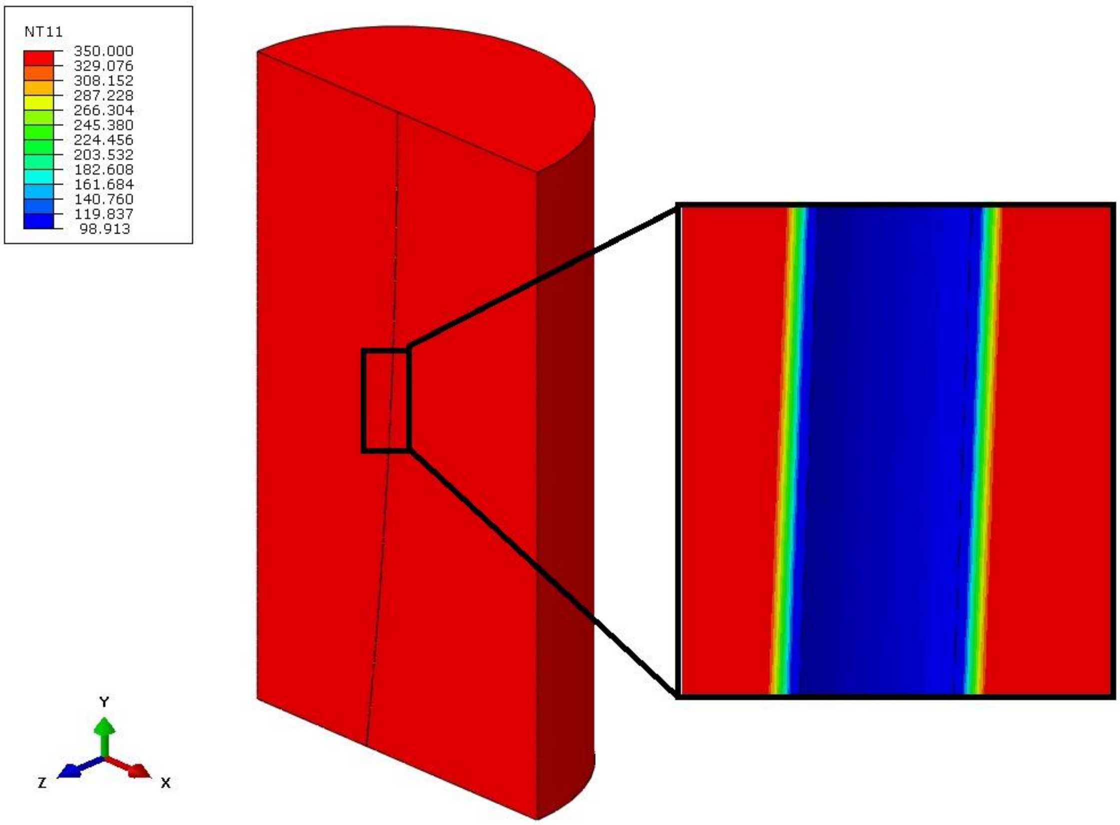

Figure 50 **Heat transfer analysis results for deviated well**

Note this view has the x and z coordinates magnified for clarity.

The cement element damage results for both the non-deviated well and the deviated well are shown in Figure 51 to Figure 52 respectively.

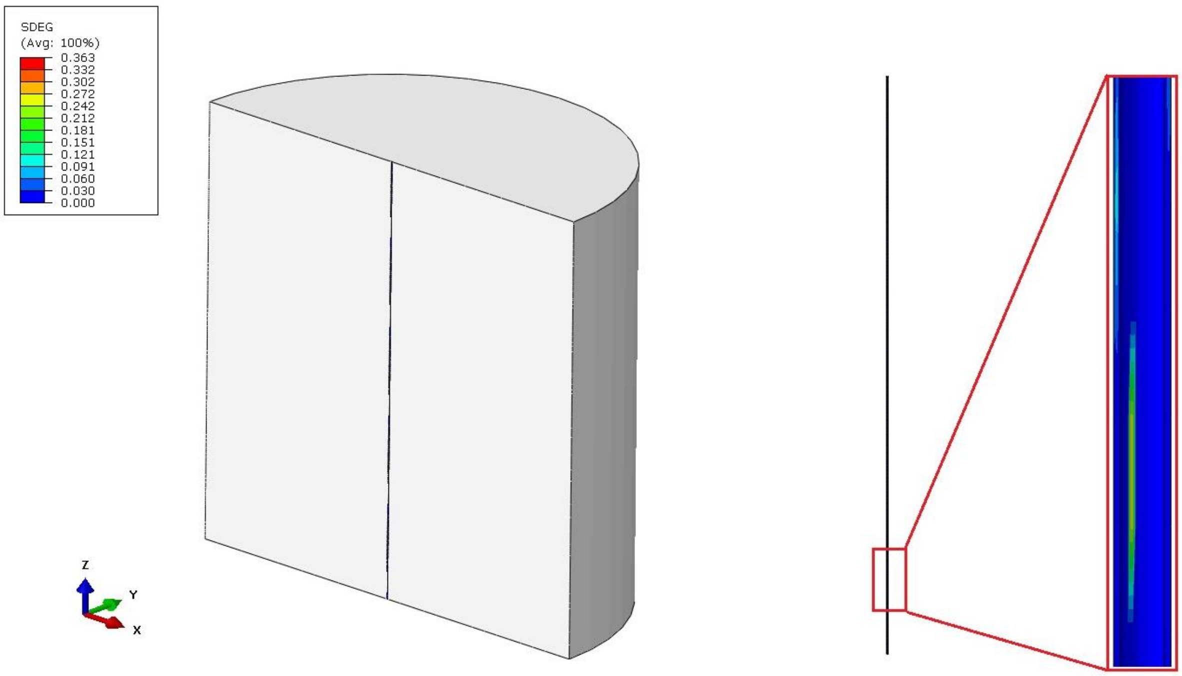

Figure 51 **Cement damage results for vertical well**

Note this view has the x and z coordinates magnified for clarity.

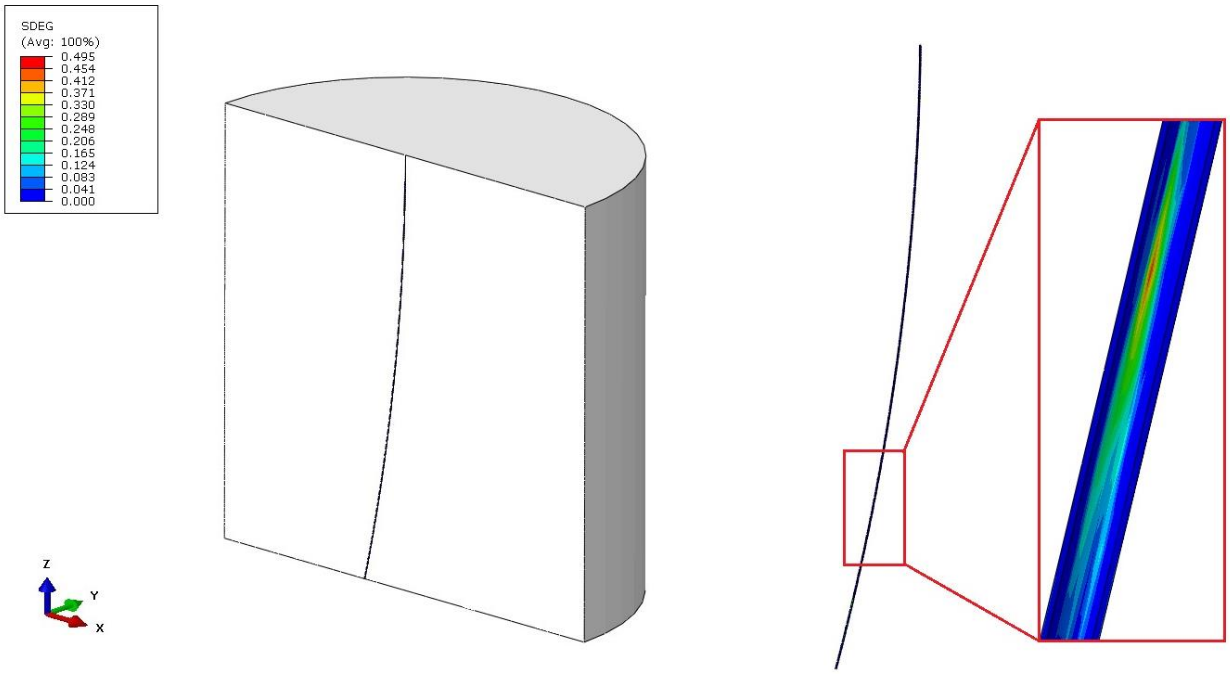

Figure 52 **Cement damage results for deviated well**

Note this view has the x and z coordinates magnified for clarity.

6.4 Conclusions

The FEA modelling performed has indicated that the definition of "thermal shock" as defined in Task 2 and Appendix A is a reasonable definition. It also confirmed some of the response from operators in the advisory group that production/shut-in is not as significant driver of damage in the well as stimulation. The long term durability of the well is highly associated with proper cement selection and quality of the cement placement.

A shut-in of a producing deep water HPHT well does represent a thermal shock that can damage cement, particularly in the upper part of the well, however a large accumulation of production/shut-in cycles is required to significantly damage the barrier. This is in line with the opinions from some of the members of the advisory group.

Stimulating a well does significantly more damage to the cement than a normal production/shut-in cycle and that damage can extend a significant distance up the well bore. It therefore represents a greater risk to the well barrier system. However, damage in the wellbore cement does not always indicate a loss of isolation.

The HPHT well investigated was able to maintain zonal isolation for a complete production life of 20 years. As mentioned above stimulating the well did significantly more harm to the well than just production/shut-in cycles alone. It was noticed that after a stimulation event the damage in the upper portion of the well would undergo a slight increase for the first couple of cycles then level off and hold steady until the next stimulation occurs. This further suggests that stimulation is more significant concerning damage in the well.

The two injection rates investigated of 14 bpm and 42 bpm (20 kbpd and 60 kbpd) revealed that the rate of injection increase of three times did cause an increase in damage in the cement, however the increase in the damage was around 10%. This indicates that the wellbore is likely more sensitive to the change in temperature than rate of change.

The stresses in the tubulars were well within the working limits for typical grades of steel used in a wellbore. Based on findings from Task 2, it appears that standard practices in the design of the tubulars, while not explicitly calling it thermal shock, do account for it in the process of checking them against thermal induced stresses. In addition the behavior of steels at higher temperatures also has been better understood historically.

The cement designs and quality of placement of cement in the wellbore during completions is very critical to the performance of the well barrier system. Although one cement mix design is not always adequate for all situations and environments it was found that in general the more brittle the cement is, the less durable and failure will occur at fewer cycles. This is true for all wells but is more pronounced in HPHT wells. A high compressive or tensile strength does not always indicate the ability to withstand a greater number of load cycles;

rather a balance of high compressive strength or tensile strengths coupled with a lower elastic modulus performed the best.

It was also revealed that a deviated well is potentially more susceptible to a higher magnitude of damage compared to a vertical well when compared under identical loading scenarios.

Mitigation recommendations are included in Task 6.

7 LABORATORY SCALE TESTING

7.1 Physical Property Testing

A series of mechanical tests have been performed to characterize material properties for the cement for input to the FEA. These are listed below:

- Shear Bond
- Tensile Strength – Indirect "Brazil test" + Direct pull
- Tensile Modulus
- Compressive strength
- Compressive modulus / Poisson's ratio
- Impact resistance

Significantly more effort was placed on this stage of the testing than in previous projects. Previously the quality of the mechanical properties, particularly the tensile strength and modulus were not at the desired level, meaning that the FE work has to estimate certain characteristics. For this project the higher fidelity achieved to gather the tensile strength and modulus means better inputs to the FE have been established.

The shear bond test apparatus used both for curing and testing the samples is shown in Figure 53, impact testing in Figure 54 and compression testing in Figure 55.

The direct tensile test utilized a new test sample set up. Instead of the more usual "dog bone" type test, a cylinder of cement was cast and cured with steel bolts embedded into it was used, see Figure 57. This allowed for a more accurate measurement of the tensile strength and modulus.

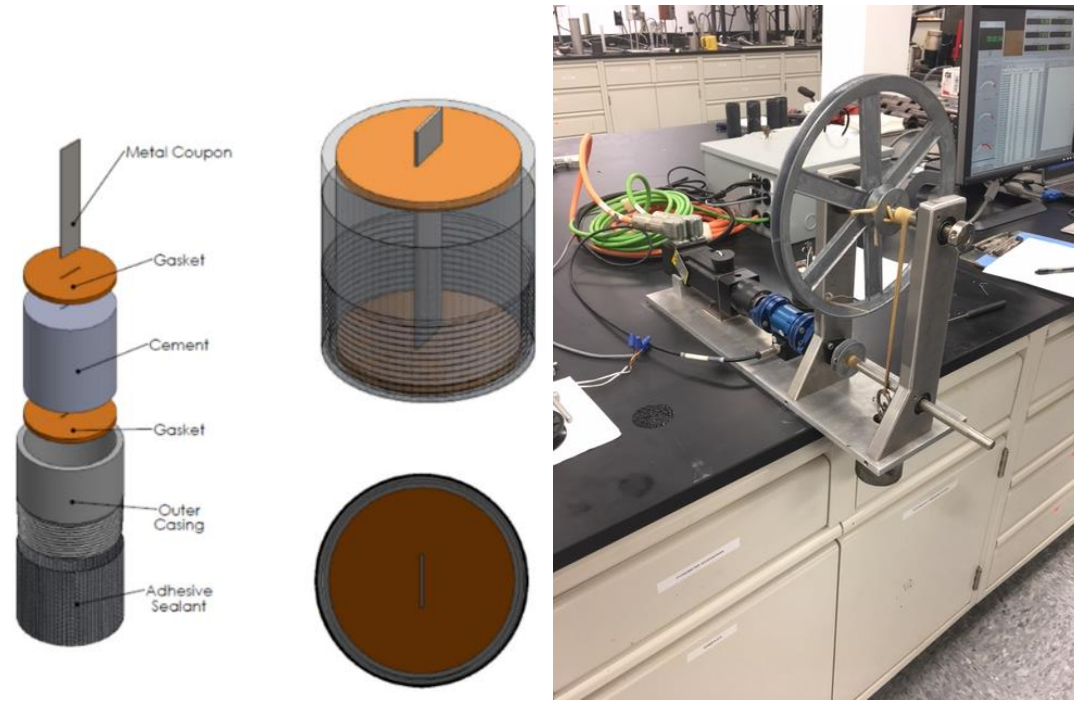

Figure 53 **Shear bond testing set-up**

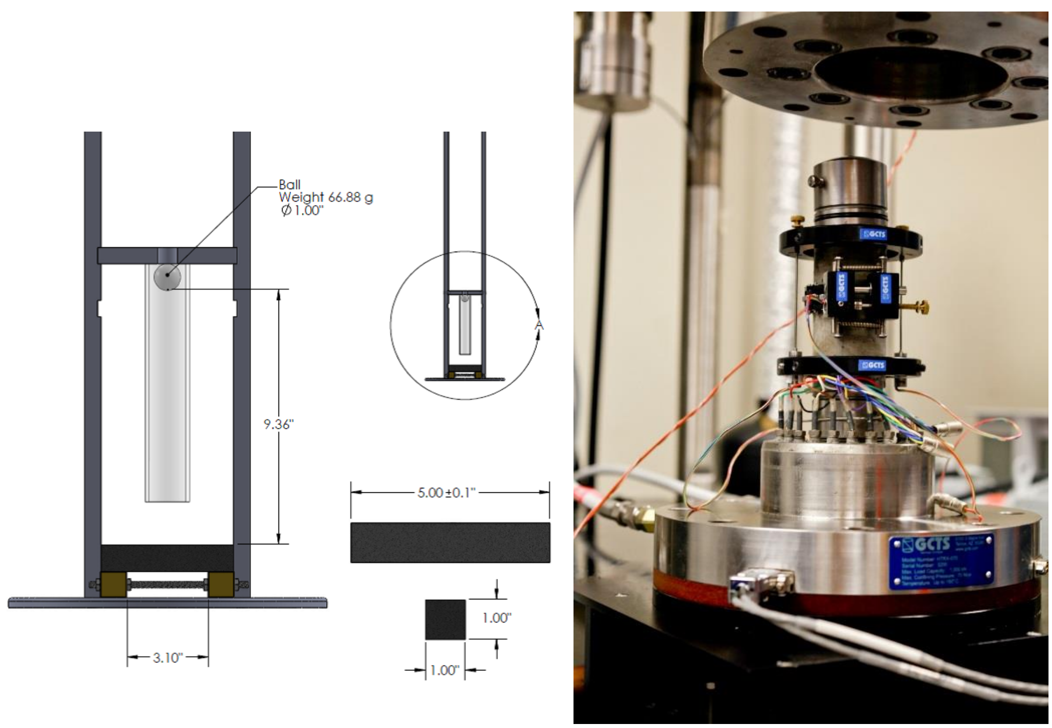

Figure 54 **Impact testing set-up LEFT / Compression testing RIGHT**

An example of the compression testing is shown in Figure 3.

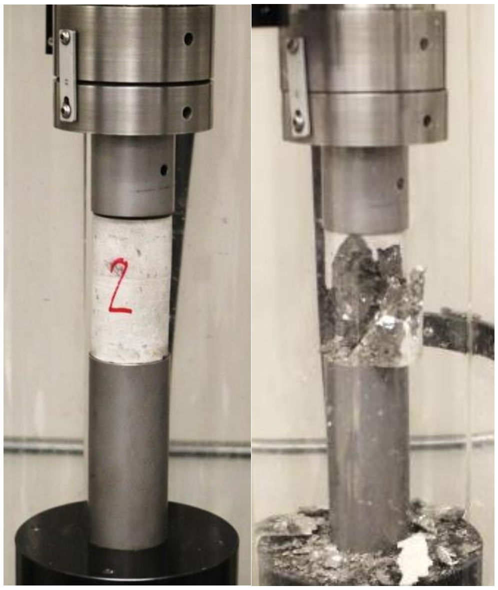

Figure 55 Compression testing – pre-failure LEFT / post failure RIGHT

Figure 56 Tensile testing – Indirect Tension – "Brazil Test"

Figure 57 **Tensile testing – direct test mould and test sample**

Cement blend samples judged to be representative of various depths through the well, typical of those used on GOM, were cured and tested. The data sheets for those cement blends are provided in Appendix A. The results and mechanical properties are summarized below.

Table 5 Cement Property Summary

ID	TVD [ft]	Casing/ Liner	Density [lb/gal]	Young's Modulus [psi]	Poission's Ratio	Strength	
						Compressive [psi]	Tensile [psi]
HDV09675-5-4d	4500	20 in	16.4	1.11E6	0.21	1309	243
HDV09675-5-1b	4200	14 in	12.0	3.18E5	0.26	448	69
HDV09675-5-5a	6700	16 in Liner	13.5	7.35E5	0.28	1858	253
HDV09675-5-2c	12100	9 5/8 in	17.0	2.20E6	0.26	6310	706
HDV09675-5-3b	16500	5 in Liner	-	1.67E6	0.27	5044	571
HDV09675-5-6d	17000	9 5/8 in	16.4	1.67E6	0.27	10732	1114

7.2 FEA Modelling

3D finite element models of the test setups were created using ABAQUS 2017 [23] and solved using the Explicit solver. The Explicit solver was chosen as modelling unreinforced concrete/cement materials can sometimes cause convergence problems in the Standard (Implicit) solver due to the extreme non-linearity caused by cracking, (as was encountered in the global model), which is even more pronounced on the smaller scaled models. The Explicit solver is computationally efficient for analysis of extremely discontinuous events, such as cracking in cement, and can be used to perform quasi-static analyses with complicated contact conditions. Time increments in the Explicit solver are influenced by the overall event time scale, element shape and mass of the system; therefore in order to reduce solve time a combination of mass scaling and reduction of step times were used. To ensure that this method did not influence the solution, energy histories for the systems were checked and the mass scaling used was varied as required.

To reduce computational expense, a one-fourth of the test setup was modelled by using symmetry planes in both the small and large scale models. The extent of the sand bed at the bottom of the cement was limited to reduce the computational expense of the model. The sand is to allow for the placement of cement in the pipes and create a space where the bottom of the cement can be pressurized when testing.

The small scale assembly is shown in Figure 58 and the large scale assembly is shown in Figure 59.

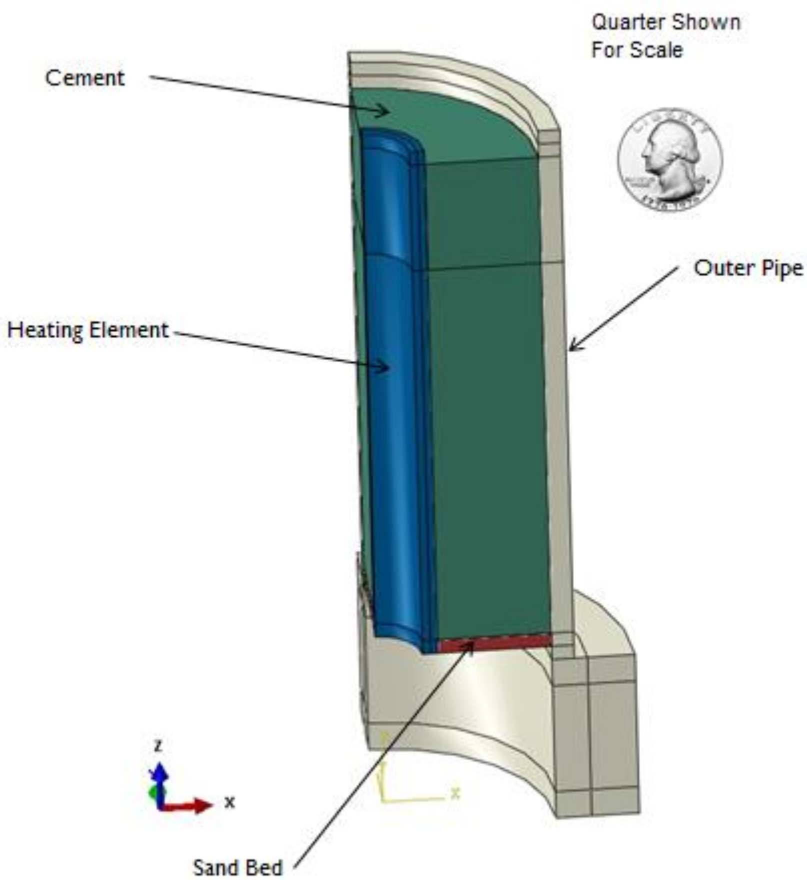

Figure 58 **Small scale FEA model assembly**

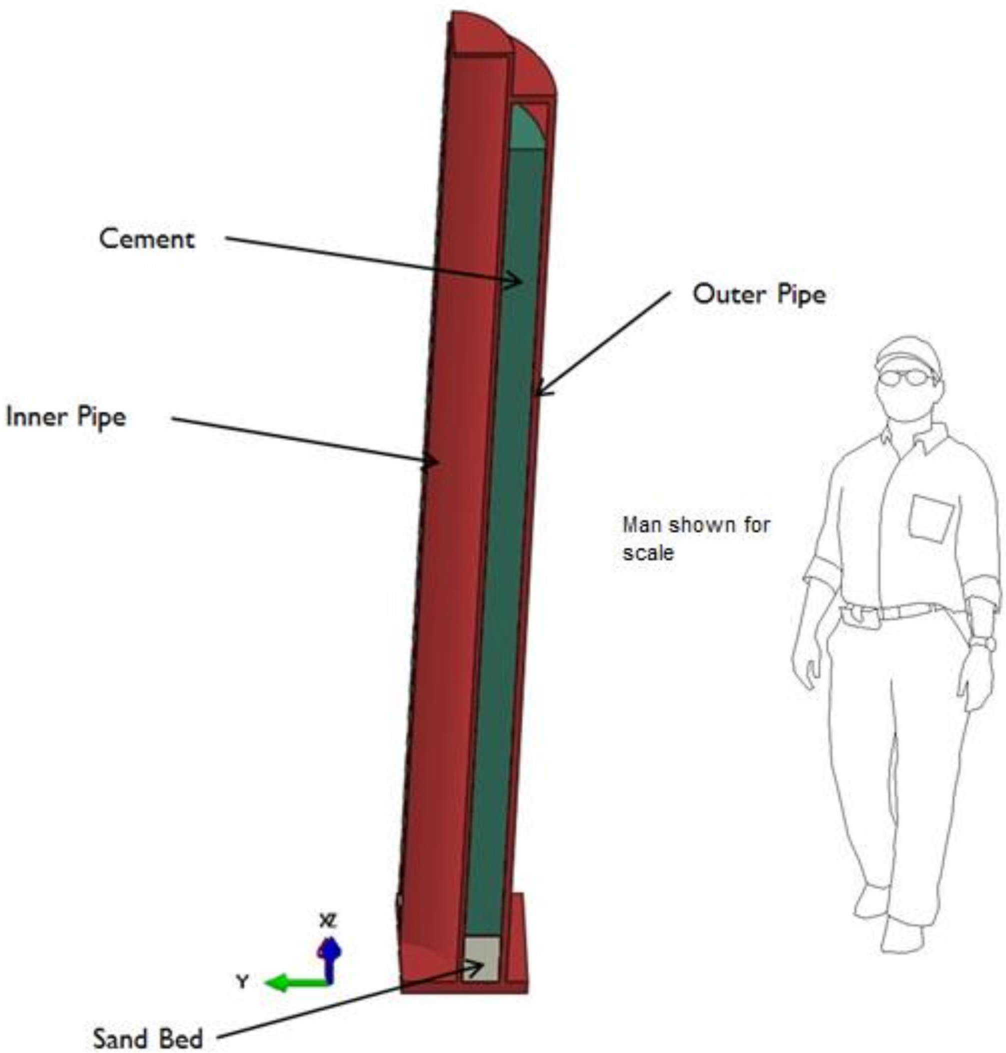

Figure 59 **Large scale FEA model assembly**

Where possible, 8 node reduced integration brick elements (C3D8R) were used. General views of the mesh used in the models are shown in Figure 60 and Figure 61.

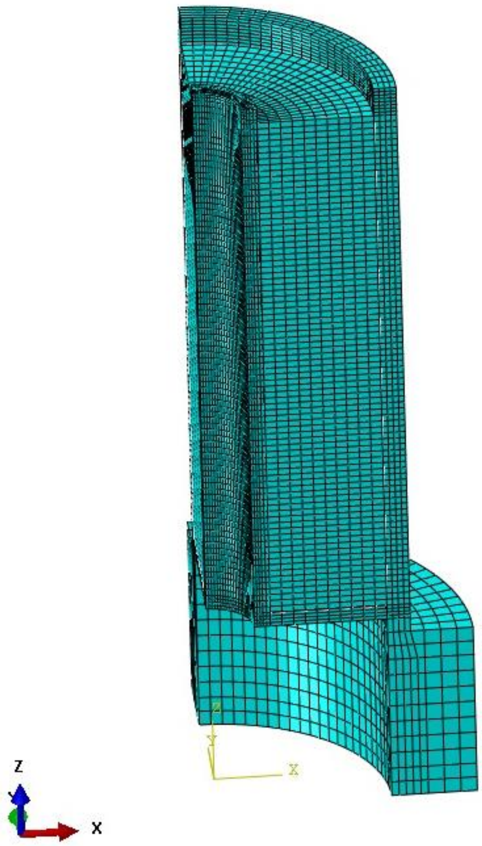

Figure 60 **Small scale FEA element mesh**

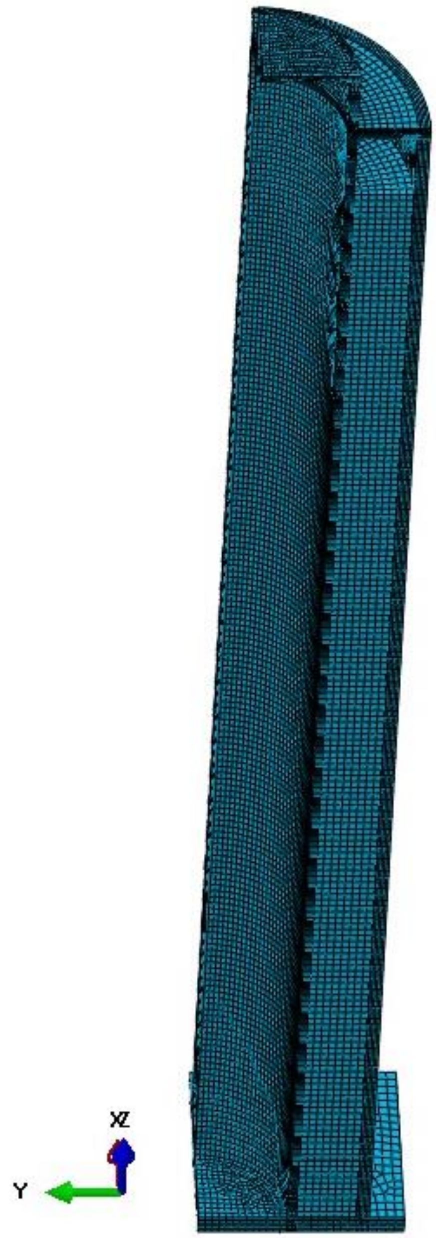

Figure 61 **Large scale FEA element mesh**

Note this view has the x and z coordinates magnified for clarity

7.2.1 Boundary Conditions and Initial Conditions

The small scale and large scale models were restrained by fixing the base of the outer pipe in the vertical and horizontal directions. Symmetry planes were used in the X and Y planes. Boundary conditions for the small scale model are shown in Figure 62. Note that the large scale model is similar.

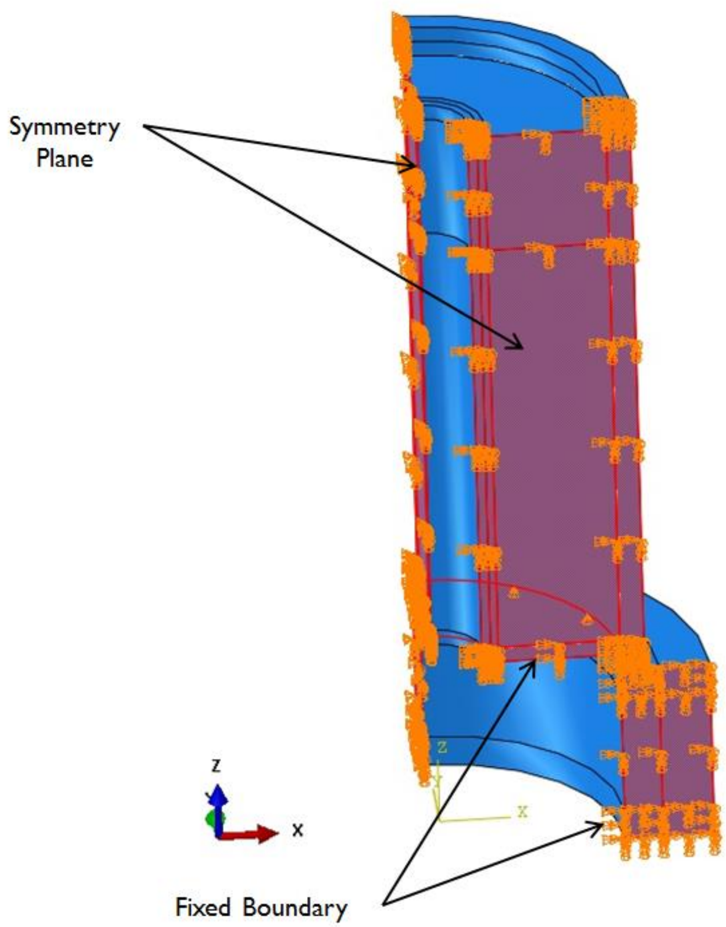

Figure 62 **Small scale boundary conditions**

7.2.2 Contact Interactions

The assembly of parts used to create the test model was held in space using contact interactions true to how the parts interact in reality. Surface to surface contact definitions were defined at the cement to coil tubing interface and at the cement to formation pipe interface. In previous lab validation the contacts were assigned a cohesive behavior utilizing a traction separation based contact enforcement method. However, the cement designs that were applied to the global model contact was modelled as either "hard contact' or using tie constraints for the scale models since contact damage was not explicitly modelled in the global model due to convergence issues. De-bonding and micro-annulus formation is still accounted for by other diagnostic means such as element damage in either tension or compression as well as the plastic strains in close proximity to the cement to pipe locations.

See Figure 63 for typical contact pairs in the small scale model, the large scale model is similar.

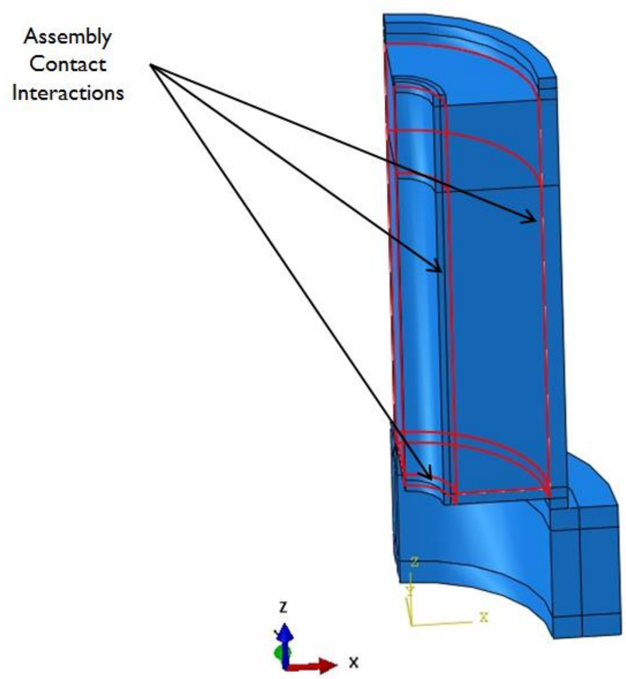

Figure 63 **Small scale interactions**

7.2.3 Cement damage modelling

The cement sheaths were modelled using the concrete damaged plasticity model in ABAQUS. It provides a general capability for modelling concrete and other quasi-brittle materials in all types of structures by using the concepts of isotropic damaged elasticity in combination with isotropic tensile and compressive plasticity to represent the inelastic behavior of concrete. It consists of the combination of non-associated multi-hardening plasticity and scalar (isotropic) damaged elasticity to describe the irreversible damage that occurs during the cracking process. The concrete damaged plasticity material model is interoperable between the Explicit and Standard solvers, therefore the defined materials can also be used in the global FEA models.

The model is a continuum, plasticity-based, damage model for concrete and cements. It is based on the assumption that the main two failure mechanisms are tensile cracking and compressive crushing of the material. The evolution of the failure surface is controlled by two hardening variables, tensile and compressive equivalent plastic strains that are linked to failure mechanisms under tension and compression loading, respectively.

The fracture energy criterion was used to model the cements brittle behavior by using a stress-displacement relationship. The stress-strain behavior of the cement in uniaxial compression outside of the elastic range is modelled by using compression hardening and strain softening.

The concrete compression damage and concrete tension damage optional parameters were used to simulate the loss of stiffness of the cement as damage occurs. Maximum compressive stiffness reduction was set to 99% and 90% for tension. Once these values are reached a complete loss of stiffness is assumed to occur. Element deactivation was enabled to remove these elements from the stiffness matrix at complete failure.

7.2.4 Thermal analysis approach

Thermal loads were applied by means of a sequentially un-coupled thermal stress analysis. To accomplish this, a transient heat transfer analysis was first solved. The nodal temperature values from the heat transfer analysis were then mapped onto the structural solution model. The material definition in the structural model included a thermal expansion coefficient and thus the model developed thermal strains with the addition of a ΔT and thermal stresses when expansion was resisted by the stiffness of the structure. Since the heat transfer analysis and stress analysis are in different time period thermal properties and convection coefficients were converted into the appropriate time scale.

A heat transfer analysis was performed for the small and large scale models. The temperature was varied over time using the load amplitude feature within ABAQUS to replicate the thermal cycling that was performed in the lab testing. A complete thermal cycle for the small scale testing consisted of activating the interior heating element for 150 minutes at approximately 215°F, then turning the heating off and then chilling the exterior of the testing fixture at 50°F for 150 minutes. The heat transfer analysis results were then mapped on to the structural model and allowed to cycle up to 50 complete cycles. The small scale testing consisted of curing the cement in the fixture at 190°F and then allowing the fixture to cool back to ambient; therefore the initial temperature of the large scale model was assumed to be at an ambient temperature of 72°F. The results from the small scale heat transfer analysis are shown in Figure 64. Note that the cooldown from ambient was accounted for but not shown in the figure.

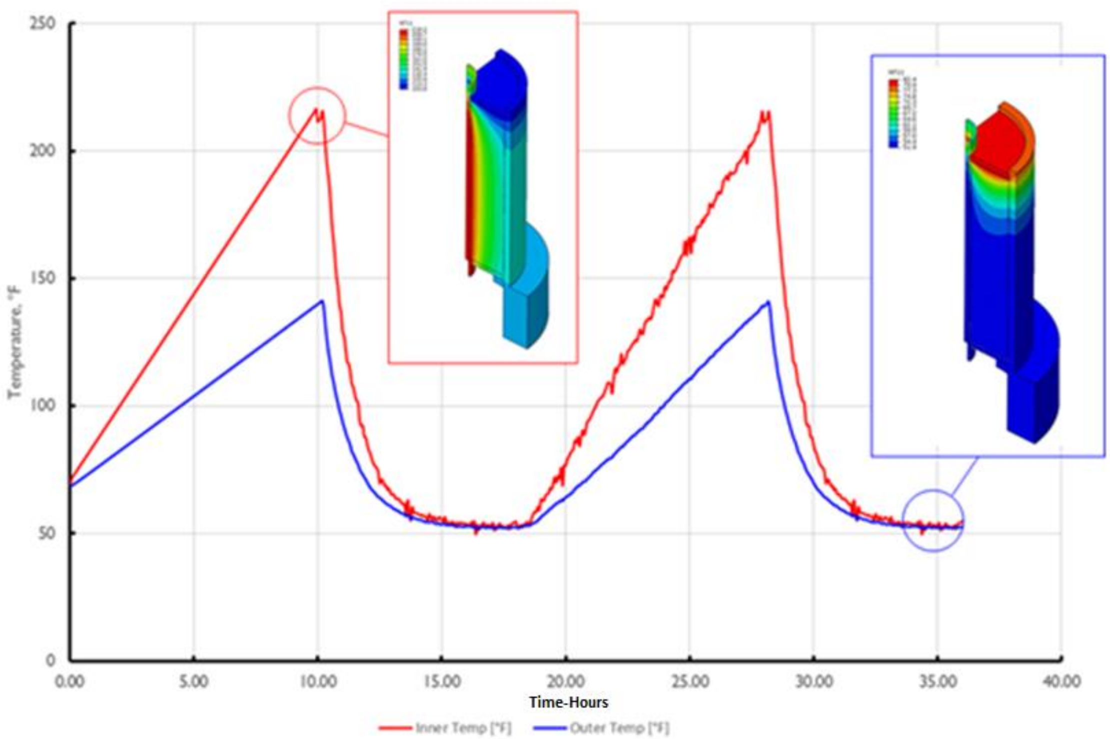

Figure 64 **Small scale heat transfer analysis results**

Thermal cycling for the large scale test was similar to the small scale with the exception that the interior pipe was cooled by circulating chilled water and the exterior was heated. A complete thermal cycle for the small scale testing consisted of circulating chilled water through the interior pipe for 150 minutes at approximately 50°F and then turning off and then heating the exterior of the testing fixture at 230°F for 150 minutes. The heat transfer analysis results were then mapped on to the structural model and allowed to cycle to failure or up to 50 complete cycles.

The large scale testing consisted of curing the cement in the fixture at 190°F and then subsequently starting the temperature cycling without allowing the fixture to cool back to ambient; therefore the initial temperature of the large scale model was assumed to be at a temperature of 190°F. The results from the large scale heat transfer analysis are shown in Figure 65.

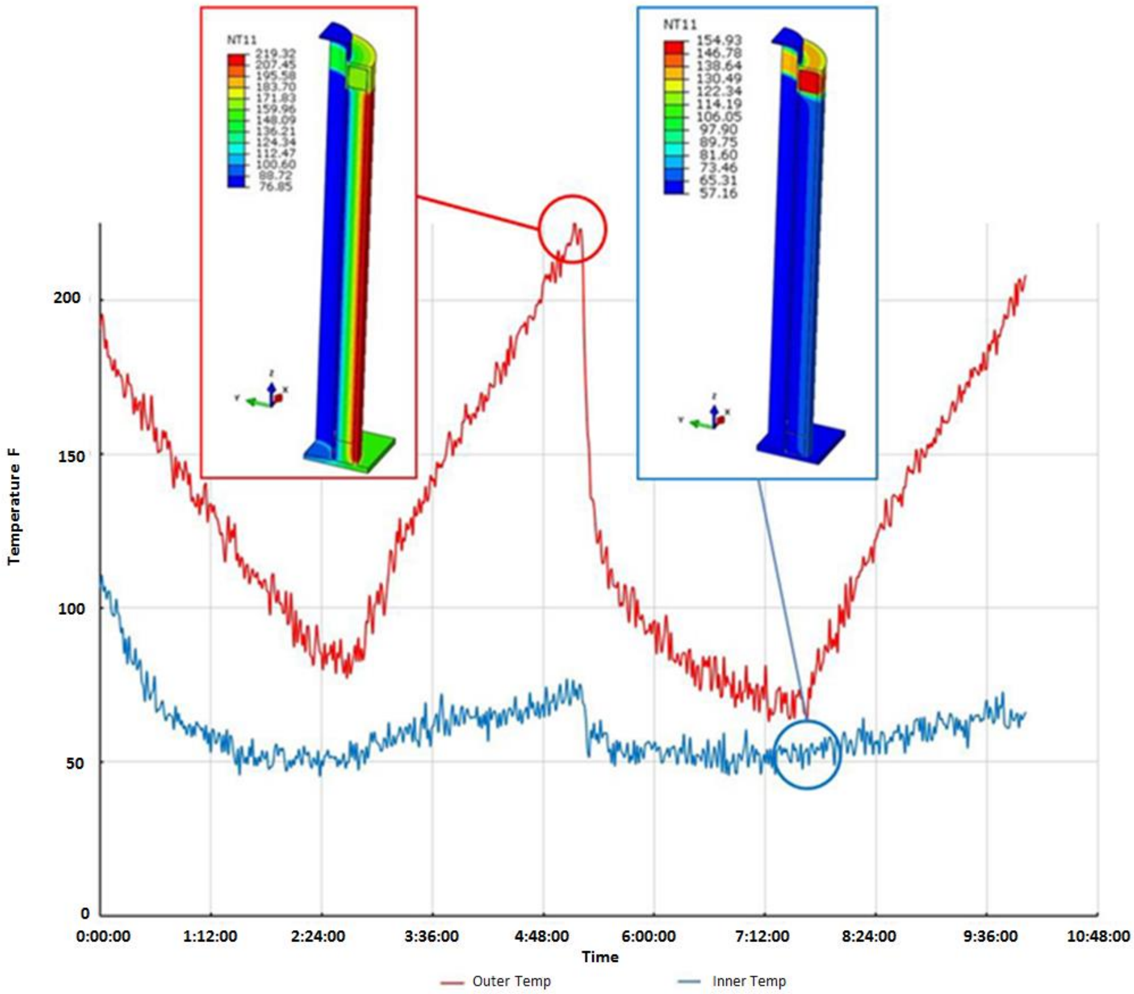

Figure 65 **Large scale heat transfer analysis results**

7.2.5 Thermal properties

Thermal expansion coefficient, conductivity and specific heat values for the cement mixes were determined by CSI and are shown in Appendix A. In order to reduce computational time, average values of the cement thermal properties were used to reduce the number heat transfer analysis required.

The thermal expansion coefficient for steel was assumed to be 6.7x10-6 in/in-°F and 4.4x10-6 in/in-°F for the soil.

7.2.6 Thermal boundary conditions

Surface boundary conditions were defined by giving the outer surfaces a convection coefficient and a sink temperature (water temperature or ambient air temperature). The surfaces exposed to water were applied with a film coefficient that was set to 580 W/m2K and for surfaces exposed to air a film coefficient of 15 W/m2K was used.

7.3 Small Scale Lab Tests

CSI performed the small scale thermal tests on the cements previously identified in Table 5

The thermal shock test apparatus is explained below and shown diagrammatically in Figure 66.

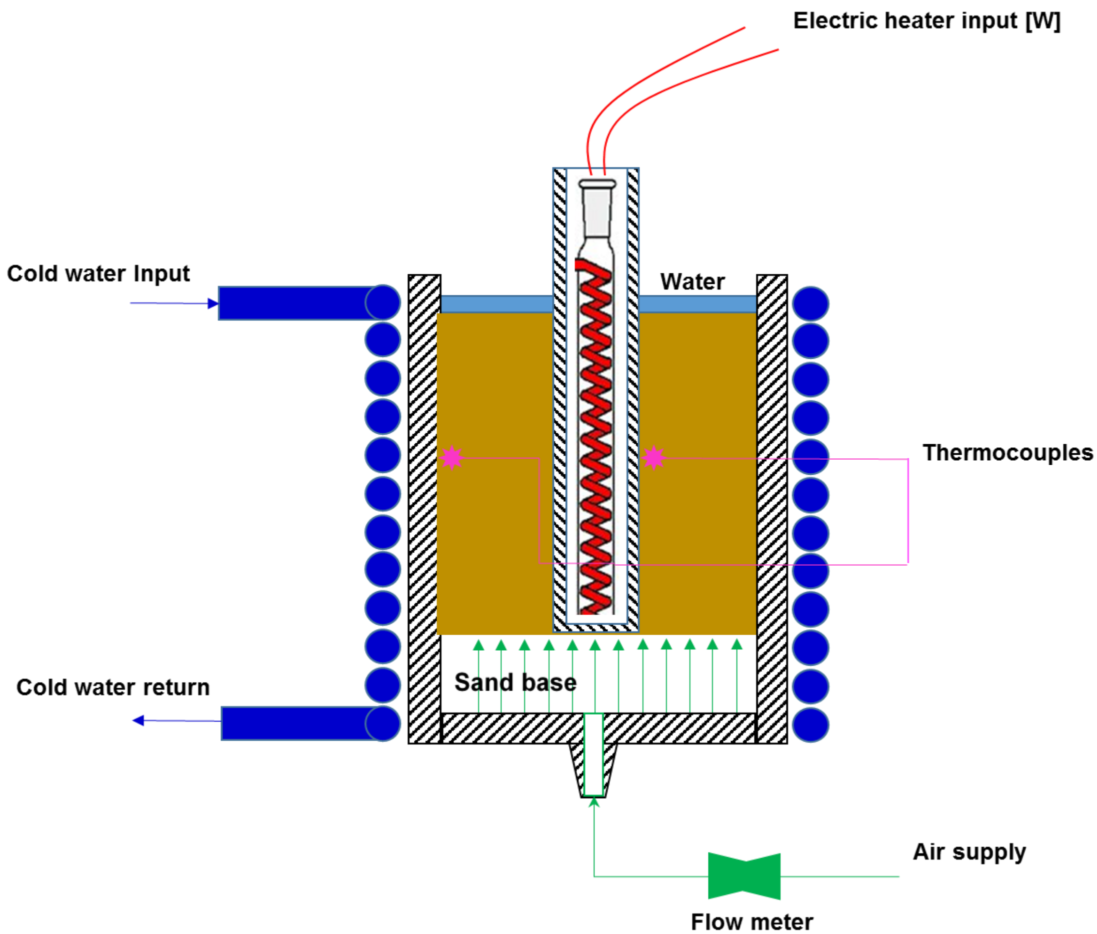

Figure 66 Thermal shock test schematic

The test specimen comprises of an electric heater element embedded in a cylinder of cement which itself is surrounded by a metal sheath inside a metal cylinder. A brass coil supplying cooling water then surrounds the outside metal cylinder.

A compressed air supply charges the base of the cement sample and flow is monitored through an inline flow meter. Thermocouples are embedded in the cement, just inside the outer wall and just outside the inner wall respectively.

Once cured, the test begins by heating the sample for a prescribed time until both thermal couples measure steady temperatures. Then the heating input is switched off and the cold water flow switched on to cool the sample. The rates of heating and cooling can be adjusted to accommodate different temperature ramps by adjusting the energy input and the cooling water temperature. This process is repeated to subject the sample to repeated thermal shocks until air bubbles appear at the top of the sample indicating the cement has failed through the height of the sample.

The actual test lab test setup is shown in Figure 67.

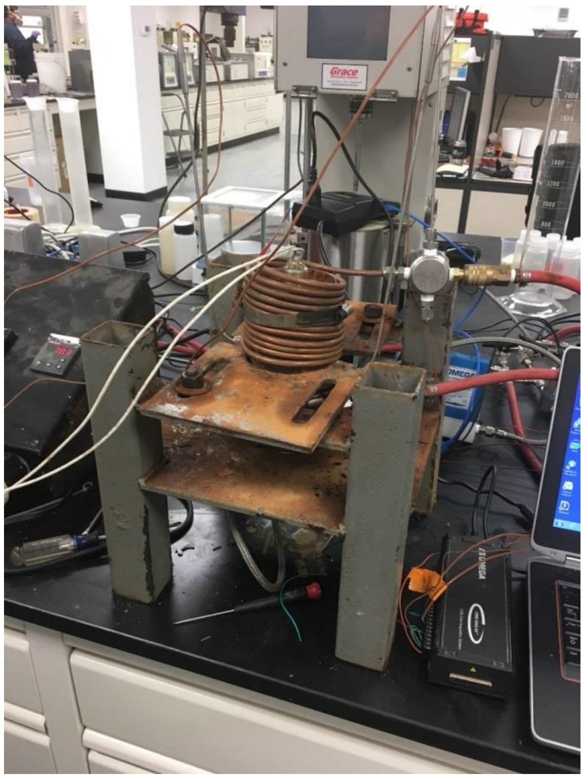

Figure 67 Thermal shock test apparatus

7.3.1 Small Scale Thermal Shock Testing – Results

Instant failure occurred on some of the tests where the air passed through the cement sample immediately; suggesting a failure of the curing process, see Figure 68. Test that failed immediately were attempted again and successful results were achieved in all but two of the cement designs as shown in Table 6. An example of a successful test is shown in Figure 69. This sampled eventually failed through a delamination of the cement to casing bond on the outer radius of the cement.

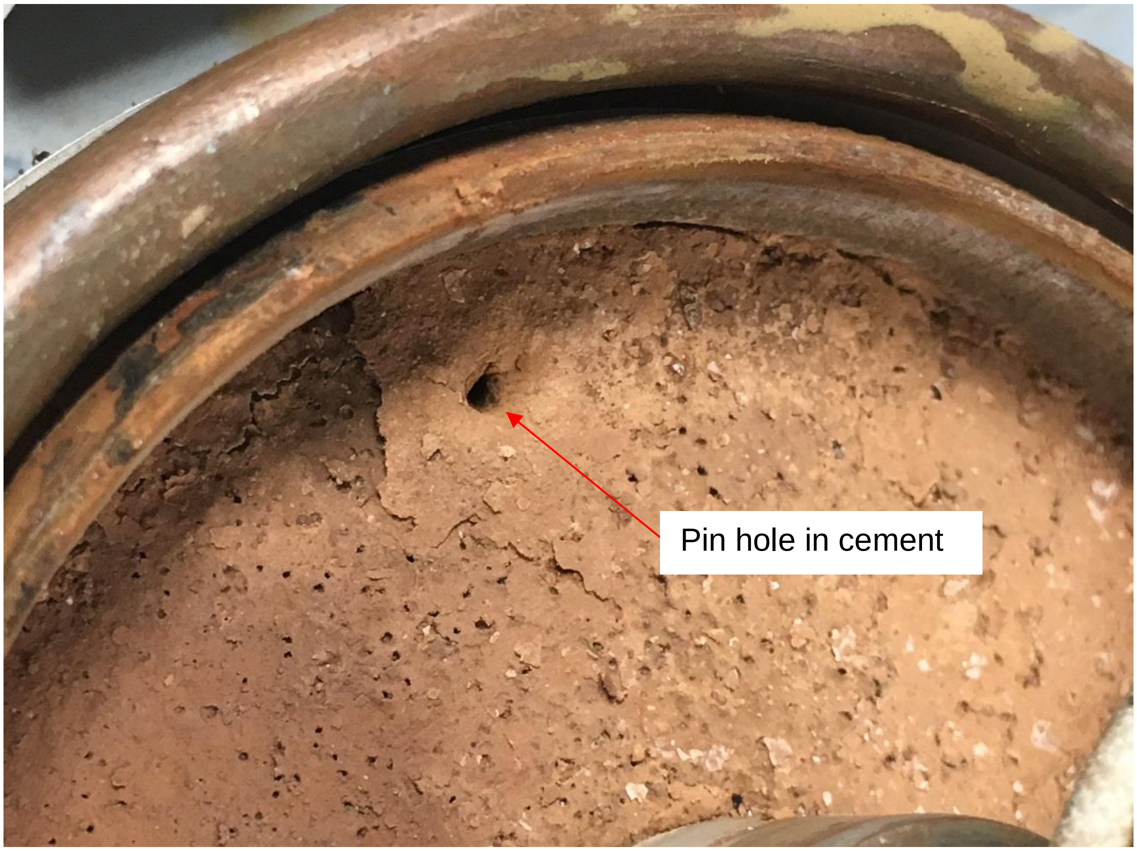

Figure 68 Thermal shock test fail – pre-mature failure

Figure 69 Thermal shock test – failure on outer radius of cement

The cycle history for a typical sample is shown in Figure 70; note that the number of cycles vary per sample.

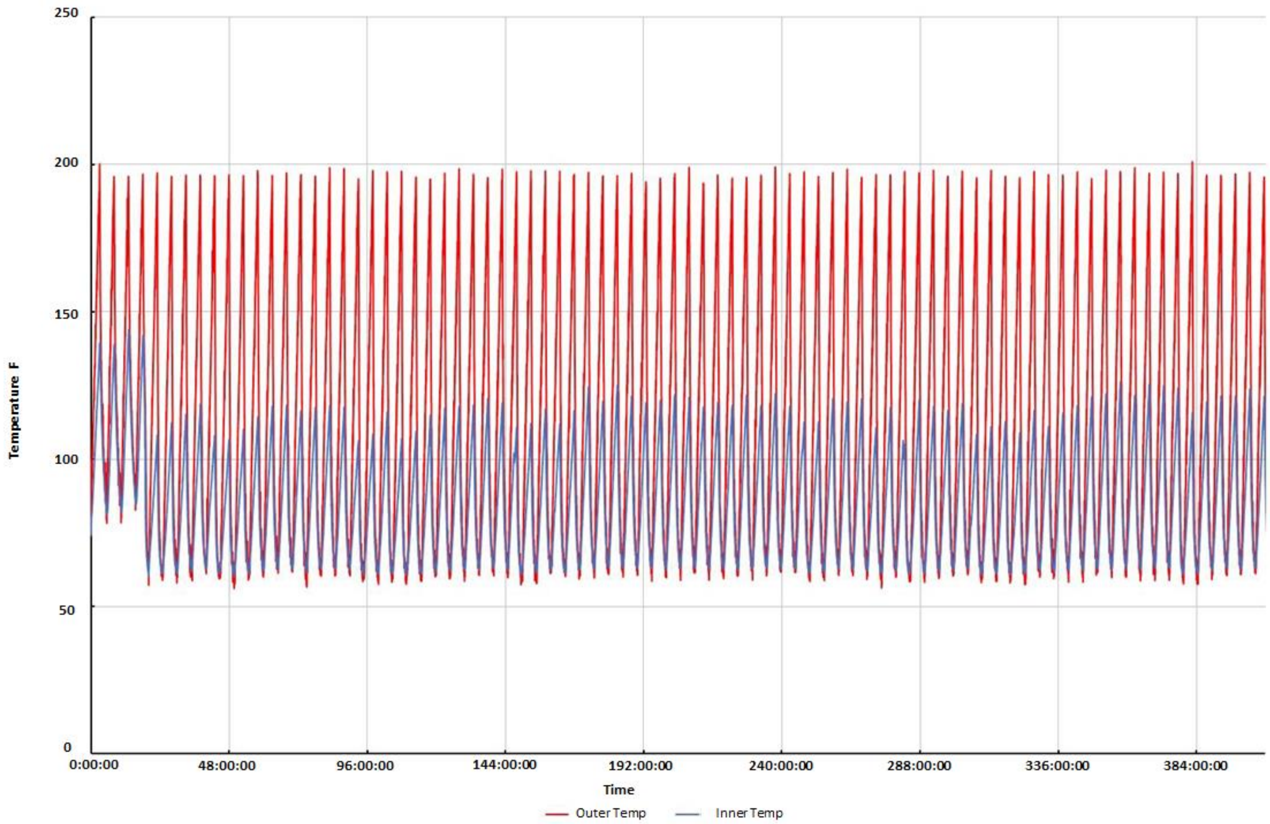

Figure 70 Thermal shock example – cycle history

The structural response for HDV09675-5-2c is shown in Figure 71. Note the magnitude has been capped to identify potential leak paths. A possible leak path is represented as the yellow line. This failure mode was observed to be similar for the other samples that failed as well.

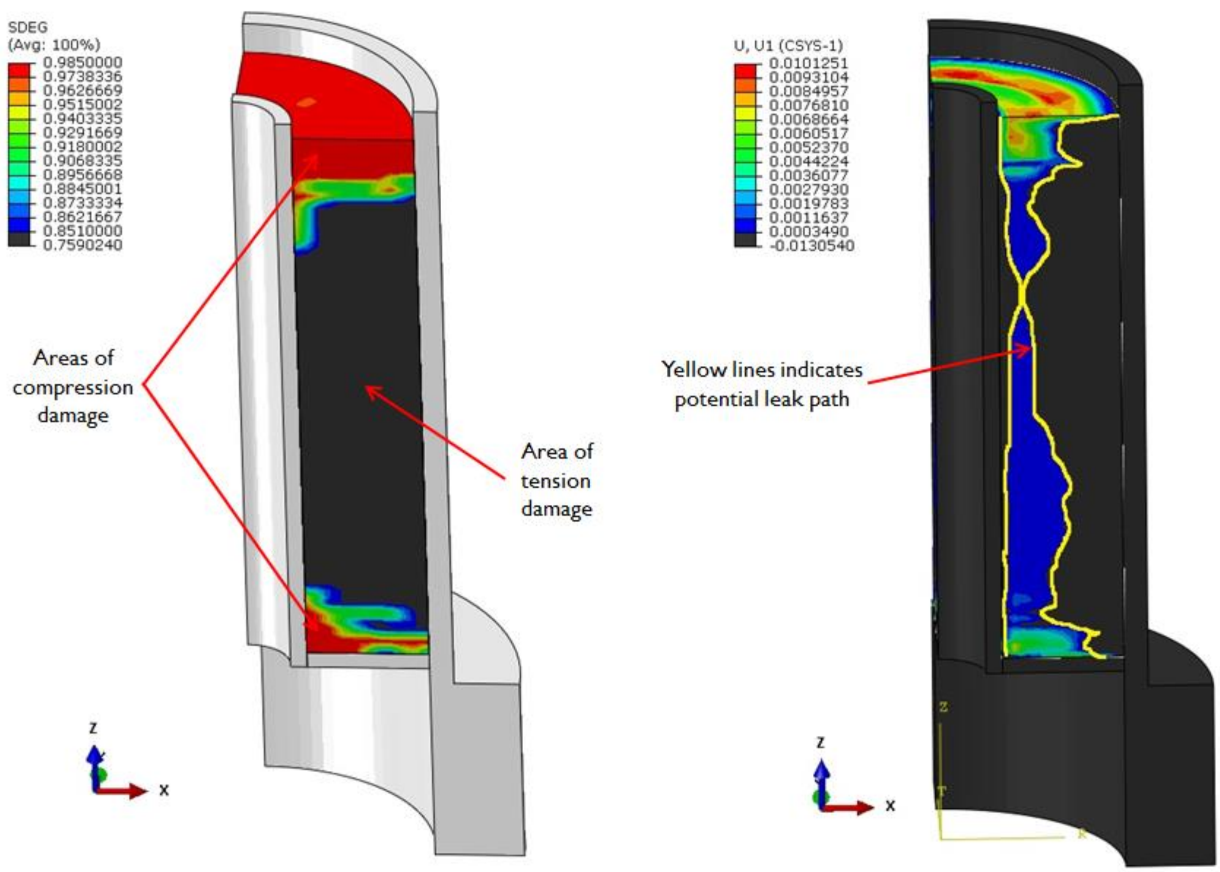

Figure 71 **Small scale failure example – FE response**

Table 6 Comparison of FEA Results and Small Scale Tests

ID	Lab results		FEA Results	
	N_{TEST}	Location	N_{FEA}	Estimated location
HDV09675-5-4d	70 cycles	Outer pipe	50 cycles	No fail up to 50 cycles[1]
HDV09675-5-1b	Instant Failure	Inconclusive	1 cycle	Path goes from inner to outer
HDV09675-5-5a	No Failure	N/A	No Failure	No fail up to 50 cycles
HDV09675-5-2c	8 cycles	Outer	7 cycles	Path goes from inner to outer
HDV09675-5-3b	Instant Failure	Inconclusive	2 cycles	Path goes from inner to outer
HDV09675-5-6d	No Failure	N/A	50 cycles	No fail up to 50 cycles
^FEA was performed up to a max of 50 cycles based on the low cycles to failure on early tests performed and prior to all of the lab tests completed.				

7.4 Large Scale Lab Tests

Four attempts to perform the large scale tests were tried using the HDV09675-5-2c mix. However, only one was able to achieve usable data suggesting that the sealing of the test fixtures is sensitive to the curing process. The test that was successfully run failed after only a few cycles. The results of this test are discussed later on. The schematic for the large scale test fixture is shown in Figure 72.

[1] This FEA model will be re-started and the cycle count will be increased until failure – results will be incorporated into final report.

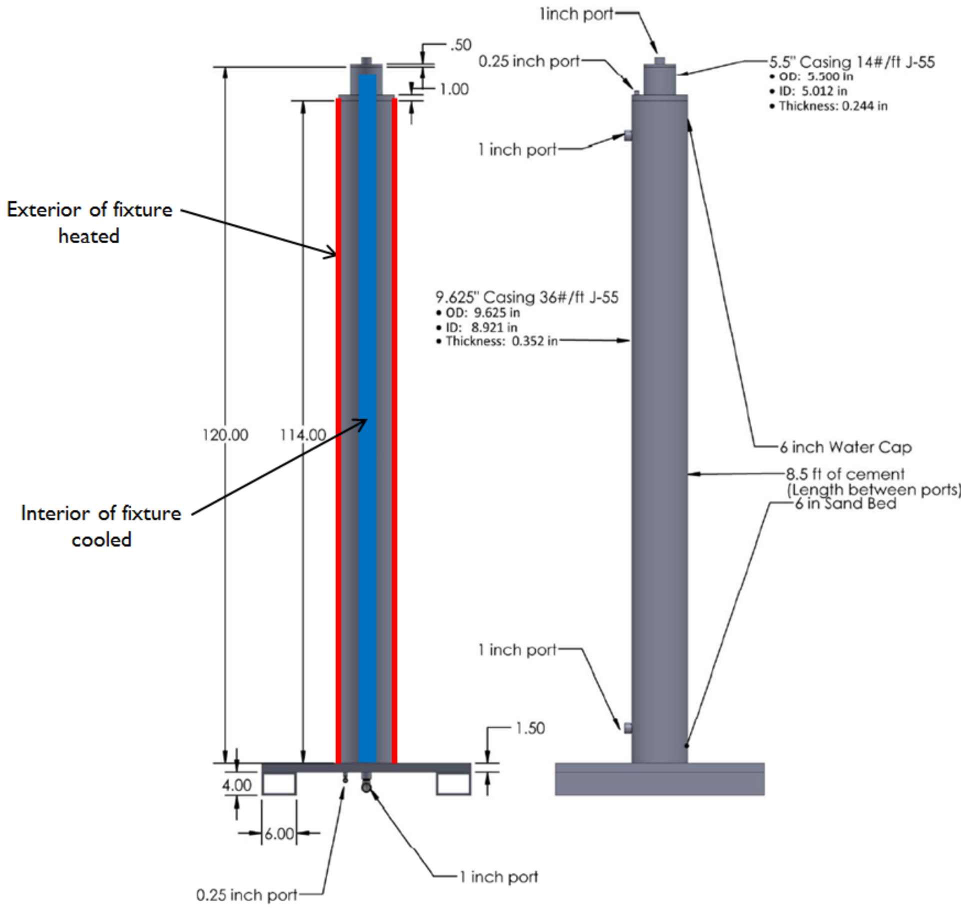

Figure 72 **Large scale test setup**

The test specimen comprises of a heater on the exterior of the fixture. Chilled water is circulated through the interior pipe to cool the system.

A compressed air supply charges the base of the cement sample and flow is monitored through an inline flow meter. Thermocouples are embedded in the cement, just inside the outer wall and just outside the inner wall respectively similar to the small scale tests.

The heating and cooling can be adjusted to accommodate different temperature ramps by adjusting the energy input and the cooling water temperature. This process is repeated to subject the sample to repeated thermal shocks until air bubbles appear at the top of the sample indicating the cement has failed through the height of the sample.

7.4.1 Large Scale Thermal Shock Testing – Results

As mentioned previously the test that was successfully run failed after only a few cycles in the lab testing. Lab testing confirmed that the seal failed at the inner diameter of the outer pipe. The damage observed in the FEA analysis indicates that failure of the cement occurs at about 1 to 3 cycles. Significant damage starts to initiate at the onset of the first cycle and progresses rapidly throughout the cycle. The FEA results for the large scale test are shown in Figure 73.

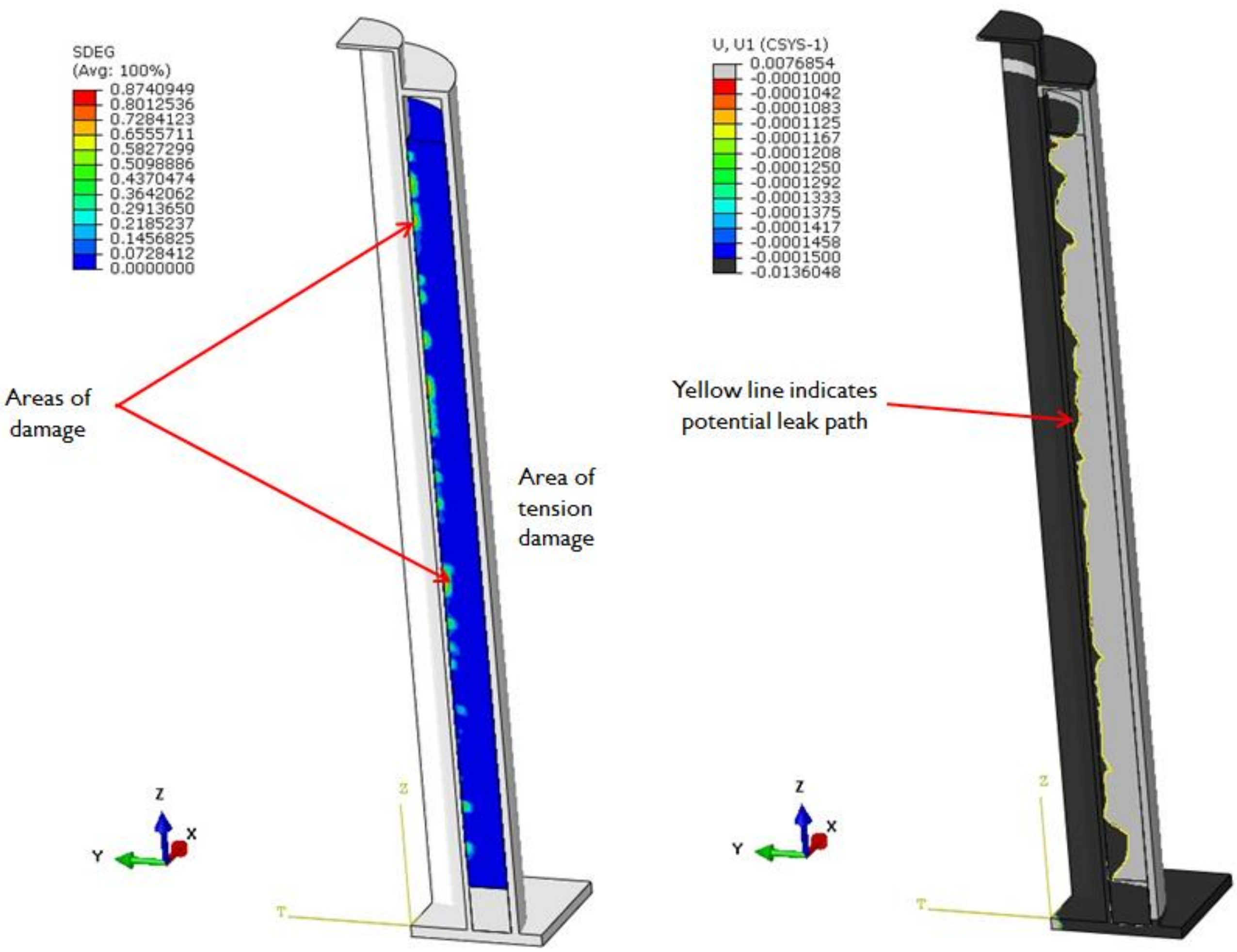

Figure 73 **Large scale FEA at failure**

7.5 Large Scale Thermal Shock Testing - Conclusions

The lab testing and FEA modelling performed show that the FEA analysis can predict the failure of the cements used in the wellbore with very good accuracy.

Although some of the samples experienced immediate failure, likely as a result of the thermal cycle induced by the curing process, it was observed that the same mixes experienced early failure in the FEA as well. It was generally observed that the samples that did not fail or had a significant number of cycles to failure in the lab also performed well in the analysis. It should be noted that cement response is influenced by many different factors such as loading conditions, confinement, etc. Meaning that one mix that does poorly in a certain scenario may perform well in another.

A positive validation of the modelling techniques was provided by the HDV09675-5-2c cement sample. It showed an excellent match at small scale test as it had 8 cycles to failure in the lab and approximately 6 cycles to failure in the FEA. The large scale test had immediate failure in one attempt and failure at 2 cycles in the lab and approximately 1-3 cycles to failure in the FEA.

Therefore a high degree of confidence in the modelling methodology was gained.

8 PROPOSE MITIGATION TECHNIQUES

Conventional cement systems are at times unable to maintain an effective seal under cyclic stressing conditions in the changing environment of the wellbore. These stresses are from thermal changes, and pressure changes such as stimulation activities like fracturing the wellbore. However, the industry has improved the cement systems that are used in wells.

- Computer simulations and models can help in the cementing design process for these challenges. It was found that many operators are including some type of computer simulations. The use of FEA programs to gain insight to better determine how the cements and mechanical barriers are behaving will help improve the cement systems and have the potential to provide information that can improve the software currently being used.
- Cement to casing bond is dependent on numerous mechanical properties, not just compressive strength. While one cement system may not be the best selection for all situations it was observed that the cements that exhibited more ductile behavior performed better in the lab and in the FEA simulations. These mixes generally had a lower Young's Modulus coupled with higher compression and tensile strengths.
- Excellent cement job execution is also critical to create a good bond. Mud removal, density control and other aspects of cement placement are important in creating a durable bond. The consequences of a poor cementing job are difficult to quantify. A better understanding of the effects of poor cementing on the durability of the bond can be gained by using FEA similar to the simulations performed in the lab in this project. The FEA could be used to perform sensitivity studies to investigate the wellbore response with reduced bond strengths.
- Quality control of the cement blending and mixing should be monitored to ensure that the strengths placed in the wellbore meet or exceed the intended design.

8.1 Cement barrier failure modes

Stresses induced on typical deep-water wells by stimulation operations result from increased casing pressure and thermal shock/cycling of the casing by fracturing fluids. The magnitudes of these stresses are not generally sufficient to be the primary cause of damage to the casings. However, the stresses can be sufficient to cause failure of the cement or to destroy the bond of cement to casing or cement to formation. This failure of the cement to casing bond can potentially increase the loading of the casing overstressing it and cause a failure.

Potential failure modes of cement from thermal shock during the combination of production-shut in cycles and stimulation can be attributed to tensile stress, compressive stress, and shear stress. The casing-cement-formation system integrity depends on mechanical properties of the cement such as Young's Modulus, Poisson's Ratio, and tensile strength. Cement failure in tension during stimulation is considered very common due to the intrinsically low tensile strength of most Portland cement systems. This can be amplified if the low tensile strength system is has a higher Young's Modulus.

Additionally, the quality of cement placement and control of unwanted fluid migration in the cemented annulus after cement placement dictate the initial condition of the system and affect the potential for stress-induced seal failure. Finally, since Portland cement mechanical properties are governed by extent of chemical hydration occurring in the cement, where this hydration rate depends on time, temperature and cement design, the mechanical properties of the cement component must be measured after curing for appropriate times at simulated down-hole conditions to accurately assess performance.

In addition to time dependence, mechanical performance of Portland cement can degrade under cyclic stress that is far below failure stress for the material. This degradation is due to the porous nature of set Portland cement and localized failure of the pore walls that can result from stresses in the elastic region. Thus, stresses lower than failure strength of cement can cause plastic strains. Stress repetition from thermal shock/cycling can result in additional plastic strain thus creating channels that allow flow at lower-stresses.

In general, failure of the casing-cement-formation system as a result of thermal shock-induced stress is complex and is not accurately described by solely one or two cement mechanical property values. Primary failure points are within the cemented annulus. Failure is governed by cement composition, quality of cement placement, extent of hydration as governed by time interval between cement placement and stimulation treatment, and stimulation treatment temperatures and pressures.

8.2 Mechanical barrier failure modes

In general, a failure to a casing/tubular in the wellbore would occur after a failure or significant damage occurred within the cement annulus. While the design of the tubulars typically does not consider thermal shock explicitly, it is accounted for in the thermal loading applied. If a failure to a tubular is the primary cause of failure in the wellbore, the most likely cause will be due to a failed connection. This type of failure is not typically caused by thermal shock alone, but rather an additional factor such as:

- Improper design or exposure to loads exceeding rated capacity
- Failure to comply with make-up requirements
- Failure to meet manufacturing tolerances
- Damage during storage and handling
- Damage during production operations
  - e.g., corrosion and wear

The most common failure modes of the tubulars would be characterized as:

- Ballooning
- Collapse
- Connection Failure

Existing design tools are considered adequate to design tubular barriers for thermal shock, see Section 4.2. Mitigating against the effects of temperature variation in the design of the tubulars depends upon the failure mode but design solutions are likely to be available provided the temperature loading is accounted for in the first instance.

Mechanical seal failure could be caused by high temperatures but provided the design basis for the seal components account for the temperatures and the temperature range the seals will be exposed to then the seal designs should be able to mitigate against the risk of barrier failure.

In the case of the HPHT Deepwater wells being considered in this project, thermal shock caused either by shutting in a producing well or by stimulating a well should not pose a particularly onerous design constraint for mechanical seals at or near the mudline. Seals near the mudline, for example in the well head, are likely to benefit from the temperature being higher in the bore than in the environment, provided the seal materials are rated for the highest temperatures they will be exposed to. The temperature gradient from bore temperature to environment should assist sealing, as the inside will want to expand rather than contract assisting rather than compromising sealing. For seals deeper in the well, for example the production packer, the opposite is true and cooling of the inner string, for example during stimulation, would result in a less favourable temperature gradient. But provided the temperature conditions surrounding the packer are accounted for in the packer basis of design, the risk of packer failure can be mitigated through design.

9 GUIDELINES AND BARRIER RISK RANKING

The work performed in this study has highlighted that thermal shock can damage the cement barriers throughout the well bore. The magnitude of the damage to cement is governed by the amplitude of the thermal shock and design of the cement. A significant finding of the simulation work performed is the importance of designing cement sealants for durability up and down the well. Intervention or remediation can induce sufficient thermal stresses to induce cement failure in well locations not usually considered high risk (mud line or mid well). While induced stresses may not be as high as those deeper downhole, typical mechanical properties of the cement design for these locations may be much lower for those seemingly lower-risk applications. If the cements designed for these regions are not subjected to extra design evaluation the risk of seal failure increases.

The risk of cement barrier damage and hence barrier failure is also dominated by stimulation conditions rather than the production/shut-in cycles as the amplitude of the thermal shock is greatest in these circumstances. Provided appropriate consideration is given to thermal shock in the cement design, the risk of barrier failure can be mitigated. It should be noted that this project considered a maximum bottom hole temperature of 350˚F. As oil and gas exploration goes even deeper and hotter, then as bottom hole temperatures exceed 350˚F the risked posed by thermal shock will increase.

While the term thermal shock is not prevalent in most of the regulations surrounding the construction of a well, CFRs, [28,29,30], do capture the need to address the well design conditions throughout the life of the well and for the cement design to be certified by a licensed professional engineer that is it fit for purpose, [29]. CFR 250.415 makes reference to API RP 65 Part 2, [31], which does acknowledge that the mechanical parameters of the cement are critical to the integrity of the cement over the life of the well. The API also acknowledges that cements with high tensile strength and low Young’s modulus tend to resist damage more effectively. This is supported by the findings of this study as this combination performed the best. CFR 250.415 further requires a written description of how the well designer has evaluated the best practices included in API RP 65 Part 2. Therefore there does not appear to be a need to generate a raft of new guidelines concerning well design to accommodate thermal shock, however, temperature variations within the well lifetime and how they will be accommodated by the cement design should be given greater scrutiny to ensure the intent of the existing regulations is met.

From the work performed the impact of thermal shock on the cement system appear to be dominated by the amplitude of the temperature change experienced by the well, rather than the rate of change of temperature. Design guidelines and recommended practices for HPHT well design do emphasise the need to consider the well conditions the barrier system will be exposed to over the life of the well, even if the specific term thermal shock is not used regularly.

For mechanical barriers, both the amplitude and the rate of change of temperature could be a more important factor. If there is a significant temperature gradient across the barrier and that gradient changes with operating conditions, the sealing effectiveness could be impacted, albeit perhaps only temporarily. Therefore as well as taking into account the temperature amplitude the differential temperature across the barrier and how that changes with time should be accounted for in the design of the barrier. Under normal production-shut-in cycles the timescales of temperature change should limit this effect but the impact may be greater during stimulation when a sudden cooling of the well bore is much more pronounced. However good design practise and a proper understanding of the loads those barriers are exposed to should be adequate to mitigate the risk of barrier failure.

The mechanical barriers deeper in the well may be more susceptible than at the mudline. At the wellhead the environment is always colder than the bore, even during stimulation, and so the temperature gradient in the well cross-section should act in favour of the seal. The risk of this type of failure is consider low since it can be mitigated through design, provided temperature is correctly address in the design basis of the barrier elements.

Tubulars are undoubtedly affected by the temperature changes resulting from thermal shock but as with mechanical seals the design tools currently available should be sufficient to allow barriers to be designed to meet the temperature changes over the life of the well provided temperatures and temperature changes over the well life and their impact on the cement sheaths are adequately addressed at the design stage. It is also important to note that some design tools widely used for that purpose assume a competent cement sheath exists at all times. The integrity of the tubular or other aspects of the well design could be compromised if the cement fails. This emphasises the importance of getting the cement design correct. Furthermore, prudent engineering design should examine the impact of a degraded cement sheath on the tubular system.

In attempting to rank the risk to the cement barriers it would be convenient to simply use the magnitude of thermal shock as the governing metric. However an important conclusion of this study is that, while clearly the highest thermal shock occurs deeper in the well during stimulation, the damage to the barrier, if poorly designed, can extend across a significant length of the well and the vulnerability of the cement barrier to temperature change is dependent upon the design of the cement. Lower modulus high tensile strength cements tend to perform better in response to large changes of temperature but it is also apparent that one cement design that does well in one circumstance may not perform as well in another and simple designing for the maximum compressive strength may not be sufficient to produce a cement barrier that will last the lifetime of the well. Use of appropriate analysis, such as described in this study, would help ensure the cement is fit for purpose regardless of its location in the well.

Overall risk ranking for the barriers within a well is primarily a task that should be carried out on a well by well basis taking the overall well integrity into account. While it may be more likely that a cement barrier is damaged during the operating life of the well, leading to barrier failure if the damage is extensive enough, the impact of that failure would be governed by the overall barrier philosophy of the well design. A risk assessment of the well's integrity should be carried out and the susceptibility of the cement designs to temperature change throughout the entire well should be included as part of that risk assessment. This study recommends that approach rather than attempting to produce a generic risk ranking for barriers in a well.

10 ACADEMIC SCRUTINY

University of Texas at Austin has been added to the team to provide independent scrutiny of the FE and testing activities, Task 4 and 5, as well as providing input during Task 6 which will look at mitigating the effects of thermal shock.

Dr Richard Schultz was approached by the WWC project team to engage with them on this project as an Academic Partner. This engagement draws upon Dr Schulz's work in reservoir geomechanics and subsurface asset integrity as Senior Research Scientist with the Center for Petroleum and Geosystems Engineering at The University of Texas at Austin (UT), and industry-funded research programs at UT including the Fracture Research and Application (FRAC) Consortium. The Petroleum and Geosystems Engineering Department's undergraduate and graduate degree programs were consistently ranked as #1 in the nation (again through 2018) by U.S. News and World Report; the Center is the research arm of the Department. While at UT Dr Schulz was also an instructor in subsurface integrity with TopCorp, a multi-university consortium that provided technical training to state oil and gas regulators; prior to that he was Principal Geomechanicist and a key member of the company-wide subsurface containment assurance team at ConocoPhillips.

Dr Schulz's role in this project is to support and assist the Wild Wells team in three main tasks described above, from a partnering and advisory role; the intention is not to duplicate efforts but to apply his academic perspective to supplement the execution and interpretation of the technical work of these tasks.

Several meetings between U of T and WWC and CSI have taken place and U of T has reviewed the work performed by the WWC team.

11 REFERENCES

1 Topic 1, Well Bore Thermal Shock Technology, of BSEE Broad Agency Announcement (BAA) Solicitation Number E16PS00024: Proposed Research on Safety and Technology Verification Research in the U.S. Outer Continental Shelf (OCS)

2 E16PC00010 Wellbore Thermal Shock Technology, Modification 001, 27 Sept 2017

3 AMRA 2012, Radial cracking of a borehole by pressure and thermal shock; Tarasovs, S and Ghassemi, Texas AandM University and University of Latvia.

4 AMRA 2013, Numerical modelling of tensile thermal stresses in rock around a cased well caused by injection of a cold fluid; Lavrov, A. and Cerasi, P, SINTEF Petroleum Research, Trondheim, Norway

5 SPE-117709-PA An Innovative Methodology for Designing Cement-Sheath Integrity Exposed to Steam Stimulation; Garnler, Saint-Marc, Bols and Kermanac'h, Total, 2010

6 SPE-182510-MS Risk-Based Analysis of Thermal Well Integrity Through Integration of Caprock Geomechanics and Cement Sheath Design, Glover, Priolo and Heinricks, 2016

7 BSEE Project E14PC00037 "Well Stimulation Effects on Annular Seal of Production Casing in OCS Oil and Gas Operations", CSI Technologies, 2015

8 SPE 106998 FE Studies of Near-Wellbore Region During Cementing Operations – Part 1, Gray, Podnos, Becker, UT Austin, March 2009, SPE Drilling and Completions

9 ARMA-2016-246 Well Integrity Analysis - 3D Numerical Modelling of Cement Interface Debonding, Feng, Podnos, Gray

10 SPE 168001 FE Studies of Hoop-stress Enhancement for Wellbore Strengthening, Feng, Arlanoglu, Podnos, Becker and Gray

11 ARMA-2014-7109 Near-well Integrity and thermal effects - a computational road from laboratory to field scale, Lavrov, Torsaeter, Albawi. Todorovic, Opedal and Cerasi (SINTEF and Statoil), 2014

12 SPE-171430-MS Preventing String Inegrity Failure in Production and Stimulation for HPHT Wells, Aditya, Subiantoro, EMP, 2014

13 OTC-24852-MS Importance of Thermal Stress Loading Analysis for Tubulars in HPHT Wells, Shahreyar, Finley, Halliburton, 2014

14 SPE-166142-PA Environmental Risk Arising From Well-Construction Failure - Barrier v Well Failure and Failure Frequency, G. King, Apache Corp and D. King WG Consulting, 2013

15 SPE-182460-MS Well Failure Mechanisms and Conceptualisation of Reservoir-Aquifer Failure 2016, Wu, Dodle, Turnadge and Mallants, 2016

16 Best Practices For Prevention And Management Of Sustained Casing Pressure, JIP for MMS, 2001

17 SPE169814 Assessing Wellbore Integrity in Sustained-Casing-Pressure Annulus, Rocha-Valadez, Hasan, Mannan and Kabir, 2013

18 API 6A - Specification for Wellhead and Christmas Tree Equipment, 20th Ed, 2010 plus errata and addenda

19 API RP 96 Deepwater Well Design and Construction, 1st Ed, March 2013

20 API 17 TR8 HPHT Design Guidelines, 1st Ed, 2015

21 API RP 90-2 Annular Pressure Management for Offshore Wells, 1st Ed, April 2016

22 WellCAT Casing design software, https://www.landmark.solutions/WELLCAT

23 ABAQUS Finite Element Software, https://www.3ds.com/products-services/simulia/

24 Drillbench Dynamic Drilling Simulation Software, https://www.software.slb.com/products/drillbench

25 eDrilling, http://edrilling.no/products-services/wellsim/

26 TubeFlowPIC, http://www.btechsoft.com/TubeFlow_PIC.aspx

27 DIANA FEA, http://dianafea.com/content/TechDatOilGas, General Purpose FE code with Oil and Gas applications

28 CFR 250 Oil And Gas And Sulphur Operations In The Outer Continental Shelf, Subpart D - Oil and Gas Drilling Operations, Subject Group 81, General Requirements 250.400 through 250.409

29 CFR 250 Oil And Gas And Sulphur Operations In The Outer Continental Shelf, Subpart D - Oil and Gas Drilling Operations, Subject Group 82, General Requirements 250.410 through 250.418

30 CFR 250 Oil And Gas And Sulphur Operations In The Outer Continental Shelf, Subpart D - Oil and Gas Drilling Operations, Subject Group 83, General Requirements 250.420 through 250.428

31 API RP 65-2 Isolating Potential Flow Zones During Well Construction, Second Edition, December 2010 Reaffirmed, November 2016

APPENDIX A– CEMENT MATERIAL CHARACTERISTICS

CSI TECHNOLOGIES
A SUPERIOR ENERGY SERVICES COMPANY

HDV0965-5 - 4d

Laboratory Data Summary

Test Date:	May 19, 2017	Depth MD (ft):	4,500	Job Size / Type:	20 (in) Casing
Project No:	HDV0965-5 - 4d	Depth TVD (ft):	4,500	Well Fluid Density (lb/gal):	10.5
Company:	WWC/BSEE	BHST (°F):	80	Test Schedule:	Casing - 9.4
0		BHCT (°F):	65		
0		Test Pressure (PSI):	2,840		

Cement Slurry Design

Slurry Density (lb/gal): 16.4 — Slurry Yield (ft^3/sk): 1.06 — Total Mixing Fluid (gal/sk): 4.35

Cement Blend	Sack Weight, lb	% of Total Sack Weight	Prod Weight, lb/sk	CSI Log #
Cement - Class H (Lehigh)	94	100	94.00	labstock

Mix Water	Concentration	Units	CSI Log #
Deionized Water	4.272	gal/sk	labstock

Function	Additive	Concentration	Units	CSI Log #
Foamer	APF-27	0.080	gal/sk	R5083

Test Results

Measured Density

Cement (lb/gal): 16.4

Slurry Mixing

Additional Time to Mix: 10sec
Vortex at Low RPM: Yes
Maximum RPM: 12,063

Desired Thickening Time 6-10 hrs

Total Thickening Time - Cement

BHCT (°F):	40 Bc	70 Bc	
65	05:22	06:44	hr:min

Desired Free Fluid 0.00

Free Fluid

Conditioning Temp. (°F): 65
Test Angle: Vertical
Measured Free Fluid: 0.0 mL / 250 mL
Calculated Free Fluid: 0.00%

Rheological Properties

Fluid / Mixture	Temp °F	300	200	100	60	30	6	3	PV	YP	Gel Strength 10 sec	Gel Strength 10 min
Cement	80	76	60	44	36	32	16	12	60	21	15	17
Cement	65	100	80	60	50	40	20	16	1412	39	19	19
									cP	$lb_f/100ft^2$	$lb_f/100ft^2$	

Note: Rheology measured using R1-B1-F2.0 confirguration and reported as R1-B1-F1.0

Hydraulic Bond

	Flow Rate		
psi	Pipe 1	Pipe 2	Pipe 3
50	0	0	0
100	0	0	0
200	0	0	0
300	0	0	0
400	0	0	0
500	0	0	0
600	0	0	0
700	0	0	0
800	0	0	0
900	max	max	max
1000			

Splitting Tensile Strength

Test 1 211 psi
Test 2 269 psi
Test 3 249 psi
Average 243 psi

Unconfined Compressive Strength

1309 psi

Young's Modulus

\# 1.01E+06

Poisson's Ratio

0.212

Coupon Pull Test

Test 1 42.5 psi
Test 2 220 psi

Thermal Conductivity

0.8459 W/mK

Thermal Diffusivity

0.3081 mm^2/s

Specific Heat

2.747 MJ/m^3K

Shear Bond

Test 1 1.9955 inch plug traveled ? in at 370 psi
Test 2 1.928 inch plug traveled ? in at 338 psi
Test 3 2.007 inch plug traveled ? in at 488 psi
Average shear bond 399 psi

Impact Test

Weight of Ball 66.89 gms, Distance 11.25 inches
Test 1 4.9035 x 1.0035 x 1.018 inch sample broke on 3 impact
Test 2 4.9175 x 1.0125 x 1.0055 inch sample broke on 4 impact

Comments / Recommendations:

Shear Bond Test 1 1.948" ID, 2.547 pipe length, 0.2305" top to cement, 0.321" bottom to cement; Test 2 1.962" ID, 2.4815" Pipe length, 0.225" top to cement, 0.3285" bottom to cement; Test 3 2.0185" ID, 2.5665 Pipe length, 0.256" top to cement, 0.3035" bottom to cement.

Coupon Pull test 1: 2.9455" coupon length, 0.59" coupon width, 0.0655" coupon thickness, 2.398"pipe length, 2.003" Pipe ID, 0.613" top of coupon to top of cement, 0.254" bottom of coupon to bottom of cement, 115.9lbf achieved a break; Test 2: 2.955" coupon length, 0.5895" coupon width, 0.0645" coupon thickness, 2.5150" Pipe length, 2.003"Pipe ID, 0.6385" top of coupon to top of cement, 0.2380" bottom of coupon to bottom of cement, 599 lbf achieved a break.

Tensile Test 1: 1.16" Length, 2.009" Diameter, 773.6 lbf; Test 2: 1.023" Length, 2.002" Diameter, 865.2 lbf; Test 3: 0.784" Length, 2.000" Diameter, 612.3 lbf.
UCS sample 3.389" Length, 2.012" Diameter; YM/PR sample 3.4225" Length, 2.0115" Diameter.
All reported mechanical property tests were performed on the foamed design to 13.5 lb/gal.

Project Coordinator: Paul Sonnier — Position: ______

CSI TECHNOLOGIES
A SUPERIOR ENERGY SERVICES COMPANY

HDV0965-5 - 1B

Laboratory Data Summary

Test Date:	March 13, 2017	Depth MD (ft):	4,200	Job Size / Type:	14 (in) Casing
Project No:	HDV0965-5 - 1B	Depth TVD (ft):	4,200	Well Fluid Density (lb/gal):	9.5
Company:	WWC/BSEE	BHST (°F):	122	Test Schedule:	Casing - 9.4
		BHCT (°F):	101		
		Temp. Grad. (°F/100ft):	1.		
		Test Pressure (PSI):	2,440		

Cement Slurry Design

Slurry Density (lb/gal): 12.0 Slurry Yield (ft³/sk): 2.24 Total Mixing Fluid (gal/sk): 12.81

Cement Blend	Sack Weight, lb	% of Total Sack Weight	Prod Weight, lb/sk	CSI Log #
Cement - Class H (Lehigh)	94	65	61.10	L4560
POZMIX (74)	74	35	25.90	L3627

Mix Water	Concentration	Units	CSI Log #
Deionized Water	12.808	gal/sk	0

Function	Additive	Concentration	Units	CSI Log #
Defoamer	Defoamer 7011	0.300	%bwoc (DB)	L4878
Light Weight	Gel (Bentonite)	8.000	%bwoc (DB)	P2272

Test Results

Measured Density
Cement (lb/gal): 12.0

Slurry Mixing
Additional Time to Mix: 0 sec.
Vortex at Low RPM: Yes
Maximum RPM: 12,016

Desired Thickening Time 4-6 hrs
Total Thickening Time - Cement
BHCT (°F): 101 — 40 Bc: 04:17 — 70 Bc: — hr:min

Compressive Strength
Test Temperature (°F): 122

50	psi at	10:51	hr:min
500	psi at	N/A	hr:min
54	psi at	12:00	hr:min

Desired Free Fluid <2%
Free Fluid
Conditioning Temp. (°F): 101
Test Angle: Vertical
Measured Free Fluid: 4.0 mL / 250 mL
Calculated Free Fluid: 1.60%

Shear Bond
Test 1 2.02 inch plug traveled 0.2 in at 75 psi
Test 2 1.96 inch plug traveled 0.17 in at 52 psi
Test 3 1.98 inch plug traveled 0.21 in at 43 psi
Average shear bond 170 psi

Impact Test
Weight of Ball 66.9 gms, Distance 11.25 inches
Test 1 4.99 x 1.013 x .991 inch sample broke on 1 impact
Test 2 4.99 x 1.001 x 0.984 inch sample broke on 1 impact

Rheological Properties

Fluid / Mixture	Temp °F	300	200	100	60	30	6	3	PV	YP	Gel Strength 10 sec	Gel Strength 10 min
Cement	80	52	50	48	46	44	27	20	24	35	19	19
Cement	101	66	62	58	54	50	27	21	37	38	19	26
									cP	lb/100ft²	lb/100ft²	

Note: Rheology measured using R1-B1-F2.0 configuration and reported as R1-B1-F1.0

Hydraulic Bond

	Flow Rate		
psi	Pipe 1	Pipe 2	Pipe 3
50	0	0	0
100	0.6	0.6	0.8
200	0.6	1	2
300	0.6	1	2.5
400	0.6	3.2	max
500	1.2-1.3	max	
600	4.4-4.6		
700	max		
800			
900			
1000			

Splitting Tensile Strength
Test 1 58 psi
Test 2 64 psi
Test 3 85 psi
Average 207 psi

Unconfined Compressive Strength
448 psi

Young's Modulus
3.18E+05

Poisson's Ratio
0.26

Coupon Pull Test
Test 1 52 psi
Test 2 54 psi
Average 53 psi

Thermal Conductivity
0.749 W/mK

Thermal Diffusivity
0.196 mm²/s

Specific Heat
3.823 MJ/m³K

Project Coordinator: Paul Sonnier **Position:** Research Manager

CSI TECHNOLOGIES
A SUPERIOR ENERGY SERVICES COMPANY

HDV0965-5 - 2c

Laboratory Data Summary

Test Date: April 04, 2017
Project No: HDV0965-5 - 2c
Company: WWC/BSEE

Depth MD (ft): 12,702
Depth TVD (ft): 12,100
BHST (°F): 245
BHCT (°F): 190
Temp. Grad. (°F/100ft): 1.36
Test Pressure (PSI): 11,230

Job Size / Type: 9 5/8 (in) Liner
Well Fluid Density (lb/gal): 16.4
Test Schedule: Liner - 9.20

Cement Slurry Design

Slurry Density (lb/gal): 17.0
Slurry Yield (ft³/sk): 1.40
Total Mixing Fluid (gal/sk): 5.08

Cement Blend	Sack Weight, lb	% of Total Sack Weight	Prod Weight, lb/sk	CSI Log #
Cement - Class H (Lehigh)	94	100	94.00	L4560

Mix Water	Concentration	Units	CSI Log #
Deionized Water	5.077	gal/sk	labstock

Function	Additive	Concentration	Units	CSI Log #
Weighting Agent	Hematite	8.000	%bwoc (DB)	P0481B
Silica	Silica Flour	10.000	%bwoc (DB)	L4372
Defoamer	Defoamer 7011	0.100	%bwoc (DB)	L4878
Fluid Loss	FL-17	0.900	%bwoc (DB)	P2274
Dispersant	NC-S-1	0.800	%bwoc (DB)	C4170
Strength	Sand-100 Mesh	25.000	%bwoc (DB)	L4373
Retarder	FR-1	0.100	%bwoc (DB)	L4869

Test Results

Measured Density
Cement (lb/gal): 17.0

Slurry Mixing
Additional Time to Mix: 10 sec
Vortex at Low RPM: Yes
Maximum RPM: 12,174

Desired Thickening Time 6-10 hrs

Total Thickening Time - Cement

BHCT (°F):	40 Bc	70 Bc	
190	09:41	09:58	hr:min

Compressive Strength
Test Temperature (°F): 245

50	psi at	03:28	hr:min
500	psi at	03:51	hr:min
3,224	psi at	12:00	hr:min
3,921	psi at	24:00	hr:min
	psi at	-	hours

Desired Fluid Loss < 100mls

Static Fluid Loss
Test Temp (°F): 190
Collected Fluid (mL): 26
Collection Time (min.): 30
API Fluid Loss (mL/30min): 52

Desired Free Fluid 0.00

Free Fluid
Conditioning Temp. (°F): 190
Test Angle: Vertical
Measured Free Fluid: 0.0 mL / 250 mL
Calculated Free Fluid: 0.00%

Rheological Properties

Fluid / Mixture	Temp °F	300	200	100	60	30	6	3	PV	YP	Gel Strength 10 sec	Gel Strength 10 min
Cement	80	284	209	118	76	42	11	6	282	14	6	15
Cement	190	150	107	63	43	25	8	5	145	10	4	36
									cP	lb/100ft²		lb/100ft²

Note: Rheology measured using R1-B1-F2.0 configuration and reported as R1-B1-F1.0

Hydraulic Bond

psi	Flow Rate Pipe 1	Flow Rate Pipe 2	Flow Rate Pipe 3
50	0	0	0
100	0	0	max
200	0	max	
300	0		
400	0		
500	0		
600	max		
700			
800			
900			
1000			

Splitting Tensile Strength
Test 1 696psi
Test 2 631 psi
Test 3 792 psi
Average 706 psi

Unconfined Compressive Strength
6310 psi

Young's Modulus
2.20E+06

Poisson's Ratio
0.2645

Coupon Pull Test
Test 1 221 psi
Test 2 +271 psi

Thermal Conductivity
1.3027 W/mK

Thermal Diffusivity
0.39389 mm²/s

Specific Heat
3.3198 MJ/m³K

Shear Bond
Test 1 2.1135 inch plug traveled 0.1965 in at 331 psi
Test 2 1.947 inch plug traveled 0.229 in at 252 psi
Test 3 1.8855 inch plug traveled 0.179 in at 355 psi
Average shear bond 313 psi

Impact Test
Weight of Ball 66.89 gms, Distance 11.25 inches
Test 1 4.913 x .9455 x 1.095 inch sample broke on 69 impact
Test 2 4.8115 x 0.9475 x 1.0815 inch sample broke on 39 impact

Comments / Recommendations:
Shear Bond Test 1 2.0075" ID, 2.7080 pipe length, 0.364" top to cement, 0.2305" bottom to cement; Test 2 1.99" ID, 2.647" Pipe length, 0.3000" top to cement, 0.4000" bottom to cement; Test 3 2.0005" ID, 2.5470 Pipe length, 0.4045" top to cement, 0.2570" bottom to cement.
Coupon Pull test 1: 2.9556" coupon length, 0.59" coupon width, .0575" coupon thickness, 2.5115"pipe length, 2.007" Pipe ID, 0.6295" top of coupon to top of cement, 0.3045" bottom of coupon to bottom of cement, 579.38 lbf achieved break; Test 2: 2.9525" coupon length, 0.583" coupon width, 0.0535" coupon thickness, 2.461" Pipe length, 2.008"Pipe ID, 0.7995" top of coupon to top of cement, 0.2970" bottom of coupon to bottom of cement, 640 lbf did not achieve a break
Tensile Test 1: 0.9805" Length, 2.018" Diameter, 2164 lbf; Test 2: 1.0475" Length, 2.018" Diameter, 2096 lbf; Test 3: 1.0655" Length, 2.0025" Diameter, 2654 lbf.
UCS sample 3.573" Length, 2.017" Diameter; YM/PR sample 3.771" Length, 2.013" Diameter.

Project Coordinator: Paul Sonnier
Position: Research Manager

CSI TECHNOLOGIES
A SUPERIOR ENERGY SERVICES COMPANY

HDV0965-5 - 3b

Laboratory Data Summary

Test Date:	April 04, 2017	Depth MD (ft):	17,000	Job Size / Type:	5 (in) Liner
Project No:	HDV0965-5 - 3b	Depth TVD (ft):	16,500	Well Fluid Density (lb/gal):	17.8
Company:	WWC/BSEE	BHST (°F):	350	Test Schedule:	Liner - 9.22
		BHCT (°F):	284		
		Temp. Grad. (°F/100ft):	1.64		
		Test Pressure (PSI):	16,510		

Cement Slurry Design

Slurry Density (lb/gal): 18.5 Slurry Yield (ft³/sk): 1.75 Total Mixing Fluid (gal/sk): 6.32

Cement Blend	Sack Weight, lb	% of Total Sack Weight	Prod Weight, lb/sk	CSI Log #
Cement - Class H (Lehigh)	94	100	94.00	L4560

Mix Water	Concentration	Units	CSI Log #
Deionized Water	6.318	gal/sk	labstock

Function	Additive	Concentration	Units	CSI Log #
Weighting Agent	Hematite	40.000	%bwoc (DB)	C2730
Silica	Silica Flour	10.000	%bwoc (DB)	C3196
Defoamer	Defoamer 7011	0.100	%bwoc (DB)	C4174
FW/Susp Aid	LTSA-1	0.200	%bwoc (DB)	P3587
Fluid Loss	FL-17	1.000	%bwoc (DB)	P2274
Dispersant	NC-S-1	0.500	%bwoc (DB)	C4170
Strength	Sand-100 Mesh	25.000	%bwoc (DB)	L4373
Retarder	PCR-3	1.000	%bwoc (DB)	C1989
	MicroMax	24.000	%bwoc (DB)	Z2061

Test Results

Desired Thickening Time 6-10 hrs

Total Thickening Time - Cement

BHCT (°F):	40 Bc	70 Bc	
284	06:25	06:29	hr:min

Compressive Strength

Test Temperature (°F): 350

50	psi at	05:34	hr:min
500	psi at	06:35	hr:min
3,044	psi at	12:00	hr:min
4,292	psi at	24:00	hr:min
	psi at	-	hours

Desired Fluid Loss <50mls

Stirred Fluid Loss

Test Temp (°F): 284
Collected Fluid (mL): 14
Collection Time (min.): 30
API Fluid Loss (mL/30min): 28

Desired Free Fluid 0.00

Free Fluid

Conditioning Temp. (°F): 190
Test Angle: Vertical
Measured Free Fluid: 0.0 mL / 250 mL
Calculated Free Fluid: 0.00%

Rheological Properties

Fluid / Mixture	Temp °F	300	200	100	60	30	6	3	PV	YP	Gel Strength 10 sec	Gel Strength 10 min
Cement	80	552	396	224	154	104	57	49	509	54	49	94
Cement	190	292	214	129	89	54	18	12	280	24	15	32
									cP	lb/100ft²		lb/100ft²

Note: Rheology measured using R1-B1-F2.0 configuration and reported as R1-B1-F1.0

Hydraulic Bond

	Flow Rate		
psi	Pipe 1	Pipe 2	Pipe 3
50	0	0	0
100	0	0	0
200	0	0	0
300	0	0	0
400	max	0	max
500		max	
600			
700			
800			
900			
1000			

Splitting Tensile Strength
Test 1 533psi
Test 2 589 psi
Test 3 590 psi
Average 571 psi

Unconfined Compressive Strength
5044 psi #

Young's Modulus
1.57E+06

Poisson's Ratio
0.271

Coupon Pull Test
Test 1 0 psi
Test 2 80 psi

Thermal Conductivity
1.5523 W/mK

Thermal Diffusivity
0.4905 mm²/s

Specific Heat
3.175 MJ/m³K

Shear Bond
Test 1 2.059 inch plug traveled 0.1645 in at 367 psi
Test 2 1.9896 inch plug traveled 0.1915 in at 377 psi
Test 3 1.8815 inch plug traveled 0.1785 in at 378 psi
Average shear bond 313 psi

Impact Test
Weight of Ball 66.89 gms, Distance 11.25 inches
Test 1 4.8875x 1.0175 x 1.0015 inch sample broke on 32 impact
Test 2 4.8810x 1.011 x 0.9950 inch sample broke on 42 impact

Comments / Recommendations:

Shear Bond Test 1 1.925" ID, 2.5345 pipe length, 0..1795" top to cement, 0.2960" bottom to cement; Test 2 1.9845" ID, 2.4935" Pipe length, 0.2325" top to cement, 0.3215" bottom to cement; Test 3 2.1.9835" ID, 2.399 Pipe length, 0.2215" top to cement, 0.2960" bottom to cement.

Coupon Pull test 1: 2.9545" coupon length, 0.5925" coupon width, 0.057" coupon thickness, 2.5195"pipe length, 1.995" Pipe ID, 0.222" top of coupon to top of cement, 0.3090" bottom of coupon to bottom of cement, 0 lbf achieved break; Test 2: 2.9555" coupon length, 0.5905" coupon width,
0.0635" coupon thickness, 2.6285" Pipe length, 1.962"Pipe ID, 0.6935" top of coupon to top of cement, 0.3760" bottom of coupon to bottom of cement, 198 lbf achieved a break

Tensile Test 1: 1.0405" Length, 2.018" Diameter, 1759 lbf; Test 2: 1.0595" Length, 2.014" Diameter, 1973 lbf; Test 3: 1.0345" Length, 2.0105" Diameter, 1927 lbf.
UCS sample 3.7730" Length, 2.0145" Diameter; YM/PR sample 3.8255" Length, 2.0155" Diameter.

Project Coordinator: Paul Sonnier **Position:**

CSI TECHNOLOGIES
A SUPERIOR ENERGY SERVICES COMPANY

HDV0965-5 - 5a

Laboratory Data Summary

Test Date:	March 29, 2017	Depth MD (ft):	6,700	Job Size / Type:	16 (in) Liner
Project No:	HDV0965-5 - 5a	Depth TVD (ft):	6,700	Well Fluid Density (lb/gal):	11.9
Company:	WWC/BSEE	BHST (°F):	91	Test Schedule:	Liner - 9.17
		BHCT (°F):	80		
		Temp. Grad. (°F/100ft):	.16		
		Test Pressure (PSI):	4,740		

Cement Slurry Design

Slurry Density (lb/gal): 13.5 Slurry Yield (ft³/sk): 1.72 Total Mixing Fluid (gal/sk): 9.27

Cement Blend	Sack Weight, lb	% of Total Sack Weight	Prod Weight, lb/sk	CSI Log #
Cement - Class H (Lehigh)	94	100	94.00	L4561

Mix Water	Concentration	Units	CSI Log #
Lab Sea Water	8.824	gal/sk	Labstock

Function	Additive	Concentration	Units	CSI Log #
FW/Susp Aid	LTSA-1	0.200	%bwoc (DB)	C3974
Light Weight	Sodium Silicate Liquid	0.150	gal/sk	C8173
Fluid Loss	FL-17 Liquid	0.300	gal/sk	C3963

Test Results

Measured Density
Cement (lb/gal): 13.5

Slurry Mixing
Additional Time to Mix: 0 sec.
Vortex at Low RPM: Yes
Maximum RPM: 12,025

Desired Thickening Time 6-10 hrs
Total Thickening Time - Cement

BHCT (°F):	40 Bc	70 Bc	
80	09:12	11:53	hr:min

Compressive Strength
Test Temperature (°F): 91

50	psi at	09:01	hr:min
500	psi at	34:42	hr:min
109	psi at	12:00	hr:min
353	psi at	24:00	hr:min
	psi at	-	hours

Desired Fluid Loss <50mls
Static Fluid Loss
Test Temp (°F): 80
Collected Fluid (mL): 15
Collection Time (min.): 30
API Fluid Loss (mL/30min): 30

Desired Free Fluid 0.00
Free Fluid
Conditioning Temp. (°F): 80
Test Angle: Vertical
Measured Free Fluid: 0.0 mL / 250 mL
Calculated Free Fluid: 0.00%

Rheological Properties

Fluid / Mixture	Temp °F	300	200	100	60	30	6	3	PV	YP	Gel Strength 10 sec	Gel Strength 10 min
Cement	80	172	132	82	60	38	14	10	162	20	11	25
Cement	80	164	130	82	60	40	12	8	156	20	13	23
									cP	lb/100ft²	lb/100ft²	

Note: Rheology measured using R1-B1-F2.0 configuration and reported as R1-B1-F1.0

Hydraulic Bond

	Flow Rate		
psi	Pipe 1	Pipe 2	Pipe 3
50	0	0	max
100	0	0	
200	0	0	
300	0	0	
400	0	0	
500	0	max	
600	max		
700			
800			
900			
1000			

Splitting Tensile Strength
Test 1 266 psi
Test 2 216 psi
Test 3 277 psi
Average 253 psi

Unconfined Compressive Strength
1858 psi

Young's Modulus
7.39E+05

Poisson's Ratio
0.2765

Coupon Pull Test
Test 1 +260 psi
Test 2 252 psi

Thermal Conductivity
0.899 W/mK

Thermal Diffusivity
0.246 mm²/s

Specific Heat
3.654 MJ/m³K

Shear Bond
Test 1 1.7855 inch plug traveled 0.2 in at 266 psi
Test 2 1.7685 inch plug traveled 0.2 in at 290 psi
Test 3 1.606 inch plug traveled 0.20 in at 266 psi
Average shear bond 274 psi

Impact Test
Weight of Ball 66.89 gms, Distance 11.25 inches
Test 1 4.985 x .9957 x 0.993 inch sample broke on 24 impact
Test 2 5.0065 x 1.0105 x 0.998 inch sample broke on 11 impact

Comments / Recommendations:
Shear Bond Test 1 1.9795" ID, 2.5510 pipe length, .4570" top to cement, .30850" bottom to cement; Test 2 1.9790" ID, 2.5575" Pipe length, .5275" top to cement, .2615" bottom to cement; Test 3 1.986" ID, 2.5355 Pipe length, .5395" top to cement, .39" bottom to cement.
Coupon Pull test 1: 2.956" coupon length, 0.5880" coupon width, 0.054" coupon thickness, 2.5215"pipe length, 2.006" Pipe ID, 0.844" top of coupon to top of cement, 0.3135" bottom of coupon to bottom of cement, 600lbf maximum did not break; Test 2: 2.96" coupon length, 0.5855" coupon width, 0.0535" coupon thickness, 2.5315" Pipe length, 2.096" Pipe ID, 0.797" top of coupon to top of cement, 0.2845" bottom of coupon to bottom of cement, 602.59 lbf achieved a break.
Tensile Test 1: 1.05" Length, 2.008" Diameter, 880 lbf; Test 2: 1.075" Length, 2.007" Diameter, 733.5 lbf; Test 3: 1.031" Length, 1.993" Diameter, 895.5 lbf.
UCS sample 3.661" Length, 2.003" Diameter; YM/PR sample 3.741" Length, 2.003" Diameter.

CSI TECHNOLOGIES
A SUPERIOR ENERGY SERVICES COMPANY

HDV0965-5 - 6d

Laboratory Data Summary

Test Date:	March 31, 2017	Depth MD (ft):	18,359	Job Size / Type:	9 5/8 (in) Casing
Project No:	HDV0965-5 - 6d	Depth TVD (ft):	16,922	Well Fluid Density (lb/gal):	15.2
Company:	WWC/BSEE	BHST (°F):	201	Test Schedule:	Casing - 9.10
		BHCT (°F):	162		
		Temp. Grad. (°F/100ft):	.72		
		Test Pressure (PSI):	14,330		

Cement Slurry Design

Slurry Density (lb/gal): **16.4** Slurry Yield (ft³/sk): **1.06** Total Mixing Fluid (gal/sk): **4.36**

Cement Blend	Sack Weight, lb	% of Total Sack Weight	Prod Weight, lb/sk	CSI Log#
Cement - Class H (Lehigh)	94	100	94.00	L4905

Mix Water	Concentration	Units	CSI Log#
Deionized Water	4.028	gal/sk	labstock

Function	Additive	Concentration	Units	CSI Log #
Defoamer	Defoamer 7011-L	0.010	gal/sk	C4174
Fluid Loss	FL-17 Liquid	0.300	gal/sk	C3963
Retarder	Kelig 32L	0.020	gal/sk	L4869

Test Results

Measured Density

Cement (lb/gal): 16.4

Slurry Mixing

Additional Time to Mix:	10 sec
Vortex at Low RPM:	Yes
Maximum RPM:	12,167

Desired Thickening Time **6-10 hrs**

Total Thickening Time - Cement

		40 Bc	70 Bc	
BHCT (°F):	162	06:22	**06:29**	hr:min

Compressive Strength

Test Temperature (°F): 201

50	psi at	02:04	hr:min
500	psi at	02:49	hr:min
3,097	psi at	12:00	hr:min
4,081	psi at	24:00	hr:min
	psi at	-	hours

Desired Fluid Loss **<50 mls**

Static Fluid Loss

Test Temp (°F):	162
Collected Fluid (mL):	10
Collection Time (min.):	30
API Fluid Loss (mL/30min):	20

Desired Free Fluid **0.00**

Free Fluid

Conditioning Temp. (°F):	162
Test Angle:	Vertical
Measured Free Fluid:	0.0 mL / 250 mL
Calculated Free Fluid:	0.00%

Rheological Properties

Fluid / Mixture	Temp °F	300	200	100	60	30	6	3	PV	YP	Gel Strength 10 sec	Gel Strength 10 min
Cement	80	470	350	207	138	79	20	10	463	30	13	62
Cement	162	460	354	221	154	90	26	13	448	42	15	49
Note: Rheology measured using R1-B1-F2.0 configuration and reported as R1-B1-F1.0									cP	lb/100ft²		lb/100ft²

Hydraulic Bond

psi	Flow Rate Pipe 1	Flow Rate Pipe 2	Flow Rate Pipe 3
50	0	0	0
100	0	0	0
200	0	0	0
300	0	max	0
400	max		0
500			0
600			0
700			max
800			
900			
1000			

Splitting Tensile Strength

Test 1 1103 psi
Test 2 991 psi
Test 3 1248 psi
Average 1114 psi

Unconfined Compressive Strength

10732 psi #

Young's Modulus

1.53E+07

Poisson's Ratio

0.5

Coupon Pull Test

Test 1 318 psi
Test 2 248 psi

Thermal Conductivity

1.0594 W/mK

Thermal Diffusivity

0.449 mm²/s

Specific Heat

2.3983 MJ/m³K

Shear Bond

Test 1 1.797 Inch plug traveled 0.189 in at 397 psi
Test 2 1.786 Inch plug traveled 0.198 in at 527 psi
Test 3 1.769 Inch plug traveled 0.1835 in at 449 psi
Average shear bond 458 psi

Impact Test

Weight of Ball 56.89 gms, Distance 11.25 Inches
Test 1 4.872 x 1.0285 x 0.8995 Inch sample broke on 24 Impact
Test 2 4.8975 x 1.022 x 0.8915 Inch sample broke on 104 Impact

Comments / Recommendations:

Shear Bond Test 1 1.9995" ID, 2.5635 pipe length, .4285" top to cement, .3380" bottom to cement; Test 2 1.984" ID, 2.5095" Pipe length, .4665" top to cement, .2570" bottom to cement; Test 3 1.9795" ID, 2.585 Pipe length, .5165" top to cement, .2995" bottom to cement.

Coupon Pull test 1: 2.9535" coupon length, 0.5845" coupon width, .0635" coupon thickness, 2.5855"pipe length, 2.006" Pipe ID, 0.896" top of coupon to top of cement, 0.3115" bottom of coupon to bottom of cement, 600lbf maximum did not break, pushed with GCTS and obtained 719 lbf; Test 2: 2.9565" coupon length, 0.5895" coupon width, 0.0600" coupon thickness, 2.5245" Pipe length, 2.008"Pipe ID, 0.9865" top of coupon to top of cement, 0.291" bottom of coupon to bottom of cement, 541.92 lbf achieved a break.

Tensile Test 1: 1.067" Length, 2.027" Diameter, 3747 lbf; Test 2: 1.079" Length, 2.01" Diameter, 3375 lbf; Test 3: 1.0785" Length, 2.0055" Diameter, 4240 lbf.
UCS sample 3.389" Length, 2.012" Diameter; YM/PR sample 3.4225" Length, 2.0115" Diameter.

APPENDIX B – TASK 2 DEFINITION

Definitions, Assumptions and Search Parameters

The following will be applied to help focus Task 2 and provide some boundary conditions/limits for search parameters.

Thermal Shock Definition:

- Wells with a bottom hole temperature of 350°F or above combined with a minimum ambient temperature as low as 40°F .
- Thermal shock could be initiated by shutting in a producing well and allowing it to cool to ambient or by stimulating a well, although these thermal shocks are less severe than stimulation and damage mainly caused by the cyclical nature.
- Thermal shock not only depends on the temperature range but also the rate at which temperature changes. The rate of cooling of the well would depend on the operations considered, e.g. natural cooling post shut-in or cooling during well stimulation for example.
- While the expectation is that further refinement of the definition of thermal shock may be made in Task 3, the public domain search effort for task 2 will use the above definition to determine if research has been done into well thermal shock caused either by shut-in or stimulation.

Initial Well Configuration:

- Wells in the Lower Tertiary[2] associated with Deepwater operations will be used to define the target operating conditions for the search parameters. Task 2 will define and use a representative well configuration to assist in the search but should not rule out any other information the search uncovers.
- It was acknowledged at the project kick-off meeting that BSEE's focus is on OCS Gulf of Mexico but that relevant knowledge from other regions, if readily uncovered by the public domain search, would be considered.[3]
- Sensitivities to well parameters such as true vertical depth, measured depth, casing schedule, deviation, top of cement and hole size do not need to be explored in Task 2. Task 2 will catalogue all of the variables that could have some impact on the thermal shock response of the well and the impact of these will then be explored in Task 4.

[2] Wells in the Cascade and Chinook fields are considered typical of the target wells
[2] This could include Arctic conditions for example, which could also prove to be worst-case?

- Task 2 will catalogue all of the variables that could have some impact on the thermal shock response of the well and the impact of these will then be explored in Task 4, however;
- Task 2 excludes attempts and efforts by research team members to conduct a sensitivity analysis on the relative impact of the variables, and
- Task 2 includes acquisition of any previously conducted sensitivity studies or related research, if any exists.

Materials:

- It is acknowledged that there are multiple variants of all of the primary well materials with steel, cement and elastomers each having subtly different mechanical and thermal properties that may have some bearing on thermal shock response. Indeed a range of steel grades will likely be used through a typical casing program and these may also have slight differences in thermal properties. However, Task 2 should not attempt to use all possible permutations of the materials as parameters for public domain information searches but rather identify whether typical well construction materials have been the subject of research into thermal shock as defined above. The following boundary definitions apply:
  - To be considered, steel used in all casing strings that extend to the mudline. (Liners re excluded unless tied-back to the mudline.);
  - To be considered, steels (and any elastomers) in the wellhead and below, likely to be 4-6 different alloys that exhibit variations in hardness, brittleness an thermal-induced properties
  - The tree does not need to be considered within the scope of this project